Dipl.-Ing. Lukas Andreas Jagiello

Separation and thickening of pulp fibers and fines in the lab scale and application thereof

DOCTORAL THESIS

to achieve the university degree of

Doktor der technischen Wissenschaften

submitted to

Graz University of Technology

Supervisor

Univ.-Prof. Dipl.-Ing. Dr. techn. Wolfgang Bauer

Institute of Pulp, Paper and Fibre Technology
Graz University of Technology

Graz, February 2017

AFFIDAVIT

I declare that I have authored this thesis independently, that I have not used other than the declared sources/resources, and that I have explicitly indicated all material which has been quoted either literally or by content from the sources used. The text document uploaded to TUGRAZonline is identical to the present doctoral thesis.

Date

Signature

Acknowledgements

The current work was carried out at the Institute of Paper, Pulp and Fiber Technology at Graz University of Technology (TUG). The work was carried out within the frame work of the project of Flippr° (Future Lignin and Pulp Processing Research).

First of all, I would like to thank my supervisor Prof. Dr. Wolfgang Bauer for giving me the possibility to write my doctoral thesis at the Institute for Paper, Pulp and Fiber Technology. I wish to express special thanks to Prof. Dr. Wolfgang Gindl-Altmutter for evaluating my thesis. I am very grateful to my "non-official" supervisor Dr. Rene Eckhart for helping me and for inspiring discussions. Thanks to Dr. Wolfgang Fischer for his support in academic writing for my publications and for stimulating discussions and his supervision. I am thankful to Claudia Bäumel and Kerstin Schefzik for their administrative support. I am also very grateful to Adelheid Bakhshi, Kerstin Roschitz and Harald Streicher for the support in the laboratory and especially to Harald Streicher for his IT-support. I am thankful to the Institute of Process and Particle Engineering for helping me with the Tube Flow fractionation device and for stimulating discussions. Special thanks to Christian Probst and Michael Dauer for helping me with the design and construction of several devices as well with programming. Samir Kopacic, Georg Urstöger, Raphael Giner Tovar, Wolfgang Fuchs, Marina Jajcinovic, Jussi Lahti and Melanie Mayr, for being great colleagues and friends. Finally, I would like to express my warmest thanks to my family. My mother Ingrid for making this work possible and for her support in good times and bad times. Teresa, Jan, Daniel for their motivation. In the end, I would like to thank my girlfriend Bettina for her support in all aspects of my life.

Lukas Jagiello

Graz, 08.02.2017.

Abstract

Any given pulp being it mechanical or chemical pulp of any kind of wood species is a composition of particles ranging from the nanometer scale to several millimeters in length and up to 100 µm in width. The proportion of the single fractions can also vary greatly, for example the fines fraction (particles passing a 76 µm hole screen) can represent 1 or 2 and also up to 40 % of a pulp mass. The different fractions show quite different technological properties based on size, chemical composition and specific surface area making them beneficial or detrimental depending on a given application. To be able to take a closer look at the different fractions and especially on the fines fraction methods for separation of these fractions are necessary.

In this thesis two different separation approaches focused on the fines fraction are discussed. The first approach deals with fractionation/separation as an analytical tool for characterization of the single fractions. It is based on so called tube flow fractionation and also addresses the influence of secondary flow in a coiled tube setup under different parameters such as curvature and flow velocity. These secondary flows have not been investigated yet and strongly affect the separation performance. The second approach deals with the separation of larger amounts of the fines from different pulp sources for subsequent lab trials regarding their technological properties and their applicability in products outside the paper industry. For this task a pressure screen with a 100 µm hole screen was implemented. Results show a high separation efficiency and depending on the original fines content of a pulp quantities of more than 100 g of fines (oven dry mass) can be produced within one hour.

Still, due to a very low solids content of the fines fraction (accept flow) subsequent trials such as chemical modification or formation of handsheets cannot be performed without a thickening procedure. To perform this task, a dissolved air flotation cell (DAF) was developed with a clear focus on fines thickening performance. Experiments with different pulp fines show that the DAF process has a high separation efficiency (up to 90 %) and thickening from 0.01 % up to more than 3 % consistency is possible without the use of any kind of chemical additives that would contaminate the material. Such a process does also seem reasonable in a given industrial application as 99 % of the water can be removed at very low costs. The device is used in-line with the pressure screen to yield large quantities of fines for further experiments within reasonable time.

Keywords: Fines fractionation, Dean Flow, Tube Flow Fractionation, Pressure Screen, Dissolved Air Flotation (DAF)

Kurzfassung

Zellstoff, egal ob mechanisch oder chemisch aufgeschlossen und egal von welcher Holzart, ist immer eine Mischung aus Partikeln, welche eine Länge von einigen Nanometern bis Millimetern und eine Breite von bis zu 100 µm aufweisen. Das Verhältnis von einzelnen Fraktionen zueinander kann sich sehr unterscheiden, so kann zum Beispiel die Feinstofffraktion (Partikel die ein 76 µm Lochsieb passieren) 1 bis 2 aber genauso bis 40 % der Gesamtmasse ausmachen. Die erhaltenen Fraktionen weisen unterschiedlichste technologische Eigenschaften basierend auf Partikelgröße, chemischer Zusammensetzung und spezifischer Oberfläche auf. Um einen tieferen Einblick in unterschiedliche Fraktionen zu erhalten, sind geeignete Methoden zur Fraktionierung notwendig. Die vorliegende Arbeit behandelt zwei unterschiedliche Ansätze zur Fraktionierung im Labormaßstab. Ein Ansatz dient der analytischen Fraktionierung. Die Versuche wurden mit einem Tube Flow Fraktionierer durchgeführt, wobei insbesondere der Einfluss von Sekundärströmungen auf die Fraktionierung, durch Änderung von Parametern wie zum Beispiel Krümmung und Strömungsgeschwindigkeit untersucht wurde. Diese Strömungen haben starken Einfluss auf das Fraktionierergebnis und wurden bis zum heutigen Zeitpunkt noch nicht untersucht. Der zweite Ansatz behandelt Feinstoffabtrennung im größeren Maßstab für weiterführende Laborversuche bezüglich technologischer Eigenschaften und Anwendbarkeit von Produkten außerhalb der Papierindustrie. Um diese Anforderungen zu erfüllen, wurde ein Labordrucksortierer mit einem 100 µm Sieb implementiert. Der Sortierer zeigt eine hohe Effizienz bezüglich der Abtrennung von unterschiedlichen Feinstoffen und es können stündlich mehr als 100 g Feinstoff abgetrennt werden. Jedoch liegt die abgetrennte Feinstoffsuspension stark verdünnt vor, sodass eine direkte Anwendung wie zum Beispiel Blattbildung oder chemische Modifikation nicht möglich ist. Aus diesem Grund wurde eine Druckentspannungsflotationszelle entwickelt mit einem Hauptaugenmerk auf die maximale Eindickung der Feinstofffraktion. Ergebnisse zeigen, dass eine sehr hohe Abtrennungseffizienz aus der Wasserphase (mehr als 90%) erreicht werden kann, wobei die Suspension von 0.01% auf über 3% eingedickt wird. So ein Prozess erscheint in Bezug auf eine industrielle Anwendung sinnvoll, da man mehr als 99% des Wassers vergleichsweise energiesparend abtrennen kann. Die Flotationsanlage wurde in-line mit dem Drucksortierer betrieben, so dass größere Mengen an Feinstoff innerhalb kurzer Zeit bereitgestellt werden konnten.

Schlagwörter: Feinstoffabtrennung, Dean Flow, Tube Flow Fraktionierung, Drucksortierer, Druckentspannungsflotation

Contents

1 Introduction

1.1 General research framework

This doctoral thesis was carried out within the framework of the project "Future Lignin and Pulp Processing Research" (Flippr°). This project is a cooperative research project between four different company partners of the Austrian pulp and paper industry as well as three universities. The target of Flippr° is a higher resource efficiency in utilization of the components of wood. To achieve the goal of a higher value obtained from the resource wood, there are two interconnected research areas dealing with lignin on the one hand and pulp fibers on the other (Timmel [2014]). The Flippr° project is divided into three different areas:

- Lignin
  The goal is to use the in process existing lignin sources as a product instead of using it to produce energy and electricity via thermal conversion
- Pulp fibers
  This research field deals with the investigation of fiber fractionation, characterization and modification methods as well as their possible applications. One goal of utmost importance of area 2 is the utilization of fines as a product based on fiber fractionation.
- Life cycle assessment
  In this project, the aim is to assess environmental impacts associated with all stages of a product during its lifetime. Further, this field deals with the comparison of existing products/prices and the economic and ecological impacts

In the fiber research in the Flippr° project, two institutes from Graz University of Technology are involved, the Institute for Paper, Pulp and Fiber Technology (IPZ) and the Institute for Process and Particle Engineering (IPPT). The major part of

this thesis was carried out at the Institute for Paper, Pulp and Fiber Technology. Chemical analysis as well as application trials dealing with fines were carried out in corporation with the Institute of Wood Technology and Renewable Materials - BOKU Wien.

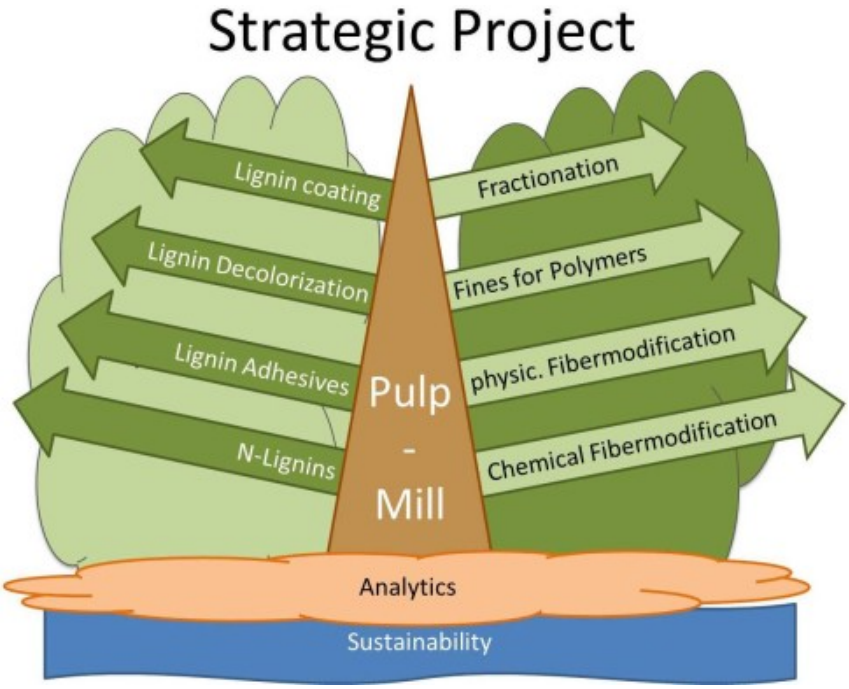

Figure 1-1 *Basic layout of the Flippr° project (Flippr° [2013]).*

The current thesis is part of the Area 2 "Advanced Utilization of Primary Fibers", where the main objective is to focus on opportunities for optimized utilization of fiber resources within the pulp and paper process. Furthermore, possible applications for pulp fibers or certain fiber fractions outside the standard product chain are in the focus of this area. Pulp fractionation and subsequent utilization of these fractions is a key procedure in this research area to get a deeper insight into different properties.

Different fiber fractions of pulp provide different properties in a paper sheet. Pulp fines play an import role with regard to the optical and physical properties of a paper sheet. The addition of suitable fines can enhance the final paper properties (Retulainen et al. [1993]). The influence of fines regarding size, shape and chemical composition was discussed by several authors (Luukko and Paulapuro [1999], Sirvio and Nurminen [2003], Lindqvist et al. [2012]). In addition, when trying to understand and to control the properties of a cellulosic pulp, it is important to consider not only the bulk amount of long fibers, but also the fines, which comprise 1 and 40 % of pulp.

Fractionation of pulp provides information regarding morphology, chemical composition of fines and the influence especially in papermaking. The main characteristic of fines is their large specific surface area associated with their size. The chemical composition, charge and magnitude of their surface area are the basis of interactions with different pulp and paper components such as extractives, fillers and retention aids.
To investigate the full potential of fractionation, this project deals with laboratory fractionation using standard methods as well as novel methods already partly described in literature (e.g. tube flow fractionation).
A further objective was to provide large amounts of isolated fines (>100 g oven dried fines) from different pulp sources for further investigations and applications.
An additional focus was set on the investigation of the influence of secondary flow in a coiled tube set-up of a tube flow fractionation device by changing parameters such as curvature and flow velocity. This was done to investigate the influence of secondary flow on the separation performance of different fiber and fines fractions. Further it was investigated, whether this secondary flow provides a possibility for improved fines separation with the TFF device.

1.2 Outline of the thesis

After this introduction chapter, the present thesis is divided into the following four chapters:

- Chapter 2 gives an overview about fibers and especially fines including fundamentals of fiber-fines fractionation methods in the laboratory scale as well in the industrial scale

- Chapter 3 describes materials and methods for studying the defined research questions

- Chapter 4 presents the design and implementation process of different laboratory fractionation equipment either for analytical fiber-fines fractionation or for fines separation and thickening methods where quantities of more than 100 g fines (oven dried) are required

- Chapter 5 concludes this thesis by giving an outlook on potential industrial methods and applications

1.3 List of publications

Papers

1. Jagiello, L. A., Redlinger-Pohn, J. D., Fischer, W. J., Eckhart, R. and Bauer, W. (2016). The effect of Dean Flow in a tube flow fractionation device. Nordic Pulp and Paper Research Journal 31(4), 641 - 647.
2. Redlinger-Pohn, J. D., Jagiello. L. A., Bauer, W., and Radl, S. (2016). Mechanistic understanding of size-based fiber separation in coiled tubes. International journal of multiphase flow, 83, 239-253.

Contribution to conference proceedings

1. Jagiello, L. A., Fischer, W.J., Eckhart, R. and Bauer W. (2016). Fines separation and thickening in the lab scale by means of screening and microbubble flotation. In: Progress in Paper Physics Seminar, Darmstadt, Germany.
2. Giner, R., Mayr, M., Jagiello, L., Fischer, W., Eckhart, R., and Bauer, W. (2016). Characterization of pulp fines and their technological properties. In: ACS National meeting Computers in Chemistry, San Diego, United States.

Oral Presentations

1. Jagiello, L. A. (2015). Implementierung eines Tube Flow Fraktionierers. 11. Minisymposium Verfahrenstechnik, 181-185
2. Jagiello, L.A. Novel approaches in fiber fines fractionation, European Doctoral Students (EDS) Summer Conference 2016, Arlanda, Sweden
3. Fischer, WJ., Schmiedt, R., Andreas, M., Jagiello, L. A., Mayr, M., Giner Tovar, R. et al (2016). Pulp fines - Investigating the smallest constituent parts of the paper network, 2nd EPNOE Junior Scientists Meeting, Sophia-Antipolis, France.

Posters

1. Jagiello, L.A., Fischer, W.J., Eckhart R., Bauer, W. (2016). Novel laboratory methods of fines separation and thickening, 2nd EPNOE Junior Scientists Meeting, Sophia-Antipolis, France.

2 Pulp fiber fractions

Wood - A versatile raw material
Wood is a very old material that has been used for thousands of years for fuel and tools. Wood is the hard and fibrous tissue of a tree that comprises the major part of stems, branches and roots. Its function in a living tree is the transport of water, providing mechanical support, storage of food and to produce secretions. The use of wood from trees, as timber, has become a versatile material with a multitude of uses. In converted forms such as plywood, particleboard or fiberboard, wood has become an important building material. Last but not least, wood is the basic material for pulp and paper, fibers, films, additives and many other materials.

2.1 Pulp sources

The observation of different wood species does not only show differences between softwood and hardwood, but also differences within one sample, such as sapwood, heartwood, growth rings, earlywood and latewood (see Figure 2-1).
The cells in wood are connected to each other with different openings, called pits, which are responsible for the transport of water and nutrients (Parham and Gray [1984]).
Softwoods are structured relatively simple as they consist of 90-95% tracheids, which are long cells with flattened closed edges. The tracheids are ordered in radial files and their longitudinal extension is oriented in the direction of the stem axes. The development from earlywood to latewoods shows a smaller cell diameter while the cell wall thickness increases. The change between earlywood and latewood is visible to the eye as an annual or growth ring.

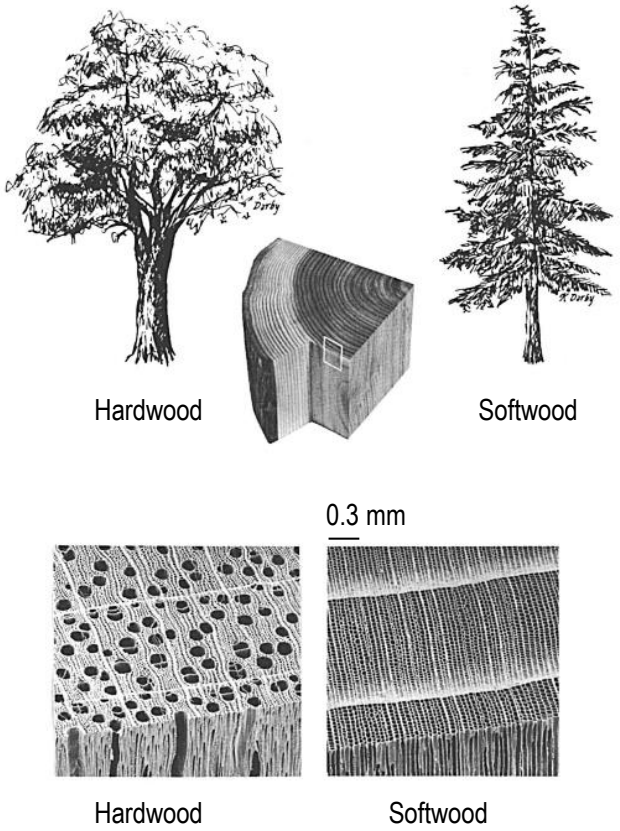

Figure 2-1 *Difference between softwood and hardwood. The wood tissue consists mainly of dead wood, that arrange a composite material of substantial viod volume (adapted from Parham and Gray [1984]).*

The latedwood tracheids, which show a thick wall provide strength, while the earlywood tracheids mainly conduct water and minerals within the tree. Several softwood species such as larch (*Larix spp.*), spruce (*Picea spp.*), pine (*Pinus spp.*) and Douglas fir (*Pseudotsuga menziesii*), also contain radially oriented tracheids associated to the ray parenchyma cells.
The transport and the storage of assimilates occur within the parenchyma cells, which exist in softwood predominantly as radially running rays. Epithelial cells surround the resin canals which are vertical and radial cavities within the tissue of softwoods (Fengel and Wegener [2003]).
Hardwoods consist of strength containing libriform fibers and fiber tracheids. Within this strengthening structure, vessel cells are embedded (see Figure 2-2). These vessel cells form long pipes reaching a maximum length of up to some meters and they are responsible for liquid transport in a hardwood tree. The dimensions of hardwood fibers are smaller than those of softwood tracheids. They consist of a smaller

lamellar but thicker cell wall and also the differences in wall thickness and lumen are smaller between earlywood and latewood as in softwoods.

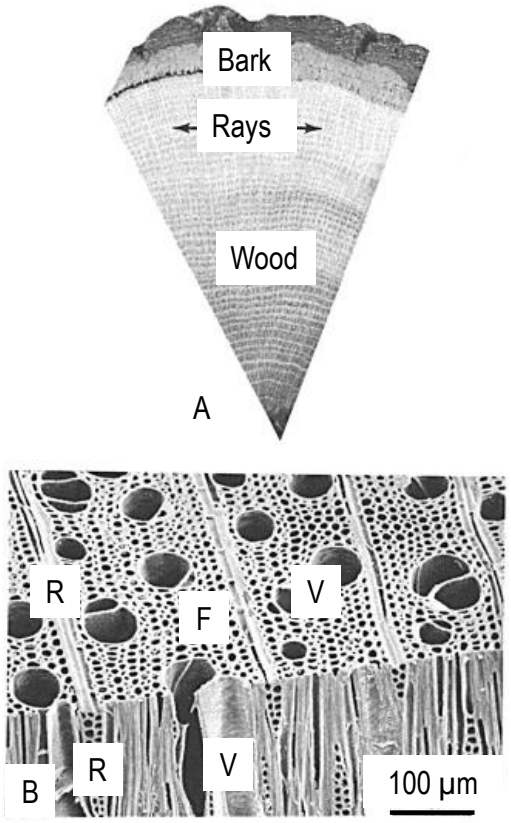

Figure 2-2 *(A) Wood ray cells located in the stem. (B) SEM picture of wood rays (R), vessels or pores (V), and wood fibers (F) of a maple tree (adapted from Parham and Gray [1984]).*

The parenchyma cells are short cells with chunky ends. There are a higher number of parenchyma cells in the hardwoods than in softwoods, which reveal a large number of longitudinal parenchyma. The wall thickness of the tracheids as well as the number and diameter of the vessels and the number of parenchyma cells determine the density of woods (Fengel and Wegener [2003]).

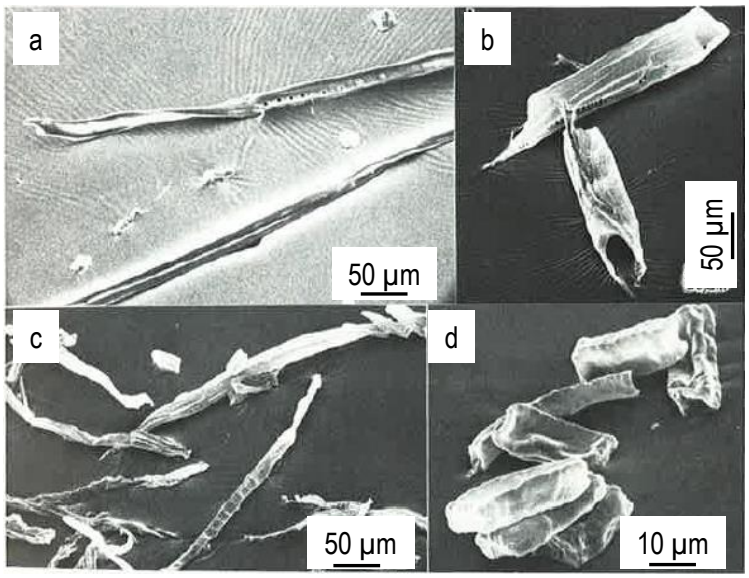

Figure 2-3 *SEM pictures of cells and fibers of softwood and hardwoods at the same level of magnification. (a) shows softwood trackeids, (b) hardwood vessel elements, (c) hardwood fibers and (d) hardwood parenchyma cells (adapted from Fengel and Wegener [2003]).*

2.2 Pulping

The production of pulp is the most important technique for the chemical conversion of wood and the principal reason for pulping is to liberate fibers from a wood matrix. In general, the pulping process can be divided into either chemical, mechanical or into a combined treatment (see Table 2-1). The chemical pulping process disintegrates wood chemically into fibers by cooking wood chips and converting the lignin in the middle lamella into a soluble form. Thus, fibers can be separated from each other without being destroyed. During the cooking process, lignin and hemicelluloses are dissolved or softened to some extent. Chemical pulp can either be produced by kraft (sulfate) or sulfite process (Sjöström [1993]). In the case of chemical pulp, the pulp has to be mechanically treated (refined) for most paper applications (Lönnberg [2009]).

The mechanical pulping process can be divided into grinding (pressing wood logs against a rotating grindstone) and refining, where wood chips are disintegrated with a disc refiner. The yield of mechanical pulping ranges typically between 93-97 % (PGW 98.5 %) for Norway spruce, while the yield from chemical pulp ranges from 35-65 % (Lönnberg [2009]). Norway spruce, aspen or radiata pine can be used for both pulping processes. Scots pine, eucalyptus and birch are preferably used for

chemical pulping (Fardim [2011]). In Table 2-1, the commercial pulp types available on the global market are presented.

Pulp type	Yield % of wood
(A) Chemical	35 - 65
Acid sulfite, Bisulfite, Multistage sulfite, Anthraquinone alkali sulfite, Kraft, Polysulphide-kraft, Prehydrolysis-kraft, Soda	
(B) Semichemical	70 - 85
NSSC, Green liquor, Soda	
(C) Chemimechanical	85 - 95
Chemithermomechanical (CTMP), Chemigroundwood (CGW)	
(D) Mechanical	93 - 97
Stone groundwood (SGW), Pressure groundwood (PGW), Refiner mechanical (RMP), Thermomechanical (TMP)	

Table 2-1 *Commercial pulp types (Sjöström [1993]).*

The main advantages in mechanical pulping are the low production costs (high yield) and the simple technology. Mechanical pulps have a higher light scattering coefficient, a fairly high brightness and good formation characteristics. The drawbacks of mechanical pulps compared to chemical pulps are the lower bonding ability of the fibers and this leads to lower strength properties. Mechanical pulps contain impurities and lignin which cannot be bleached to the same extent as chemical pulps, which results in a poorer brightness stability (Lönnberg [2009]).

2.3 Characteristics of chemical and mechanical pulps

2.3.1 Properties of alkaline pulps

The sulfate process or kraft process and the soda process are the two main alkaline pulping techniques and are also the basis for modified alkaline processes such as kraft pulping after a hydrolysis step for the production of dissolving pulp (Blom et al. [1981]). Sodium hydroxide is the main cooking chemical used in both processes, while in sulfate pulping sodium sulfide is an additional active pulping component. Both processes received their names from the regeneration chemicals which are used to compensate for the loss of sodium hydroxide, namely sodium carbonate and sodium sulfate. The chemical and the mechanical properties of alkaline pulps depend on the wood type and the pulping conditions. A basic factor for every chemical pulp is the chemical composition, which also affects the pulp yield, strength properties and color. The character of a pulp can be determined by the degree of delignification or

of the polysaccharide reactions in alkaline medium. The criterium for the field of application is defined by the kappa number, which is an expression for the amount of residual lignin. Alkaline pulps usually have a dark color or low brightness, which is caused by the chromophoric groups in the residual lignin which is formed during the alkaline cooking process.
The main characteristics of kraft pulps are their excellent strength properties. They are preferably used for pulps in strong paper grades, such as the kraft liner in corrugating boards, or bag and wrapping papers. Superior strength values can be reached by kraft softwood pulps due to the characteristics of softwood fibers. Short-fiber hardwoods cannot reach the requirements in strength properties for linerboard grades and therefore in these grades only small amount of hardwood kraft fibers are mixed with softwood pulp. Required strength properties can be reached by adding softwood kraft pulps or sulfite pulps (Fengel and Wegener [2003]).

2.3.2 Properties of sulfite pulps

Sulfite offers a wide variety of chemical composition and papermaking properties regarding to opacity and strength values due to the different production processes. In the NSSC process (Neutral Sulfite Semi Chemical), the residual lignin content reaches 10-15% , but is generally in the range of 3-5% for softwood and 1-3% in hardwood pulps (Fengel and Wegener [2003]). The acidic processes are preferred for the production of dissolved pulps based on hardwoods with high alpha-cellulose contents above 90 %. Hardwood sulfite pulps show very low strength properties and are used mainly for high opacity printing papers. Magnefite softwood and hardwood pulps can be used for very different paper grades such as printing, writing and base paper for coating as well as newsprint, partly used to replace sulfate pulp (Stark and Eichinger [1979]). The brightness values of unbleached sulfite pulps are generally higher than for kraft pulps, even at high yields. Typical sulfite pulps can be beaten more easily with lower refining energy than kraft pulps to reach the maximum tensile strength (Fengel and Wegener [2003]).
Table 2-2 shows the strength values of sulfite pulp which are principally lower than those of kraft pulps. Only the alkaline sulfite pulps attain the strength properties of kraft pulps.

	Yield %	Beating time min	Tensile m	Burst index kPa*m2/g	Tear index mN*m2/g
Bisulfite - neutral sulfite	48.5	18	11400	7.26	10.2
Bisulfite - acidic sulfite	49.8	26	10000	6.38	11.8
Neutral sulfite - acidic sulfite	54.8	7	9000	5.00	7.35
Bisulfite	50.8	15	10400	6.38	9.22
Kraft	45.5	34	12900	9.81	13.7
Strength properties at 500 ml CSF					

Table 2-2 *Comparison of alkaline sulfite pulp and kraft pulp (adapted from Fengel and Wegener [2003]).*

2.3.3 Properties of mechanical pulps

Mechanical pulps show a superior opacity and light scattering compared to chemical pulps, primarily due to the special properties of mechanical pulp fines. In a mechanical pulp fraction, the long and intact fibers can be less than 20% (by weight) for groundwood and 40% for thermomechanical pulp (TMP), while in the chemical pulp the long fiber fraction can be as high as 90% (Niskanen [2008]). In Figure 2-4, the light scattering and the tear strength versus the freeness of various pulp types are shown. Mechanical pulps show a superior light-scattering coefficient compared to chemical pulps. For chemical pulps, the tear index is higher than for mechanical pulps, except chemithermomechanical pulp (CTMP).
In general, chemical pulps have a higher tear index but a lower light-scattering coefficient than mechanical pulps. There are differences in tear index between softwood and hardwood, the former has a higher tear index but a lower light scattering coefficient. Mechanical pulps such as stone groundwood (SGW) and pressure groundwood (PGW) have the highest light-scattering ability but also the lowest tear index. For refiner pulps such as CTMP or TMP, the opposite is true.

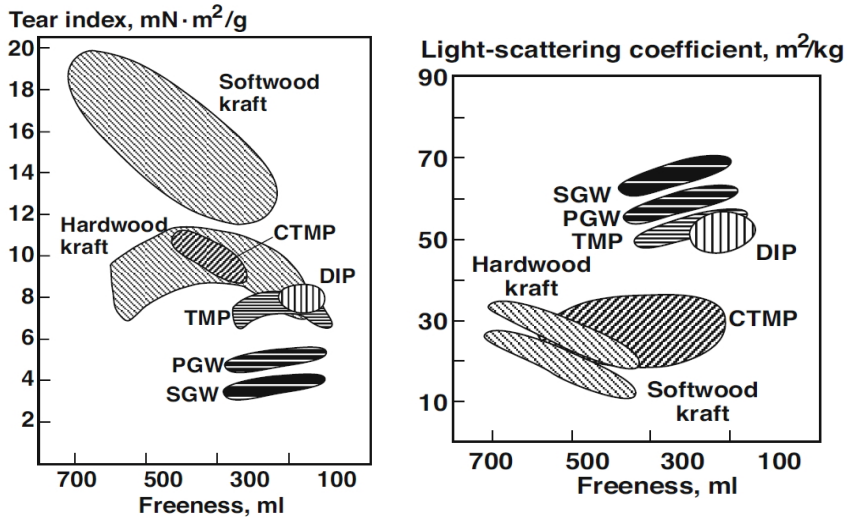

(a) Light-scattering ability of various chemical pulps and mechanical pulps based on a Norway Spruce

(b) Tear strength of various chemical pulps and mechanical pulps based on a Norway Spruce

Figure 2-4 *Light scattering and the tear strength versus the freeness of various pulp types (adapted from Sundholm [1999]).*

Table 2-3 and 2-4 show the main differences between chemical and mechanical pulps. Almost all properties differ between these two pulp types. The lignin content for mechanical pulps is approximately 30 % and almost zero in bleached kraft pulps. Due to the low lignin content of kraft pulp fibers, the wet fiber conformability and swelling ability is higher than for mechanical pulp fibers. In chemical pulps, the content of lignin and hemicelluloses is smaller than for mechanical pulps and therefore the chemical pulps have a lower pulping yield.

Property	Chemical pulps	Mechanical pulps
Yield on wood	Low	High
Amount of lignin	Low	High
Amount of hemicelluloses	Low	High
Fines content	Low	High
Degree of polymerization	High	High in cellulose
Charge in water suspension	Less anionic	More anionic
Water affinity	More hydrophilic	More hydrophobic
Long fibers per unit mass	Many	Few
Specific surface area	Small	Large

Table 2-3 *Differences between the properties of chemical pulps and mechanical pulps from softwoods (adapted from Niskanen [2008]).*

During the mechanical pulping process, fiber fragments and other small particles called fines are generated. In chemical pulps, fines include ray cells and parenchyma cells in addition to particles originating from the fiber wall. Typically, 30 % by weight of mechanical pulp and less than 10 % of chemical pulp qualifies as fines. The properties of fines will be examined in section 2.5. Mechanical pulp can be used directly, but it often undergoes bleaching. Chemical pulp is also bleached in most cases. The main use of unbleached pulps is in packaging boards and papers. Further, chemical pulp is usually processed to optimize its contribution to the mechanical properties of paper. Due to beating of chemical pulps, the pulp loosens its structure of the fiber wall (internal fibrillation) and surface (external fibrillation). Mechanical pulping produced similar effects.

Property	Chemical pulps	Mechanical pulps
Fines:		
Structure	Fibrillar	Lamellar
Bonding ability	Excellent	Good
Fibers:		
Structure	Slender, curly, kinky	Stiff, coarse, straight
Shape	Long and narrow	Short and wide
Bending stiffness	Low	High
Degree of collapse	More collapsed	Less collapsed

Table 2-4 *Main differences between the properties of mechanical and chemical pulp fibers and fines from softwoods (adapted from Niskanen [2008]).*

2.4 Fibers

Pulps mainly consist of fibers and fines. The structure of paper is primarily defined by the fibers and they are the principal structural element of paper. In addition to fibers, fines and inorganic fillers are the most typical particles in the papermaking process (Niskanen [2008]).

In general, fibers are plant cells that have a high length-to-width ratio, approximately 50-100. The average fiber length ranges between 0.8 to 7.9 mm and the fiber width from 14-65 µm. Hardwood fibers are thinner and shorter than softwood fibers. The volume fraction of fibers in wood vary between softwoods and hardwoods. 89-95 % fibers in wood for softwoods and 37-65 % for hardwoods (Ilvessalo-Pfäffli [1995]).

Detailed description of wood fibers

The concentric arrangements of cell wall layers is caused by the differences in the chemical composition and by different orientations of the structural elements. The components of cell walls must be subdivided into a structural component, i.e. cellulose, and into sub-structural, blurring components, i.e. polyoses and lignin. When the polyoses and the lignin get removed from the cell walls, the texture of the cellulosic elements called fibrils, is visible (see Figure 2-5).
Between the individual cells, a thin layer called middle lamella glues the cells together. The middle lamella is in principle free of cellulose, though single fibrils may cross this middle lamella. The transition from the middle lamella to the adjacent cells is not very clear and therefore the term compound middle lamella is used.
The primary wall consists of cellulose fibrils which are arranged in this crossing layers. Nevertheless the amount of cellulose in the primary wall is rather low. The orientation of the fibrils in the outermost lamella is more oblique. The subsequent wall layer is the secondary wall 1 (S1). In this wall layer the fibrils are arranged in a gentle helical slope and the S1 layer is mostly amorphous. There are several lamellae with counter-running helices, which can be observed as a crossed system, if they are very thin.
The secondary wall 2 (S2) is the thickest wall layer, where the fibrils run at a steep angle. Changes in the angle and differences in the packing of these fibrils results in a lamellar structure of the S2. Several studies determined the angle and the winding direction of the fibrils in the S2 in order to demonstrate the variability and to find a correlation between cell size and development. The S2 layer consists of crystalline cellulosic chains on a microstructural level.
A third secondary wall layer (secondary wall 3, S3) occurs in parenchyma cells. It is a very thin and amorphous layer (thinner than approx. 0.1 µm) that protects the fiber from bacterial attack through the lumen, which is the hollow part inside the fiber. Fibers of monocotyledones, e.g. bamboo, may have four or more secondary wall layers. The last fibrillar layer at the luminar border is defined as the tertiary wall (T). It is different to the S3 of the parenchyma cells (see Figure 2-5) and to other secondary wall layers. Figure 2-5 gives a description of the cell wall structure and the constituents of a fiber (Fengel and Wegener [2003]).

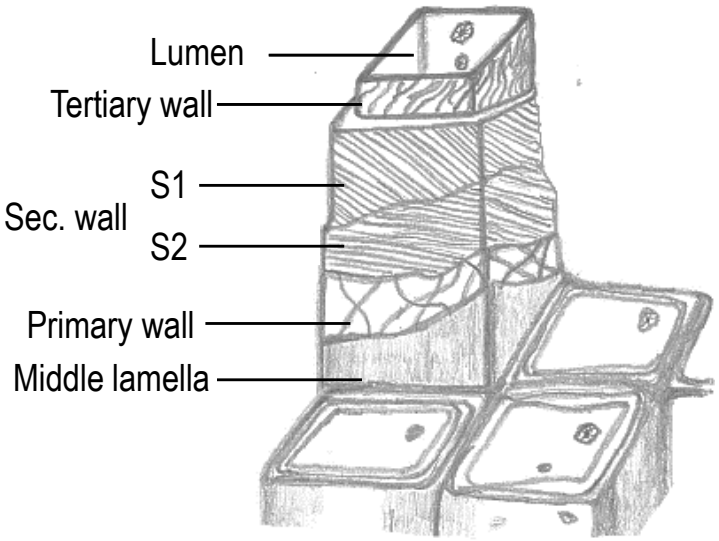

(a)

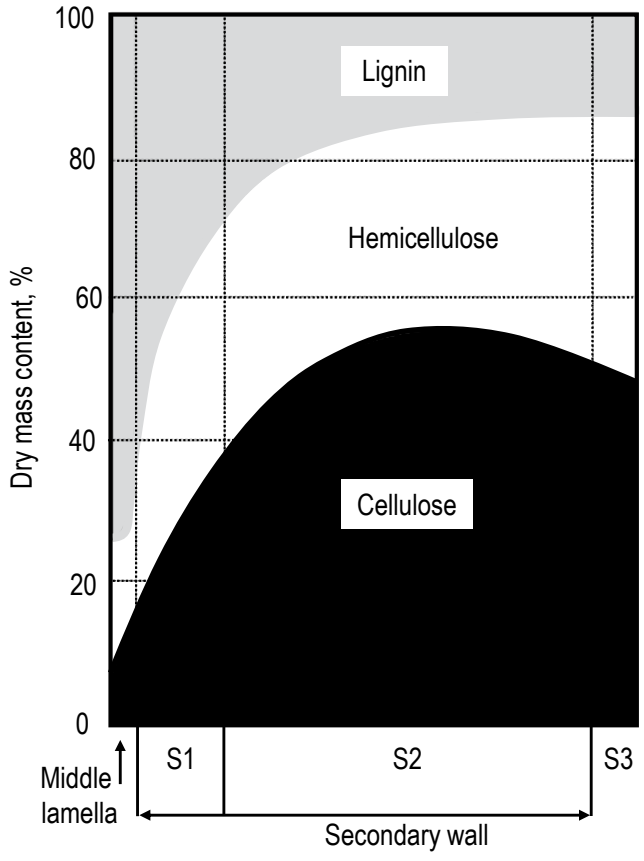

(b)

Figure 2-5 *Overview of the cell wall structure of a wood fiber (conifer tracheid), middle lamella (ML), primary wall (P), secondary wall 1 (S1), secondary wall 2 (S2), secondary wall 3 (S3) (adapted from Niskanen [2008] and (b) Cellulose, hemicellulose and lignin distribution in a cell wall of conifers (adapted from Kellomäki [2009]).*

In Table 2-5 and Table 2-6, the data for the thickness of different wall layers of sprucewoods tracheids and cells of beechwood are compiled.

Wall layer	Earlywood		Latewood	
	µm	%	µm	%
P M/2	0.09	4.3	0.09	2.1
S 1	0.26	12.4	0.38	8.8
S 2	1.66	79.0	3.69	85.8
T	0.09	4.3	0.14	3.3
Total wall	2.10		4.30	

Table 2-5 *Average thickness and percentage of the wall layers in spruce tracheids (adapted from Fengel and Wegener [2003]).*

Wall	Vessels		Libriform fibers		Fiber tracheids		Longitud. parench.		Ray parench.	
	µm	%	µm	%	µm	%	µm	%	µm	%
P	0.25	25	0.07	1	0.07	5	0.06	4		
S 1	0.25	25	0.51	10	0.24	16	0.35	21	0.50	27
S 2	0.50	50	4.32	87	0.99	67	0.78	48	0.92	50
S 3	-	-	-	-	-	-	0.37	22	0.37	20
T	0.25	25	0.10	2	0.17	12	0.09	5	0.07	3
Total wall	1.00		5.00		1.47		1.65		1.86	

Table 2-6 *Average thickness and percentage of the wall layers in beech wood cells (adapted from Fengel and Wegener [2003]).*

In general, the wall thickness varies depending on different tree species, cell type, season of growth and other factors (Lönnberg [2009]). Fiber properties are important in papermaking because:

- they affect paper structure in terms of formation and strengthening
- they are relevant for the properties of both wet and dry paper

2.5 Fines in pulp

In the following chapters, discussions about fines properties are to a large extent based on the review paper by Obadas et al. [2016].
Every pulp consists of fibers of various length and other wood tissue elements and fragments. The size of these particles ranges from a few millimeters (1-5 mm) for the largest dimension of fibers down to colloidal wood resin of 0.1-1 µm (Nylund et al. [1993], Swerin et al. [1993]). The smallest particles in a pulp are called "fines". They are defined as those particles of a fiber suspension that can pass through a

screen with a certain whole size. In general, the official standard suggests to separate fines from the long fiber fraction using a metal screen with round holes of 76 µm diameter (SCAN-CM 66:05 (2005), TAPPI T 233 cm-95). The Bauer McNett fractionator is the most commonly used device for separation of the fines fraction, which is equipped with a 200 mesh screen (200 wires per inch): therefore the term P200 is often used.

Several researchers used different definitions and screens (e.g. experiments are carried out using a P100 (De Silveira et al. [1996], Paavilainen [1990], Sundberg et al. [2000], Lindqvist et al. [2012]) (fraction received by screening with a 100 mesh screen) fraction or through a 20 µm diameter hole screen (Chen et al. [2009]) or a wire plate having an equivalent hole diameter (Lindqvist et al. [2011])). Therefore the term "fines" is not always a defined class of particles.

The general physical description of fines depends on several different specimen such as on the kind of pulp, where the fines fraction can include short fibers, fiber and fiber wall fragments and also cells of other types (Heijnesson et al. [1995b]). Fines differ from dissolved colloidal substances (DCS) which also pass through a 200 mesh wire on the one hand (i.e. retained on filter paper(SCAN-CM 66:05 (2005))) and on the other hand some of these particles are visible under a light microscope (Luukko [1998]), but the distinction is still unclear (Mosbye [2003]). Inorganic pigments, fillers, latex, salt crystals, and precipitates that are present in the papermaking process of a later process stage and also pass through a 200 mesh screen are not considered to be fines (Taipale et al. [2010]).

Fines can be obtained from mechanical as well as from chemical pulps. In mechanical pulp, the fraction of fines makes up to 20-40 % of the pulp by weight (Luukko [1998], Retulainen et al. [1993]) and is essential for the mechanical properties of the resulting paper. The fines from mechanical pulps are usually divided into fibrillar and non-fibrillar material, which originate from the early definition of Brecht and Holl [1939].

In chemical pulps fines contents are much lower, with the contents ranging from less than 1 % to about 15 % (Retulainen et al. [2002], Bäckström et al. [2008]). The interactions of fines with other components within a pulp suspension are important for the optimization of the final product quality and the dosage of additives. Table 2-7 gives an overview about the classification of fines. The differences between chemical pulp fines and mechanical pulp fines are clarified in the following chapters.

Fines type -	Origin -	Morphology -	Content %	Size µm
Mechanical fiber fines	TMP, GW	Fibrils, flakes, ray-cells, etc	10-40	Fibril length:<200 width:0.2-10 Lamellas:<20 Flour stuff: 20-300 (Marton 1964)
Primary fiber fines	Unbeaten chem. pulp	Ray-cells, lignin flakes from middle lamella	2-10	Softwood ray cells (Alén 2000) length: 10-160 width: 2-50
Secondary fiber fines	Beaten chem. pulp	Fibrils peeled off from cell wall	2-10	
Tertiary fines	DIP, broke from mill	Fiber fines, fillers coating pigments, latexes, additves, stickies, etc.	variable	variable
DCS	Wood	Very fine dispersion, which may form larger agglomerates	From spruce: 1-2	0.1-2 Nylund (1997)
Fillers	Filler addition, paper additives	Clay, calcium carbonate, talc, etc.	0-40	0.1-10

Table 2-7 *Overview about the classification of fines (adapted from Krogerus et al. [2002]).*

2.5.1 Origin of fines

When fibers are isolated from the wood matrix and are processed into a final product, smaller particles called fines are generated. The first stage in the pulping process where fines occur is where wood is chipped, but this debris is mainly removed before pulping by different screening equipments.
The definition primary fines and secondary fines is usually used for chemical pulps. Primary fines arise during the cooking process, whereas secondary fines are generated in any further development of the fiber, such as during refining (Retulainen et al. [1993], Luukko [1998]).

Fines from the mechanical pulping process

In mechanical pulping, two main types of pulping can be distinguished: the first one is the groundwood process, where debarked wood logs are pressed against a revolving grinding stone. In the other process, which is called refining, wood chips are refined

between rotating discs. Thermo-mechanical pulping (TMP), is today the most common refining process, where steam pretreatment of wood chips is implemented. In "chemithermomechanical" pulping (CTMP), lignin softening agents are used in the pretreatment stage of the woods chips. In all mechanical pulping processes, a considerable high amount of fines is produced. The lowest weight fraction of fines arises in CTMP pulping, with 20 % fines, 30 % of fines for the TMP process and 30-40 % for the groundwood pulping process. (Ek et al. [2009], Lindholm [1980]).
In the TMP process, the amount of fines can be controlled by the specific energy consumption. In this case, the amount of fines increases with an increase in specific energy consumption. In the case of groundwood pulp, the wood species affects the fines content (Miles and Karnis [1991]).

Fines from the chemical pulping process

In the chemical pulping process, during cooking, intact cells are isolated from the wood tissue and therefore just a few primary fines are generated. The obtained fines fraction consists primarily of ray cells that are liberated during cooking and hardly any fiber fragments can be found (Westermark and Capretti [1988]). Due to the more complex structure of hardwood, these species contain more primary fines than those from softwood.
During subsequent mechanical processing, further chemical pulp fines are generated (secondary fines). The difference in bonding ability of different pulp types is small (Yin et al. [2013], Chen et al. [2009]).
In case of beating, the main effect is the release of fines. During refining, where internal and external fibrillation as well as cutting of fibers and deformation takes places, fiber fragments are released (Ek et al. [2009]). and most of the secondary fines are generated (Yin et al. [2013]).

2.5.2 Morphology of fines

The morphology of fines is related to the ultrastructure of wood (see Figure 2-6). The obtained fines fraction from different pulp types may include short fibers, fiber and fiber wall fragments, fibrillar material from the secondary wall, and parts from the middle lamella. Parts of the conducting system which consists of complete or broken vessels, ray cells and other parenchyma cells of a tree tissue are also found in fines fractions (Paavilainen [1990], Sundberg et al. [2003]).

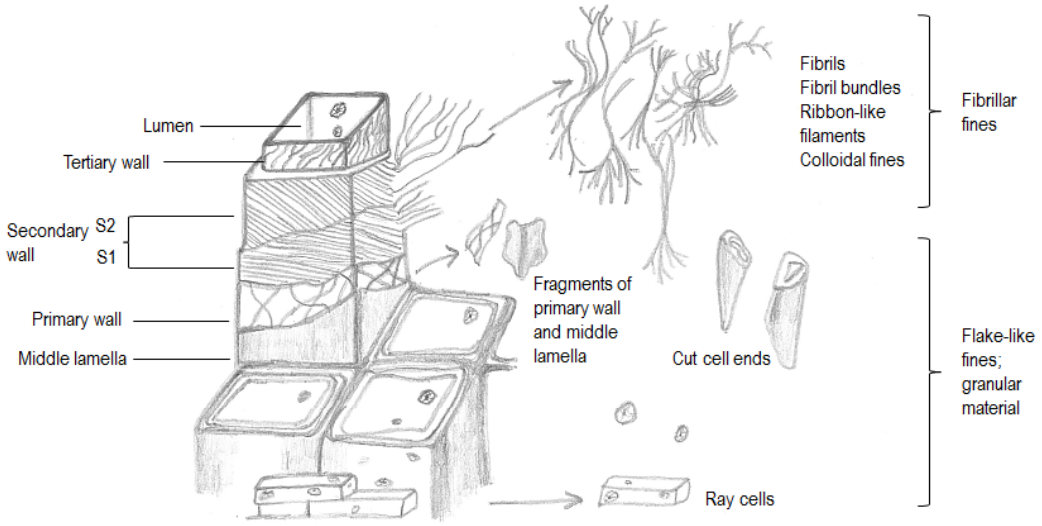

Figure 2-6 *Morphology of fines derived from different structures (adapted from Rundlöf [2002]).*

In case of mechanical pulp, Brecht and Holl [1939] distinguished fines in their fundamental work between non-swollen wood meal and swollen fibrils that were isolated from groundwood pulps with low and high strength.
In terms of the characterization of a fines fraction, the method using the content of fibrilar fines is often used for mechanical pulps which is also an index for their bonding ability (Forgacs [1963]).
Groundwood fines are more difficult to classify than TMP, because they include also a fraction of lamellae, which originate from the secondary cell wall, which has swelling abilities similar to fibrillar material. The groundwood fines fraction also consists of non-swollen wood meal which consists of stiff and compact flake-like particles from the fiber wall, middle lamella as well as ray cells (Mohlin [1977]).
Fines from groundwood pulp have a width distribution between 0.01 and 30 µm diameter (Ruck-Florjancic and Ruck [1961]) with a peak at 0.6 µm and the filamentous fines originating from the TMP process show a similar width distribution with a pronounced peak at 0.3 µm diameter (Gavelin et al. [1975]).
Mechanical pulps can also contain colloidal particles, sometime they are called microfines. These particles have no sedimentation ability and cause therefore turbidity in the water phase (Nylund et al. [1993]). In addition, the morphology of mechanical pulp fines depends strongly on the pulping process, where a higher energy input leads to higher fibril content and to thinner particles - i.e. string-like particles (for low-consistency refining) (Hafrén et al. [2014]). Due to their differences in shape, mechanical pulp fines have a large specific surface area. Different measurement methods determined a specific area of 13 m^2/g for fines from groundwood pulp (Wood and

Karnis [1996]) and 12 m^2/g for bleached CTMP pulp fines (Li et al. [2002]) (turbidity measurements) and 12-14 m^2/g calculated from microscopic images of TMP fines.

In Figure 2-7, the different appearance of fines from mechanical and chemical pulp is shown. Regarding the shape of chemical pulp fines, it can be observed that they consist mostly of rigid, rectangular ray cells (primary fines) (Westermark and Capretti [1988]). Secondary fines include sheet-like fiber wall fragments and fibrillar material generated by shear stress during the beating process. In addition, granular fragments originating from thick-walled summerwood fibers of softwood kraft pulp are generated at high beating levels (Paavilainen [1990]).

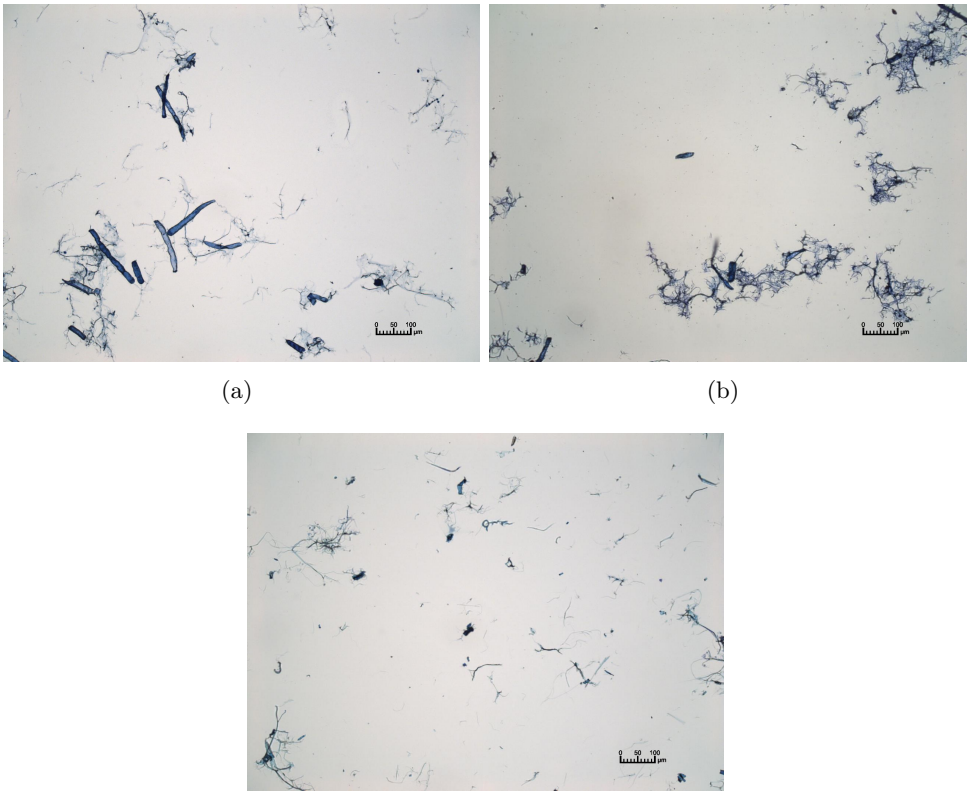

(a) (b)

(c)

Figure 2-7 *(a) Images of primary fines of chemical pulp, (b) primary and secondary fines of chemical pulp and (c) fines from groundwood (M. Mayr, personal communication, February 1^{th}, 2017).*

Compared to micro-fines of mechanical pulp, secondary fines of chemical pulps additionally show a fraction of colloidal fiber wall fragments (Kibblewhite [1975]). The specific surface area of chemical pulp fines was measured in different ways. For instance, the specific surface area of a bleached chemical pulp which was beaten to a

medium degree show a hydrodynamic surface area of the fines fraction of 8 m^2/g and and that of the fiber fraction only 1 m^2/g.
Taipale et al. [2011] determined the outer surface area of the fines fractions of different pulps by turbidity measurements where the resulting values were 6.8 and 4.4 m2/g for fines from kraft pulp analyzed before and after bleaching, respectively.

2.5.3 Chemical characterization of fines

In general, the properties of fines in a pulp suspension largely depend on the type of pulp but their chemical composition deviates from the full pulp and within one pulp, the morphological properties of fines can vary to a certain extent. Fines show lower cellulose content compared to long fibers. The reason for this phenomena can be explained by the ultrastructure of wood. In Figure 2-6, different cell wall structures of the tracheid are shown. The primary wall consists of less cellulose but of high amount of hemicellulose, pectic material and also lignin (Westermark et al. [1986]). However, a large proportion of a fiber is composed of the secondary cell wall, which consists of cellulose-rich material. Together with the tertiary cell wall, it contains almost 90 % of the total cellulose and more than 60 % of total lignin (at 27 % lignin concentration). The lignin concentration in the S1 layer is above 60 % and the proportion of non-cellulosic polysaccharides (hemicelluloses such as xylan and mannans) is equal to that of cellulose (Fengel [1969], Fengel [1970]). These specifications refer only to the composition of mechanical pulp fines.
Further, the content of lignin, hemicellulose and extractives of fines is higher than for long fibers. For instant, for an unbleached TMP pulp at 95 % yield, the components of wood are equal to those found in the mechanical pulp source, except for galactoglucomannan, which is a water-soluble component and gets removed from the pulp to a certain extent. In contrast to the fiber fraction, the overall content of cellulose is lower for the fines fraction (Sundberg et al. [2003], Ek et al. [2009]). There is also a higher cellulose content in fibrillar fines compared to flake-like fines, which can be related to the part of the fiber wall they originate from.
In case of chemical pulp fines, the chemical composition of fines is totally different, depending on the pulping process. Here, lignin and non-cellulosic polysaccharides are removed to a large extent.
Their composition can be compared to mechanical pulp fines, having less cellulose, more lignin and extractives and more xylan than the long fiber fraction (Retulainen et al. [2002], Asikainen et al. [2010a], Liitiä et al. [2001]). Their total charge is higher and they have also more carboxyl groups and metal ions (Retulainen et al. [2002], Heijnesson et al. [1995a], Asikainen et al. [2010a]).
Compared to mechanical pulps, where spruce and pine are the predominant species

for pulping, some hardwoods such as beech, birch and eucalyptus are widely used in chemical pulping. Hardwoods contain 40 % cellulose, which is similar to softwoods, but their predominant hemicelluloses are xylans and therefore a lot more xylan is found in hardwoods than in softwoods, but less arabinose, galactose and mannose (Willför et al. [2005b], Willför et al. [2005a]). Further, these differences affect the composition of the chemical pulp fines fraction as well. The relative carbohydrate composition of the fines fraction is different to the that of long fibers (Lindström and Glad-Nordmark [1978]). Therefore, a hardwood kraft pulp showed that primary fines contain less glucose but higher levels of arabinose, xylose, and galactose compared to the long fiber fraction. Secondary fines from hardwoods are closer to primary fines than to the full pulp when looking at lignin and extractives content, but their carbohydrate composition differs from the bulk pulp (Bäckström et al. [2008], Lindström and Glad-Nordmark [1978]).

Lignin and extractives

In general, the lignin content of mechanical pulp fines (mixture of all types of fines) depends mainly on their type and reaches maximum values of up to 40 %. Ray cells show a particularly high lignin content compared to other types of fines (Westermark and Capretti [1988], Sundberg et al. [2003], Sundberg and Holmbom [2004], Kleen et al. [2003]). In contrast, the overall lignin content of a mechanical pulp contains about 27 % of lignin. Although flake-like fines and fibrillar fines have similar bulk concentrations of lignin, the extent to which the lignin is located at the surface of these particles depends on the type of fines. The surface coverage of lignin is higher for flakes (54 %) and lower for fibrillar fines with about 40 % of total coverage. The content of coverage decreases the lower the fiber wall structure is they originate from (Mosbye et al. [2003]).

Unbleached sulfite pulp fines show a higher lignin content than the respective long fiber fraction, both for softwood and hardwood (Richter [1941]). For an unbleached spruce kraft pulp, again, the fines contain more lignin than the long fiber fraction. Large parts of the fines surface are covered with lignin (Lindström and Glad-Nordmark [1978], Thalib and Hultén [2006]).

Primary fines from unbleached softwood kraft pulp show a higher lignin content than secondary fines, but the differences are less notable.

The change in chemical composition of fines (chemical pulp) and long fibers (chemical pulp) depends on the processing conditions, where the lignin content decreases the more surface material is removed (lignin gradient over the fiber surface) (Heijnesson et al. [1995b]).

In kraft pulps, there are strong interactions between cellulose and the remaining

lignin. In case of the primary fines fraction, the degree of condensation of lignin is higher than for the long fiber fraction (Liitiä et al. [2001]).

Extractives

The general definition of extractives stands for "matter extractible with a given organic solvent". In several laboratory investigations, scientists have extracted their samples before studying the chemical composition of fines, using different solvents. Wood resin is composed of fatty acids and their derivatives as well as of terpenes and terpenoids, and many more components (Fengel and Wegener [1984]). Depending on process conditions such as pH, ionicity and concentration, colloidal material may adsorb onto fibers and fines (Mosbye [2003]).
In general, fines, especially flake-like fines and ray cells (from chemical pulps), are covered by more extractives than long fibers (Thalib and Hultén [2006]).
The high extractives content of chemical pulp fines was discovered early and suggested removal of the fines fraction to reduce the extractives content was suggested by Richter [1941].
In general, hardwood and softwood may contain similar amounts of extractives, but the composition differs (Fengel and Wegener [1984]). In softwoods, more than half of the resin in softwood is composed of resin acids and free fatty acids. This fraction is very small for hardwoods. In hardwoods, the resins consist mostly of esterified fatty acids, sterols, steryl esters, and other neutral components (Björklund and Nilvebrant [2009], Bergelin and Holmbom [2008]).

Charge

Fibers and fines from wood are generally negatively charged. In wood and as well in mechanical pulp fibers, the carboxyl groups of uronic acid occur most frequently (Willför et al. [2005b]). The total charge of any type of fines fraction is higher than that of the bulk pulp. Fibrillar mechanical pulp fines are more negatively charged than the respective fibers. In the case of flake-like fines, both bleached TMP and CTMP are more than twice as rich in anionic groups than unbleached TMP (Sundberg and Holmbom [2004]).
In case of chemical pulp fines, the anionicity is higher than for the long fiber fraction (Li et al. [2002], Heijnesson et al. [1995a]). It has been shown that fines from a bleached kraft pulp have 150 % higher total charge than the long fiber fraction. In addition, the specific surface charge was ten times higher for fines before beating and 17 times higher after (Wågberg and Björklund [1993]). Fines from kraft pulps

show a higher content in metal ions, such as copper, iron, magnesium, manganese and calcium than long fibers (Bäckström et al. [2008], Heijnesson et al. [1995a]).

2.6 Technological properties of fines

The content of fines in a certain pulp has a big influence on the product properties as well as in the production process. In general, fines cause a higher sheet density and improved bonding and therefore better wet and dry strength but they have also a negative impact on bleachability and they impair drainage (Paavilainen [1990], Rundlöf [2002]).

2.6.1 Influence on product quality

In general, the fiber to fines ratio can be a determining factor for many paper properties. The wet strength of a mixture of fibers and fines is higher than for long fibers alone and for a mixture of fibrillar fines and fibers it is a lot higher than for fibers only. It has been observed that there is an increase in wet strength, if the structure of fibers and fines matches - i.e. if wood meal is mixed with hard, rigid fibers and fibrillar fines are added to flexible fibers (Brecht and Klemm [1952]).
By adding of fibril-rich fines into a pulp suspension, an increase of the tensile index and sheet density of a paper sheet can be observed to a higher extent than for the same amount of flake-like fines from TMP.
The principle effect of fines in a fiber network with respect to mechanical properties is that they densify the paper sheet. They increase the number of inter-fiber bonds which is the essential factor for sheet strength besides the strength of single fibers.
In case of a chemical pulp, primary fines and secondary fines improve the strength properties of paper, but the effects are more pronounced for secondary fines (Bäckström et al. [2008], Hawes and Doshi [1986]). Figure 2-8 shows exemplary relations between mechanical properties and the fines content.
In Table 2-8, a summary of the effect of fines on pulp and paper properties with explanatory comments on the observed limitations is given (Retulainen et al. [1993]).
A sheet of paper should be bright and opaque. A model to describe the properties of brightness and opacity mathematically was introduced by Kubelka and Munk. This model depends on the light absorption coefficient and on the light scattering coefficient (Lübbe [2013]). Mechanical pulp fines show a three to four times higher light absorption coefficient than the long fiber fraction (Lindholm [1980]).
Previous studies have shown that only flake-like fines improve the light scattering, especially the smaller ones. They also mention that the increase in the light scattering coefficient of pulp is dominated by the ratio of fibrillar to flake-like fines (Luukko

and Paulapuro [1999]).

Property	Effect	Comments
Drainage time	++	
Sheet density	++	
Air permeability	–	
Wet web strength	+	There is a maximum, beyond it, more fines decrease the property value
Tensile strength	+	No increase if fibril content very low
Tear strength	+/-	There is a maximum, beyond it, more fines decrease the property value. Maximum at very low fines content
Breaking length	+	No increase if fibril content low
Specific bond strength	+	No increase if fibril content low
Compression strength	+	
Folding endurance	+	There is a maximum: beyond it, more fines decrease the property value
Tensile stiffness	+	
Shrinkage potential	+	
Light scattering		
Chemical pulp fines	(-)	The value decreases or stagnates
Mechanical pulp fines	++	
Bleachability	-	
Linting	-	

Table 2-8 *The effect of fines on pulp and paper properties (adapted from Retulainen et al. [1993])).*

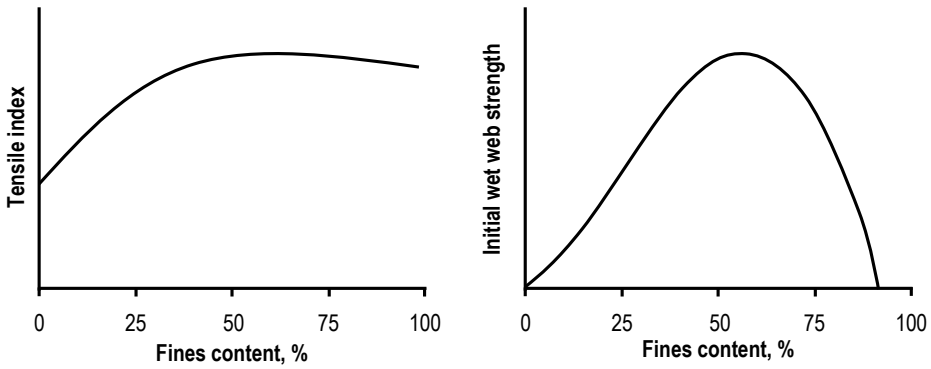

(a) (b)

Figure 2-8 *Non linear correlations between mechanical properties of paper and fines. (b) Tensile index versus fines content for a mechanical pulp and initial web strength versus fines content for a groundwood pulp (adapted from Obadas et al. [2016]).*

2.6.2 Effect on the papermaking process

Due to their small size and high surface area, fines strongly affect the speed of dewatering of newly formed paper which can be a limiting factor in paper machine productivity (Hubbe [2002]). Any type of fines increase the dewatering resistance in a paper sheet, even more with decreasing particle size (Paavilainen [1990], Lindholm [1980], Hubbe [2002]). The dewatering resistance can be determined by the Kozeny-Carman equation, which describes the flow through a bed of granulates. In this equation, the permeability of a certain bed is proportional to the reciprocal of the square of the specific surface area per volume of its particles. In other words, at an increased particle surface, the liquid gets hindered to flow through the bed they form. Smaller particles of identical shape enhance the resistance of pulp to dewatering. The Kozeny-Carman equation does not implicate the shape of particles. Another model called the choke point model describes, that fines are transported with the flow through the fiber network to a certain point where they got stuck in a narrow opening (Hubbe [2002]). Laboratory experiments proved that both primary fines and secondary fines increase the dewatering time. For secondary fines, the correlation between dewatering time and fines content is exponential (Cole et al. [2008]). This correlation is presented in Figure 2-9.
Fines have a high swelling ability due to their large specific surface area, surface charge and amount of amorphous cellulose (Paavilainen [1990]). The overall swelling of a pulp is defined by the water retention value. It is the extent to which water remains in fibrous material after centrifugation (SCAN [2000]). Chemical pulp fibers retain more water than mechanical fibers. In case of mechanical pulp fines, there is a relation between fibril content and swelling ability.

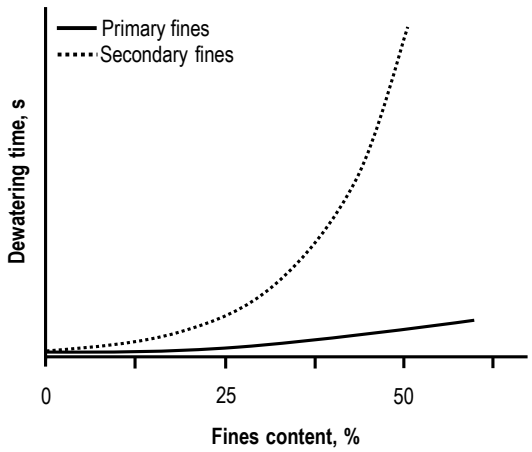

Figure 2-9 *Correlation between fines content and dewatering time for primary and secondary fines (adapted from Cole et al. [2008]).*

Primary fines of chemical pulps decelerate the dewatering of pulp suspensions, but up to 20 % they have a minor influence. On the other hand, secondary fines have a greater effect on the dewatering behavior of a pulp suspension. They inhibit the dewatering to a remarkable extent if they make up just 5 % of the pulp (see Figure 2-9 (Cole et al. [2008]). It has been shown that fines from CTMP affect the drainage more strongly than secondary fines from kraft pulp at the same level of addition. CTMP fines contain a larger number of small particles than fines from chemical pulp and therefore the dewatering time is higher, which can be attributed to the choke point effect (Chen et al. [2009]).
Due to their high surface area, higher contents of metal ions, lignin and extractives, fines consume more bleaching chemicals than the associated fiber fraction. In case of peroxide bleaching, both groundwood pulp and TMP show a less effective bleachability the higher the concentration of fines is. This drawback is compensated by better light scattering (Karlsson and Agnemo [2010]).
In case of kraft pulps, a higher final brightness can be achieved while consuming less active chlorine if the primary fines fraction is removed before bleaching (Asikainen et al. [2010a]). For softwood pulps, more effective bleaching can be achieved by the removal of ray cells. In addition, hydrogen peroxide bleaching of kraft pulp is also more effective after removing the primary fines fraction (Panula-Ontto et al. [2002]).
Chemical pulp fines have a higher swelling capacity than mechanical pulp fines. In case of chemical pulp fines, swelling is related to surface charge and the amount of amorphous cellulose.
All types of fines have a large specific surface area which leads to ample interaction with other components of the papermaking furnish. Typical substances used in the papermaking industry are solid components such as other fines, fibers, and mineral filler particles, as well as dissolved and colloidal substances. In paper production, the term firstpass retention (i.e. how much material is retained in the formed sheet) is an issue. The modern paper industry strives for closed water circuits to minimize the waste water. Colloidal and dissolved substances including a part of the fines fraction are not retained on the forming fabric get therefore into the closed water circuits where they may cause troubles. If expensive chemicals have adsorbed to fines, it is difficult to recover them from the white water (Holik et al. [2006]). Mechanical retention of small particles such as fines or fillers is poor due to their small dimensions. To retain these substances, chemical interaction between these particles must take place (Liimatainen et al. [2008]). The tendency of fines for adsorption supports to solve the problem of low retention. Retention agents are applied that interact with pulp components to generate flocculation. The flocculation of fines, fillers with fibers reduces the total hydrodynamic surface weight (corresponds to the

surface available for interactions with other solid particles) unit of solids in a paper furnish, and thereby it also improves the dewatering behavior (Hubbe [2002]).

2.7 Fines utilization

Already Brecht and Klemm [1952] had the idea of controlling the fines content for the optimization of paper strength. They suggested to balance an excess of fines by adding an unbeaten chemical pulp to increase the overall content of long fibers.
Recent investigations designed a more systematic approach where they focused on the addition of fines for an active control of paper properties. Through mixing of TMP fines and kraft pulp fines, it is possible to achieve an increase in tensile strength and light scattering coefficient.
Primary fines from bleached hardwood pulp can be used as a filler material. By addition of this material into a pulp suspension, easier refining and a higher opacity can be achieved (Retulainen et al. [1993]). By the addition of mechanical pulp fines to bleached kraft pulp, an improvement of the efficiency of dye added at the wet end via the formation of complexes between the fines and the dye which are retained in the fiber network.
In addition, fines can be removed from the papermaking process for utilization, e.g. in a biorefinery as a source of xylan, fatty acids, sterols and betulinol. Furthermore fines are used to prepare nano-ligno-cellulose by homogenization (Asikainen et al. [2010b], Osong et al. [2013]).

2.8 Fractionation

2.8.1 Laboratory fractionation methods

The two common technical solutions for isolating fines in the lab are the Bauer McNett fiber classifier and the dynamic drainage jar tester (SCAN [2005], Sundberg and Holmbom [2004]). These two devices differ slightly in their construction, but they show the same principle. Water passes through a wire and the filtrate, which contains the fines is collected. The Bauer McNett fiber classifier has the drawback of poor reproducibility and higher water requirement (Kangas and Kleen [2004], Kleen et al. [2003]). Due to the large quantities of water needed for separation, the surface properties of fines are affected. It has been shown that there is a clear difference between these two devices in the papermaking properties of the separated fines (Rundlof et al. [2000]). Some authors clearly suggest the use of a dynamic drainage jar tester. Figure 2-10 shows the Britt Dynamic Drainage Jar tester (BDDJ) and

the Bauer McNett separation device.
Both the Bauer McNett and the dynamic drainage jar tester are composed of stirred vessels (SCAN-CM 66:05 (2005), TAPPI T 233 cm-95). An other method of fines isolation is fractionation using hydrocyclones. In a hydrocyclone, particles are separated by their specific density and surface area. In addition to hydrocylones, lab-scale pressure screens are used to prepare large amounts of pulp fractions rich in fines (Ewald et al. [2014], Karjalainen et al. [2013]).
Another different procedure for the classification of pulps by their dimension is the use of a tube flow fractionation device. In the tube flow fractionation process, a non-laminar flow of water through a long tube is used to separate a pulp suspension into different fractions (Laitinen [2011]). In the tube, longer fibers move faster, because they are more easily captured by the faster middle flow. Short fibers and fines have a higher probability to stay in a region of the tube, where the flow velocity is lower. If the fines are defined by their length (particles <100µm), this fractionation device can be used to determine the fines content.
This method is still not suitable for the production of high amounts of fines, since typically less than 0.25 g of sample weight is applied for one run. In addition, the concentration of the solid material is very low (Krogerus et al. [2003]).

(a) (b)

Figure 2-10 *(a) Bauer McNett Fractionator. (b) Britt Dynamic Drainage Jar Tester (BDDJ).*

2.8.2 Industrial application methods

Industrial fractionation is used to decrease pulp processing costs and to improve the production process or the final properties of paper. The main objective of pulp fractionation is to divide the pulp into different fractions with divergent properties. Fractionation devices such as pressure screens, hydrocyclones or wire washers are available for use on an industrial scale (Niinimäki et al. [2007]).

A pressure screen is a pressurized device designed to divide a fiber suspension into two or more flows according to their particle size continuously. Pressure screens were introduced in the 1940's, where they replaced vibratory screens and "centrifugal screens" (Halonen and Ljokkoi [1989]). Several literature reviews about the general configuration of the screening device, rotor design and the geometry of the screen plate have been published (Niinimäki [1998], Ämmälä [2001]). Industrial trials have been performed using a screen basket with 250 µm holes. In this study, it was possible to produce fine fractions of bleached chemical pulp with a micro-perforated screen basket (Björk et al. [2015]).

Hydrocyclones are widely used for the separation of heavy (e.g. sand) or light (e.g. plastics) contaminants from pulp, but they can also be used for the fractionation of papermaking fibers. It has been shown, that softwood fibers can be separated according to their cell wall thickness and also hardwood vessel elements can be enriched by hydrocyclones (Asikainen [2013], Brännvall and Lindström [2006]). Fractionation in a hydrocyclone is based on the particle settling velocities, particle dimensions, shapes and densities. Hydrocyclones classify wood based cells according to their cell wall thickness, coarseness, specific surface area, specific volume and their density (Karjalainen et al. [2013]).

Several industrial washing and cleaning devices, such as wire washers, ash washers, drum washers, or the white water tank of a paper machine may be sources of different fiber or fines fractions.

It is known, that today's closure of the water circuits of a paper machine may affect the mechanical and optical properties of the paper produced (Lindström and Söremark [1977]). The closure of water circuits leads to an accumulation of dissolved and colloidal substances in the white water. If the concentration is high enough, the substances from the white water may interact with the fines and fibers and may change their properties.

2.8.3 Conclusions

As described above, the conventional laboratory fractionation devices for fiber-fines fractionation are the Bauer McNett fractionator (BMcN) and the Britt Dynamic Drainage Jar (BDDJ) tester. The main drawback when using these devices is the small amount of pulp that can be treated in a single step (10 g BMcN, 5 g BDDJ) i.e. only small amounts of fines can be produced. In case of the Bauer McNett device, more than 240 l of water are needed for one separation run. Depending on the pulp type there are only few grams of fines diluted in huge amounts of water. To allow further processing, thickening of such a highly diluted suspension is needed. Recently more and more research projects focus on areas of potential applications for fines. Therefore the need for new technologies for fines separation in a laboratory and industrial scale is of utmost importance.
In the current thesis, fines produced with a pressure screen and with a dissolved air flotation (DAF) cell are provided for other projects within this area for investigations on chemical, enzymatic and physical modification.
Further, the tube flow fractionation (TFF) method was used to fractionate particles over the entire size range of pulp particles. Pulp fractionation can be done quickly with this method and results are also comparable to screen fractionation devices such as the Bauer McNett device. The TFF device offers an interesting tool to investigate different pulp types in a more detailed way than many other conventional methods. In addition, the effect of secondary flow (Dean flow) on the separation performance in the TFF device by changing the curvature and flow velocity was investigated in this thesis.
With the current separation and thickening method using a pressure screen and dissolved air flotation as well with the analytical fractionation method using the TFF device, it is now possible to provide on the one hand high amounts of fines for further applications and on the other hand to investigate different pulp types in a analytical way.

3 Materials and methods

Methodologies and experimental procedures for studying the predefined research questions are presented in this chapter. This chapter is divided into two sections. Pulp evaluated in the current thesis are introduced in section 3.1. Different characterization methods of fiber and fines fractions using image analysis are presented in section 3.2.

3.1 Pulps used for subsequent investigations

In the current thesis, four different pulp types were used from the industry partners within the Flippr° project. Basic information of four different pulps are shown in Table 3-1.

Pulp type	Process conditions	Wood species used
Kraft unbleached	Sulfate	100 % spruce
Kraft bleached	Sulfate	100 % spruce
Sulfite bleached	Magnefite	80 % spruce, 20 % beech
Mechanical unbleached	Pressure groundwood	100 % spruce

Table 3-1 *Basic information of four different pulp types used in the current thesis.*

3.2 Characterization Methods

Britt Dynamic Drainage Jar Tester (BDDJ)

The Britt Dynamic Drainage Jar Tester (BDDJ) was used for the separation of fines from pulps. The BDDJ tester is equipped with a single screen for fiber classification

and it can be used for all kinds of pulps. The screening procedure is the same for both mechanical pulps and chemical pulps, although the sample mass varies (see Table 3-2). The separation procedure is described in the standard SCAN-CM 66:05 (2005). Figure 3-1 shows the BDDJ tester.

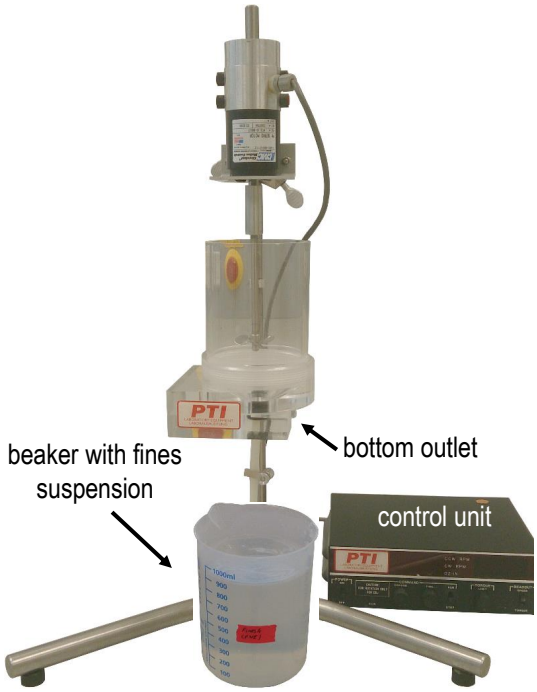

Figure 3-1 *Britt Dynamic Drainage Jar Tester (BDDJ), W.J. Fischer, personal communication, November 9th, 2016.*

After the pulp sample is disintegrated in a laboratory disintegrator (EN ISO 5269-2 2004 12) using deionized water, the pulp suspension is screened through a wire. This wire corresponds to a 200-mesh screen, or 76 µm screen of the Bauer McNett (BMcN) fractionator. The material which passes the screen and also the retained fibers are both collected in separate beakers. Subsequently, the water is removed by using a Nutsche dryers and a filter paper. After this the filter papers are dried and weighed separately. In the final step the fines content is calculated. Table 3-2 shows the mass of test portion and volume of screening for different pulps using the BDDJ tester.

Pulp type	Oven dry mass of test sample g	Total volume of water ml
Chemical pulp (fines content < 10%)	5.0 ± 0.5	5000
Mechanical pulp (fines content > 10%)	0.5 ± 0.1	2500

Table 3-2 *Mass and volume of test sample for different pulps used with the Britt Dynamic Drainage Jar Tester (BDDJ)(SCAN-CM 66:05).*

Image analysis

The Fiber Tester Plus from Lorentzen&Wettre (see Figure 3-2) was used to determine the particle size distribution of pulp suspensions. The L&W Fiber Tester Plus ("FT+") is a flow microscope developed for pulp analysis. The resolution within measurement range is 0.1 µm for an average softwood fiber (Lorentzen&Wettre [2016]). In the FT+, the sample is automatically diluted to a suitable concentration. The pulp suspension is transported through a flat, rectangular flow cell where several particles are imaged at the same time. In automatic measurement procedure, half of the volume of the diluted pulp suspension is measured first, and afterwards the results are compared to those from the second half of the sample. This procedure verifies the reproducibility of the measurements.
The recorded grayscale images are then background corrected and binarized into black and white images using a defined threshold. The particles are then divided into different classes based on size and shape. It is possible to define default settings, where particles which are longer than 200 µm with an aspect ratio over 4 and not wider than 75 µm, are classified as fibers. Particles shorter than 100 µm or 200 µm are, depending on the standard used, classified as fines.
The basic parameters calculated by the FT+ are on the one hand the area S and on the other hand the perimeter Z of a certain particle (Hyll et al. [2016]). It is assumed that the length L and the width W is equal to those of a rectangle with the same area and perimeter as the measured particle.

$$\begin{aligned} S &= LW \\ Z &= 2W + 2L \end{aligned} \tag{3.1}$$

The length and width can be calculated by solving the equation system given by the above equations. A calibration offset is added to the width. The subscript RE

stands for rectangular-equivalent.

$$L_{RE} = \frac{Z}{4} + \sqrt{\frac{Z^2}{16} - S}$$
$$W_{RE} = \frac{Z}{4} + \sqrt{\frac{Z^2}{16} - S} + offset \tag{3.2}$$

The settings of the measurement procedure was changed, that individual data from particles shorter than 200 µm (fines) were included in the raw data. The measurement time was changed according to sample size and sample concentration between 6 to 20 minutes. The FT+ was set to measure 100000 particles. Two independent samples with 200 ml volume were measured on each fraction. The raw data from the FT+ for each particle was exported including number-weighted rectangle-equivalent length, width and shape ratio for subsequent analysis.

Figure 3-2 *Fiber Tester Plus from Lorentzen&Wettre at the IPZ.*

4 Design and implementation of laboratory equipment

4.1 The tube flow fractionation device for analytical fractionation of pulps

The tube flow fractionation device (TFF) method can be used to fractionate particles over the entire size range of pulp particles. Pulp fractionation can be done quickly with this method and results are also comparable to screen fractionation devices such as the Bauer McNett device (Laitinen [2011]). The TFF device offers an interesting tool to investigate different pulp types in a more detailed way than many other conventional methods.

4.1.1 General description of the tube flow fractionation device

The tube flow fractionation device used in the present study was implemented at the Institute of Paper, Pulp and Fiber Technology at Graz University of Technology in the course of a master thesis (Jagiello [2013]).
The main component of the tube flow fractionator is a 100-meter-long teflon tube that is wound around a drum, which is shown in Figure 4-1. The sample is injected into a three way valve which is connected with a second one. These valves are used to allow any air that is inside the pipe to be removed from the fractionation system. After the sample is injected and free of air bubbles, the three-way valve (see sample inlet Figure 4-1) is set so that the continuous water flow can transport the sample into the tube system.
The tube is mounted onto a drum that is mounted on a frame construction and is positioned 700 mm above the ground to ensure easier sampling. The flow velocity as well as the time intervals for sampling can be adjusted. Parameters such as fluid temperature, inlet pressure, sample volume and consistency were kept constant.

These parameters are presented in Table 4-1. The flow rates can be adjusted accurately using a PID control unit (Bürkert 8605 PID-Control, Bürkert 8611 process controller).

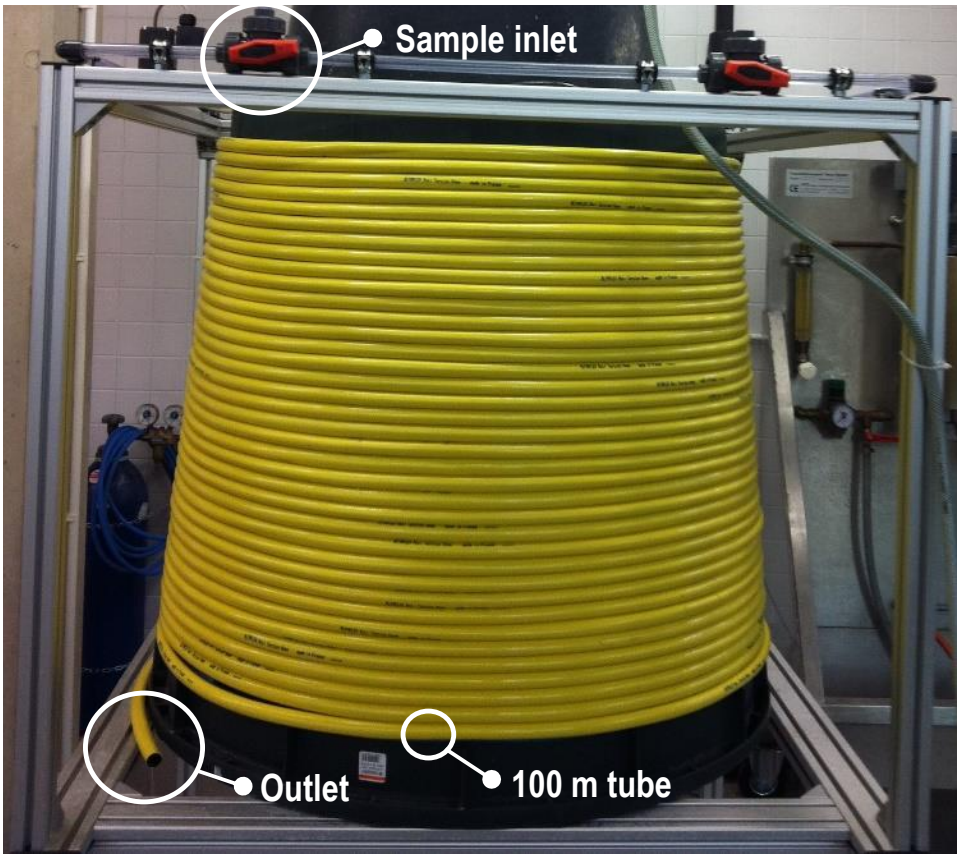

Figure 4-1 *The Tube Flow Fractionation device (TFF) at the Institute for Paper-, Pulp and Fiber Technology (IPZ).*

A tube flow fractionator (TFF) is a device used to separate particles in the lab scale according to their size. Due to the internal flow regime in the TFF, longer particles tend to accumulate in the front end of the flowing suspension, followed by consecutively smaller particles further back in the tube. This separation mechanism can be used for the separation of pulp fibers and fines into several subfractions. In theory, all particles are initially distributed randomly (see Figure 4-2 (a)). When the suspension starts to flow, the slight turbulence in the transition flow regime starts to move the particles randomly inside the flow. Smaller particles tend to remain in the fluid regime close to the tube wall and will thus spend a portion of time in that zone were the velocity is lower (see Figure 4-2 (b)). Larger particles also drift towards the tube wall. Due to their larger dimension they may show a higher probability to be captured by the faster middle flow. The probability to go along with the faster

middle flow is higher for long fibers (high aspect ratio particles) or flake like particles than for shorter ones (low aspect ratio particles). Therefore, larger particles tend to concentrate at the front end of the flow and exit the tube first (see Figure 4-2 (c)).

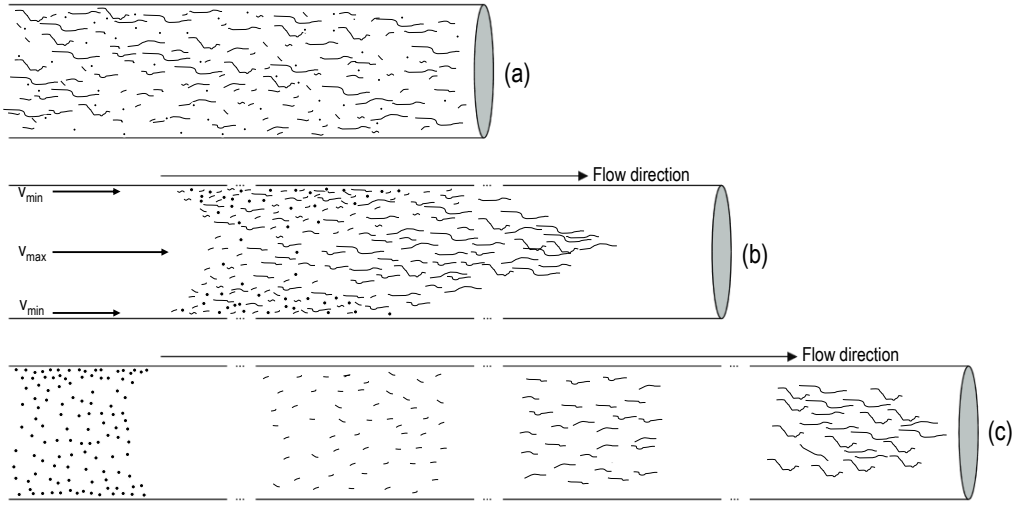

Figure 4-2 *Schematic principle of particle separation of a TFF (adapted from Laitinen [2011]).*

Sample preparation and sampling time intervals (TFF)

The duration of fractionation was determined precisely for each pulp, volume flow and curvature prior to the fractionation trials. After 100 m in the tube, an injected sample stretches over more than 20 m in tube length, depending on pulp type, volume flow and curvature of the tube. As soon as the first fibers reaches the end of the tube, the first fraction is collected in a bin for a defined time interval. The subsequent fractions are collected in separate bins using the same time interval. The whole sampling procedure is done by hand as exactly as possible using a stop watch. The fractions are numbered and later on analyzed. Depending on the flow velocity, the time intervals for sampling are adjusted respectively.

Fixed parameters	
Length of tube	100 m
Diameter of tube	16×10^{-3} m
Water temperature (1 bar)	22°C
Water density (1 bar, 22°C)	$997.773\,\mathrm{kg/m^3}$
Water viscosity (1 bar, 22°C)	0.957×10^{-6} $\mathrm{m^2/s}$

Table 4-1 *Predefined parameters for TFF.*

4.1.2 Comparison of fractions using the Bauer McNett and tube flow fractionator

The Bauer McNett fractionation device was chosen because of its recognition as the standard laboratory fractionation device for different pulp samples. The idea was, to produce similar tube flow fractions which can then be compared to Bauer McNett fractions. After pre-trials with an unbleached PGW pulp it was shown that the TFF fractions within a time range of 15 seconds provides fiber length distribution similar to those of the BMcN fractionator.

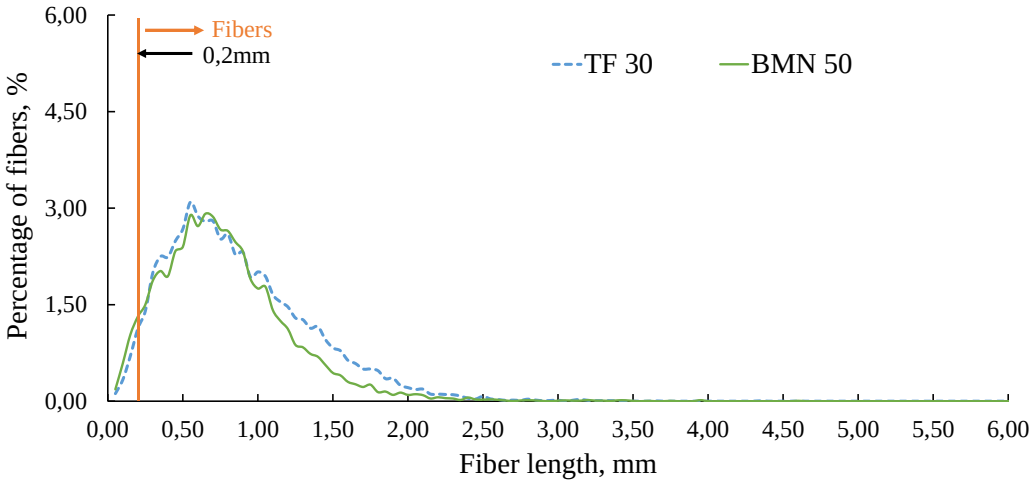

Figure 4-3 *Length weighted fiber length distribution of the TFF 30 fraction and the BMcN 50 fraction.*

Figure 4-3 shows a comparison between a 30 seconds TFF fraction and a BMcN 50 mesh fraction for an unbleached PGW pulp. It should be noted that fractions having more short fibers and fines show a very good agreement of the fiber length distribution. Results obtained from the comparison of the 75 seconds fraction to the BMcN fines fraction (see Figure 4-4) show a similar length distribution. It should be noted here, that in consideration of the right choice of time intervals of the TFF device, a comparison of the tube flow fractions and fractions from the BMcN device can be done.

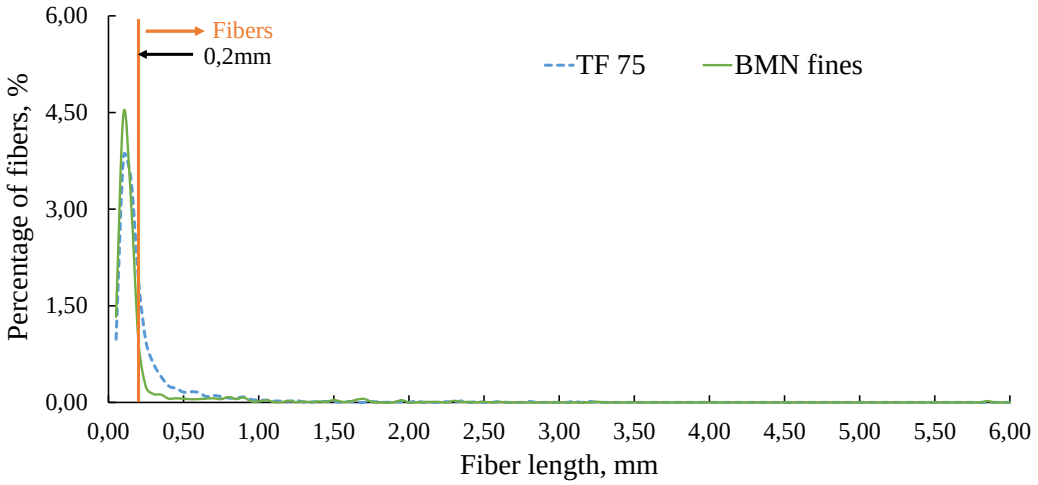

Figure 4-4 *Length weighted fiber length distribution of the TFF 75 fraction and the BMcN fines fraction.*

It can be concluded, that due to the fact that the TFF device shows no limitation regarding size of fraction length distributions, this method provides some new possibilities of investigation pulp fractions. In the knowledge that this device offers fractions with independent time intervals, many new opportunities and application are given in the laboratory analytical fractionation method.

4.1.3 Investigations on the effect of Dean Flow in a TFF device

The fractionation phenomenon in flowing pulp suspension such as in the TFF has already been investigated in 1956 by Johansson and Kubát. In this study they investigated the separation of pulp fibers in a straight glass tube. (Johansson and Kubát [1956]; Johansson et al. [1970]; Olgård [1970]).
It was found, that Reynolds numbers within the range 1,000 to 10,000 are considered to be most efficient for the separation of pulp particles (Pascal and Silvy [1993]). In 2003, Krogerus and Fagerholm [2003] used a tube flow fractionator designed by the Metso Field Systems Inc. Laitinen [2011] investigated the mechanisms of particle separation under non-laminar (Re number 8500) conditions of continuous water flow by using a Metso TFF. They explained the variation in fractionation time between different types of pulp as an effect of particle dimensions (length, width and thickness). Laitinen et al. [2011] focused on the contribution of various pulp, paper and peat particle dimensions on the observed fractionation time (the particle velocity in the flow regime). They showed, that particle length has the most significant influence on separation, while particle width and thickness have a minor, but still statistically significant effect on separation.

In case of a laboratory TFF device, where a tube is wound on to a take-up reel, it can be assumed that additional flow conditions caused by the curvature of the tube influence the separation of particles in the flow field of a tube. The influence of secondary flow (Dean Flow) in TFF has been neglected so far.
In the present study the effect of secondary flow on the separation performance in a tube flow fractionator by changing the curvature and flow velocity, referring to the tentative flow regime map (Figure 4-6), has been investigated (see also Redlinger-Pohn et al. [2016]). Secondary flow in curved pipes, even at low Reynolds numbers, are caused by the imbalance between inertial and centrifugal forces. A review on the flow in curved pipes has been given by Berger et al. [1983].
Already in 1910 and 1911, the presence of a secondary flow was shown by injecting ink into a curved pipe (Eustice [1910], Eustice [1911]).
The first theoretical analysis for an incompressible fluid (water) was given by Dean [1928]. He defined the so-called Dean number as a dimensionless value. It is denoted as De and defined for a flow in a coiled tube:

$$De = Re\left(\frac{d_\mathrm{i}}{d_\mathrm{c}}\right)^{\frac{1}{2}} = Re\sqrt{\kappa} \tag{4.1}$$

The relevant parameter κ (curvature) is defined as the ratio between the inner diameter of the tube ($\mathrm{d_i}$) and the diameter of the curvature ($\mathrm{d_c}$). It is a measure for the magnitude of the secondary flow (Berger et al. [1983]). The Reynolds number is denoted as follows:

$$Re = \frac{\rho\ u\ d_\mathrm{i}}{\mu} \approx \frac{inertial\ forces}{viscous\ forces} \tag{4.2}$$

Physically it may be understood as the ratio between inertial and viscous forces (density ρ $[kg/m^3]$, mean velocity of fluid u $[m/s]$, dynamic viscosity μ $[Pa\ s]$).
When a fluid is forced to flow through a curved pipe a secondary flow is generated in planes perpendicular to the curved centreline of the tube. Due to its coiled trajectory, a pressure gradient across the pipe, balancing the centrifugal force on the fluid, develops. The pressure reaches a maximum at the outer wall and a minimum at the inner wall of the tube. Therefore the fluid near the top and bottom of the tube moves towards the central axis and the fluid in the center is moving outwards. Two opposed vortices are formed around the center of the cross section of the tube (Cuming [1952]).
Figure 4-5 illustrates the secondary streamlines in the tube cross section and contours of constant axial velocity at low Dean number. The flow is composed of two symmetrical counter rotating helical vortices. The position of the maximum axial velocity is shifted towards the outer side (outer bend) of the tube (see Figure 4-5). An increasing Dean number leads to an increase in circumferential velocity and

therefore more fluid is being pushed into the region of the outer bend (Berger et al. [1983]).

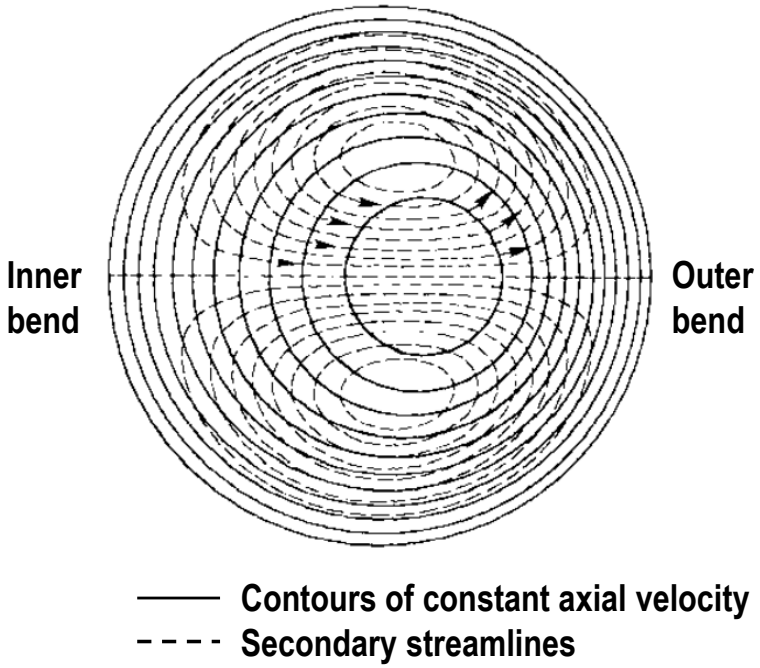

Figure 4-5 *Secondary flow field in a curved pipe at low Dean number (adapted from Berger et al. [1983]).*

Webster and Humphrey [1997] mentioned the transition to turbulent flow. Here, the increased flow resistance in curved pipes is caused by secondary circulation. This means that a laminar flow can be preserved at high Reynolds numbers (Webster and Humphrey [1997]). Based on the investigation of Webster and Humphrey [1997], Piazza and Ciofalo [2011] introduced their tentative flow regime map. The tentative flow regime map describes the change from stationary laminar to quasi periodic flow regime and the change from chaotic state to a developed fully turbulent flow (see Figure 4-6). They also observed the stable periodic solution at Re = 4108. Figure 4-6 depicts the flow regimes used in TFF experiments.

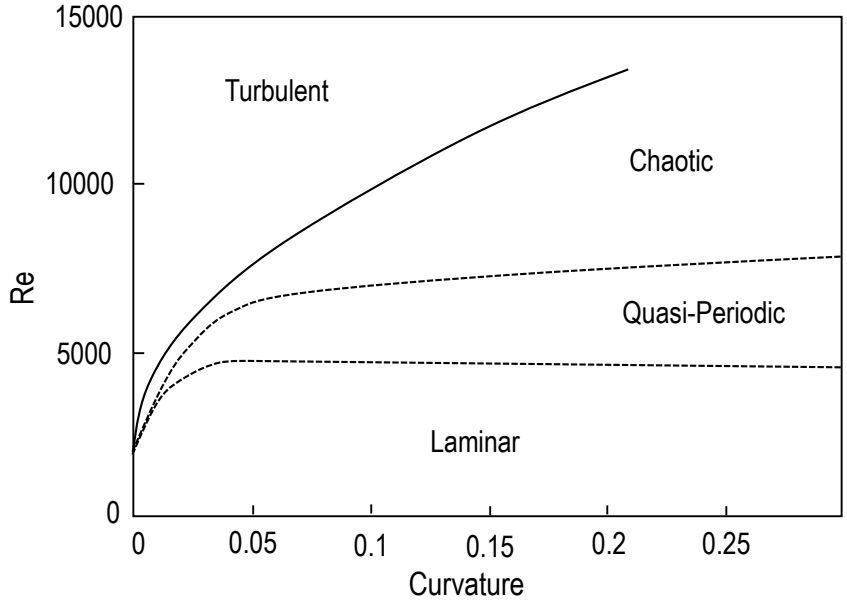

Figure 4-6 *Tentative flow regime map (adapted from Piazza and Ciofalo [2011]).*

Materials and sampling methods

In the present study two types of pulps were used. The first one was an unrefined bleached sulfite pulp (mixture of spruce (80%) and beech (20%)) and the second one was a pressurized ground wood pulp (PGW) made from spruce. For the sulfite pulp a consistency (solids content) of 0.25% and for the PGW a consistency of 0.5% was used. These consistencies are similar to those which were used in previous studies (Laitinen et al. [2011]; Krogerus and Fagerholm [2003]) and shall prevent formation of a continuous network that no longer allow fibers to move freely and thereby prevents separation.

Pulp samples (50 ml, 0.25-0.5% consistency) were injected into a 100 m long synthetic tube which is either coiled ($\kappa = 0.0432$) onto a drum or used in a straight configuration, i.e. $\kappa = 0$ (compare Figure 4-7). At the end of the tube, the obtained fractions are collected in bins. Afterwards the fiber morphology - the length distribution - of each fraction was determined using the L&W Fiber Tester Plus. The fines fraction was defined as particles with a length below 200 µm in these measurements (ISO 16065-1/2014).

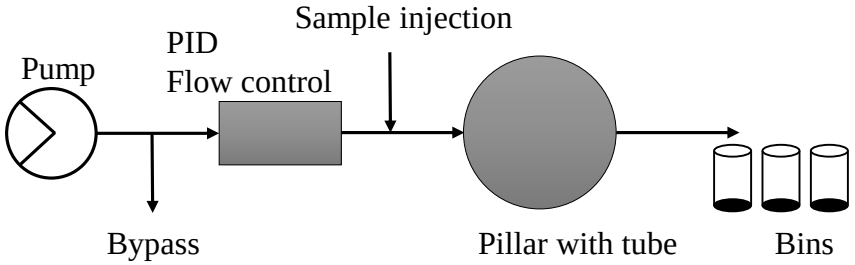

(a) Coiled setup of the TFF device

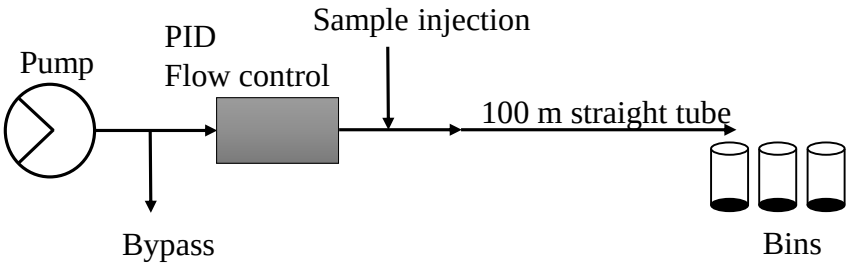

(b) Straight setup of the TFF device

Figure 4-7 *Schematic view of the TFF configuration.*

In addition, an adapter (Figure 4-16) has been developed to split the flow at the end of the tube. With this adapter, fiber mass balances between the inner and the outer bend have been performed in order to investigate the flow conditions in the cross section of the tube. The determination of the mass balances was performed by filtration, drying and subsequent measurement of the dry matter content (ISO 638/2008).

Sampling time intervals

Depending on the flow velocity, the time intervals for sampling were adjusted respectively. The time intervals were chosen in a way to yield fractions that allow statistically significant analysis with the L&W Fiber Tester Plus (at least 1000 particles per measurement). When using a volume flow of 2.5 l/min, a time interval of 10 s has proven itself to lead to precise and repeatable results. In order to compare the results obtained at 2.5 l/min, the time interval for 5.2 l/min was set to 5 s.

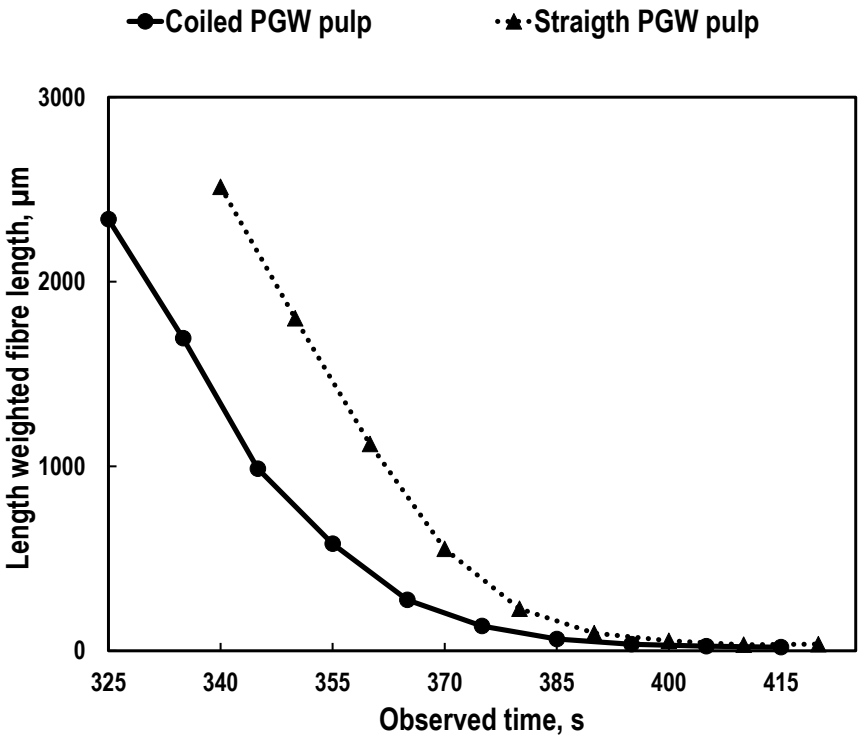

Figure 4-8 *L&W FT plus length weighted fiber length measurements of ten different TFF fractions at 2.5 l/min.*

A typical result is shown in Figure 4-8. Ten different fractions are represented by their length weighted fiber length as measured with the L&W Fiber Tester Plus. Besides the length distribution of the fractions, the residence time (time between injection and sampling) of the particles in the TFF was also of interest in the following experiments. Fig 4-8 also shows the timeline for sampling based on the first fibers reaching the end of the tube. A significant difference between the coiled and the straight tube set-up is evident at a volume flow of 2.5 l/min.

Experimental setup

Figure 4-7 shows the tube flow configurations used in the present study. It also shows on the one hand the coiled configuration in which the tube is wound onto a pillar having a diameter of 370 mm and on the other hand the straight configuration. In both configurations the flow velocity and time intervals for sampling can be adjusted for the experiments. Parameters such as fluid temperature, inlet pressure, sample volume and consistency were kept constant. These parameters are shown

in Table 4-1 (Wagner and Kruse [1998]; Vogel [1974]). The parameters which were changed during the experiments as well as the corresponding Reynolds and Dean numbers are shown in Table 4-2.
The fractionation trials were performed at flow rates of 2.5 l/min and 5.2 l/min and accurately controlled using a PID control unit (Bürkert 8605 PID-Control, Bürkert 8611 process controller). The Reynolds and Dean number depend on curvature and flow velocity (see Equation 4.1 and Equation 4.2).
The different flow rates offer the possibility to investigate the effect of secondary flow in different flow regimes. The Reynolds numbers used in this study have been calculated based on the volume flow. From Figure 4-6 it is evident that, based on these Reynolds numbers, two different flow regimes are addressed in the fractionation trials according to Piazza and Ciofalo [2011] (see Figure 4-9).

Variable parameters				
Curvature κ	0	0	0.0432	0.0432
Volume flow l/min	2.5	5.2	2.5	5.2
Reynolds number	3456	7189	3456	7189
Dean number	0	0	719	1495

Table 4-2 *Parameters changed during the fractionation trials.*

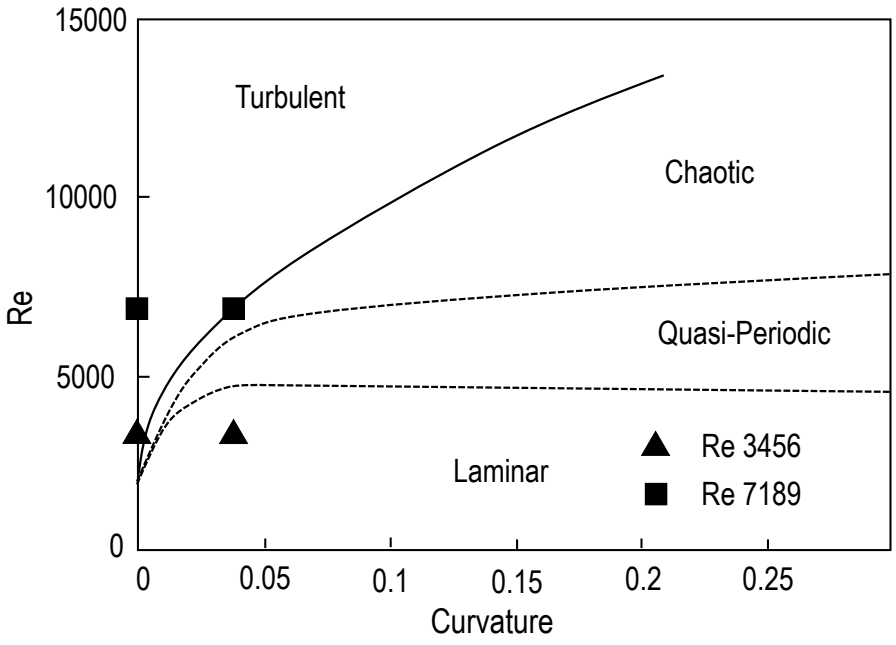

Figure 4-9 *Tentative flow regime map including Reynolds numbers and curvature (kappa) of the tube used in the TFF experiments (adapted from Piazza and Ciofalo [2011]).*

At the lower Reynolds number (3456), the flow regime is stationary (laminar). It should be mentioned here that this is true, because of the coiled setup. At a Reynolds number of 7189, the flow regime is defined to be chaotic for the coiled set up and turbulent for the straight set up. For each pulp, several fractionation trials have been performed.

Repeatability of the method

The tube flow fractionation device shows a high repeatability. Fig 4-10 shows the first fraction of three PGW pulp samples as separate length distributions. All trials show similar results with only minor changes. In Figure 4-11, the mean length distribution of the first fraction from three independent trials including 95 % confidence intervals for each class is shown. All trials show similar results with minor changes. Also the 95 % confidence interval of the length weighted mean fiber length only shows small differences between the trials.

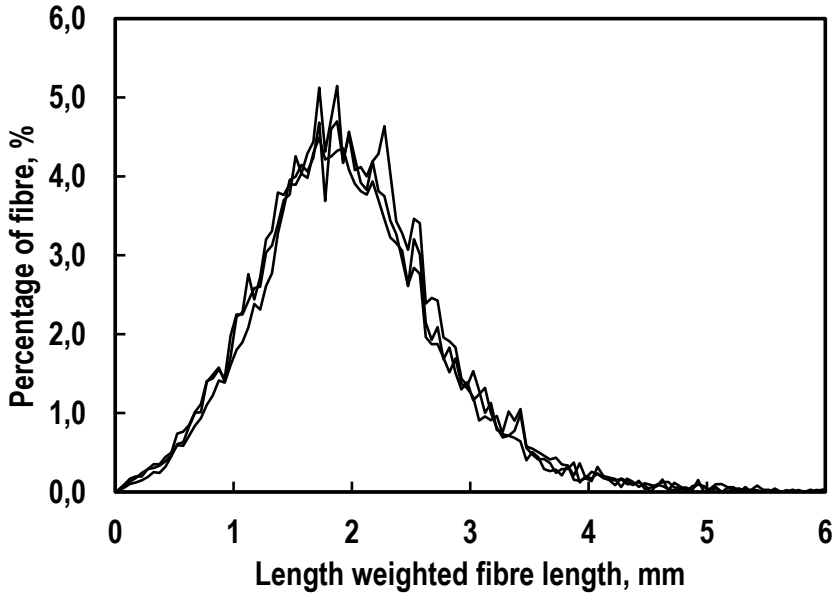

Figure 4-10 *Repeatability length weighted fiber length distribution of the 0 seconds tube flow fraction of the same PGW sample.*

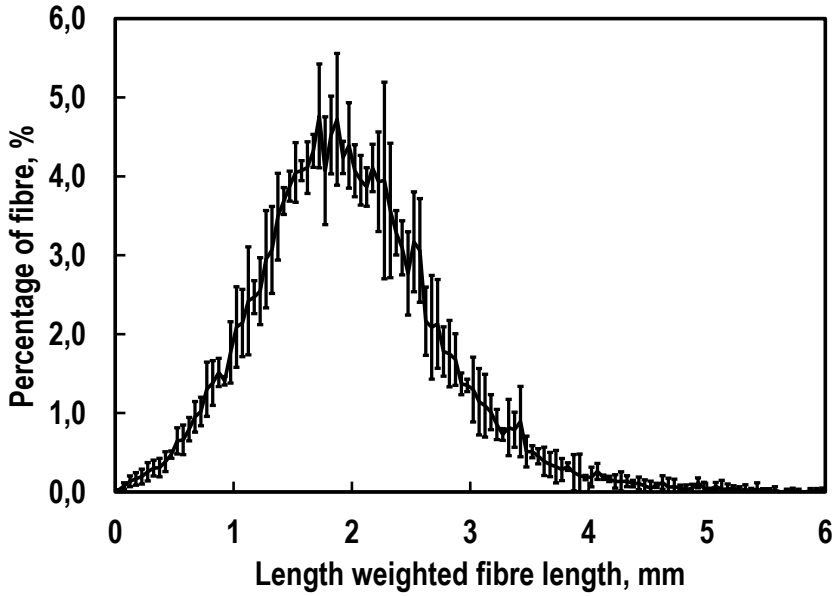

Figure 4-11 *Repeatability mean of the length weighted fiber length distribution including 95% confidence intervals of arithmetic fiber length of the 0 seconds PGW tube flow fraction.*

4.1.4 Results and Discussion

The residence time, length weighted mean fiber length, as well as fiber mass balances were used as a tool to describe the effect of secondary flow on fiber fractionation.

Investigations on secondary flow

Figure 4-8 demonstrates that different pulps show significant differences in their residence time and mean fiber length. It can be assumed that an increase of the volume flow or a change of the curvature influences the residence time of the fibers as well as the mean fiber length of each fraction.

	2.5 l/min	5.2 l/min
Straight setup (S)	340 s	170 s
Coiled setup (C)	330 s	170 s
Difference S-C	**+ 10 s**	0 s

Table 4-3 *Residence times of first sulfite pulp fibers in different TFF configurations.*

A comparison between the coiled and straight setup of the TFF for average length weighted fiber length of a sulfite pulp at 2.5 l/min is given in Figure 4-12. The x-axis represents the sample number of the fractions which corresponds to time intervals of 10 s (TFF1, TFF2, etc.). The y-axis represents the average length weighted fiber length in µm. Based on the development of fiber length over time it is obvious that the fractions obtained with the coiled configuration show a faster decrease in fiber length. The residence time of the first fibers (see Table 4-3) indicates a higher flow velocity for fibers, as the first particles reach the end of the 100 m tube 10 seconds earlier than in the straight configuration. This can be explained by an increase of the local outer flow velocity (1.6 times higher than the average velocity) in the cross sectional area of the tube due to the curvature of the pipe (Hawthorne [1951]).

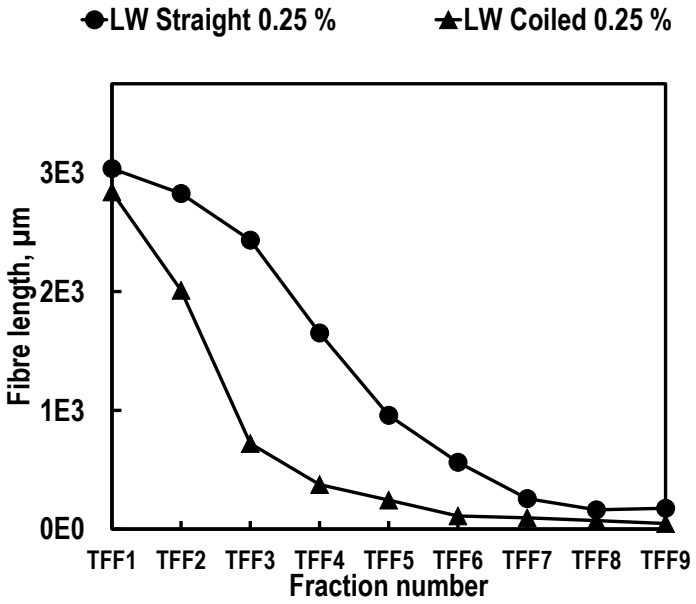

Figure 4-12 *Length weighted fiber length of tube flow fractions of sulfite pulp obtained at volume flow of 2.5 l/min.*

High aspect ratio fibers (long fibers) have a higher probability of being captured by the faster middle flow where the new position of the maximum axial velocity is shifted towards the outer side. The local maximum flow velocity is now higher compared to the one in the straight tube. Therefore long fibers reach the end of the tube within the first three fractions. The fine fraction is not that much affected by this effect since their ability of being captured by the local maximum velocity is quite lower.

The straight setup shows a smoother separation over the whole fiber length dis-

tribution (see Figure 4-12). Figure 4-13 illustrates the results for the sulfite pulp fractionated at a volume flow of 5.2 l/min. Again, the x-axis represents the sample number of the fractions but in this case it corresponds to a time interval of 5 seconds. Table 4-3 shows the effect of an increased flow velocity on the residence time. At a volume flow of 5.2 l/min it is evident, that there is no longer a difference in residence time between the coiled and straight setup. The ratio between the local maximum and mean flow velocity in the coiled set up decreases due to the transition to turbulence at the given Reynolds number of 7189. Due to the smaller flow velocity ratio as well as mixing effects the longer fibers cannot be separated in the same manner as in case of 2.5 l/min.
Concerning the fiber length distribution, Figure 4-13 shows that now the coiled configuration has a wider distribution of the long fiber fraction.

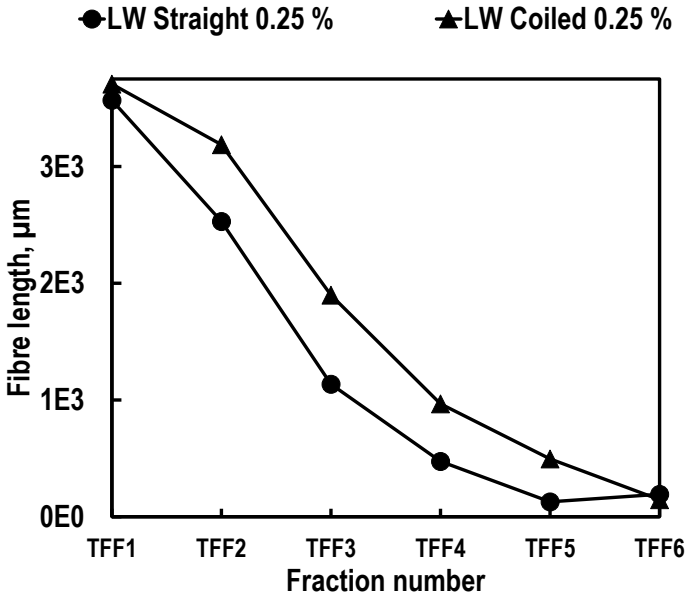

Figure 4-13 *Length weighted tube flow fractions of sulfite pulp obtained at volume flow of 5.2 l/min.*

The reason for this reversed result seems to be the more distinctly developed secondary flow at higher flow velocity. The secondary flow generates a mixing effect that mixes fine particles but especially fibers. High aspect ratio fibers (long fibers) spend now a portion of the time in a zone where the velocity is lower. This is also indicated by the no longer affected residence time (compare Table 4-3). Due to the mixing effect the sample is evenly distributed over the whole cross section and thus the - in both configurations equal - average flow velocity is the key parameter

influencing the residence time.
Compared to the straight configuration the mixing effect reduces the separation according to fiber length, as the tendency of long fibers to follow the faster flowing region is somewhat prevented by the recirculation in a low flow velocity flow zone.
The results obtained for pressurized ground wood pulp at 2.5 l/min are illustrated in Figure 4-14. In case of PGW only small differences between the straight and coiled setup can be observed. The main reason for this might be the raw material. PGW has a narrower fiber length distribution and a high amount of fine particles. In case of the 2.5 l/min fractions, there are less long fibers which can be captured by the local maximum flow velocity (minor impact regarding change of length weighted fiber length). Probably the shorter fibers of PGW pulp (low aspect ratio) show less tendency to be captured by the maximum flow velocity.

	2.5 l/min	5.2 l/min
Straight setup (S)	340 s	170 s
Coiled setup (C)	325 s	165 s
Difference S-C	**+ 15 s**	**+ 5 s**

Table 4-4 *Residence time of PGW pulp in different TFF configurations.*

Table 4-4 represents the residence time of PGW. It is evident that in the case of the coiled set-up longer fibers reach the end of the tube faster (15 s). The reason for this effect seems to be the smaller amount of long fibers and due to this they can move freely and therefore can be captured easier by the faster middle flow.
Compared to sulfite pulp (fraction obtained at 2.5 l/min) it is evident that the influence of secondary flow is totally different for different flow regimes.
Fig 4-15 shows a comparison of PGW fractionation trials using a volume flow of 5.2 l/min. From this figure it is apparent that there is a significant change in fractionation performance and residence time (Table 4-4). For each fraction the coiled configuration shows a higher average fiber length compared to the straight setup. This indicates again the influence of secondary flow due to mixing effects.

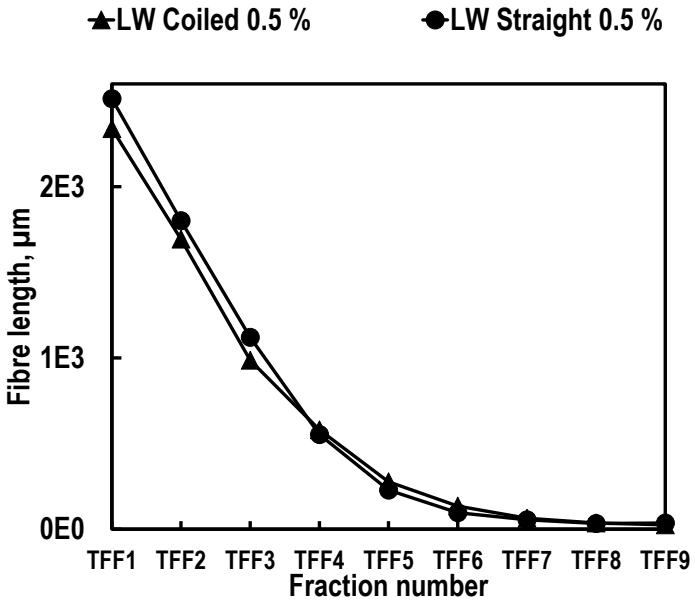

Figure 4-14 *Length weighted tube flow fractions of mechanical pulp (PGW) obtained at a volume flow of 2.5 l/min.*

Summing up it can be said that, depending on the flow velocity (Re number) and curvature of the device (κ), the secondary flow arising in a coiled tube influences the fractionation process. By changing the tube curvature and the flow velocity, it has been shown that there are significant differences in the fractionation results. This can be explained by secondary flow which affects the flow field in a given cross section of the tube. At lower average flow velocities, a region of higher flow velocity in the outer bend allows longer fibers to pass faster through the tube and compared to the straight setup a somewhat tighter network is formed.

At a higher flow velocity, the arising secondary flow is more pronounced which results in a decrease of the ratio between local maximum and mean flow velocity. This in turn leads to a rather even distribution of the fiber material over the whole cross section.

The impact is more pronounced for the chemical pulp, showing a higher proportion of longer fibers. The induced mixing due to secondary flow at higher flow rates also affects the fractionation of the PGW, showing mostly short fibers and fine fiber material.

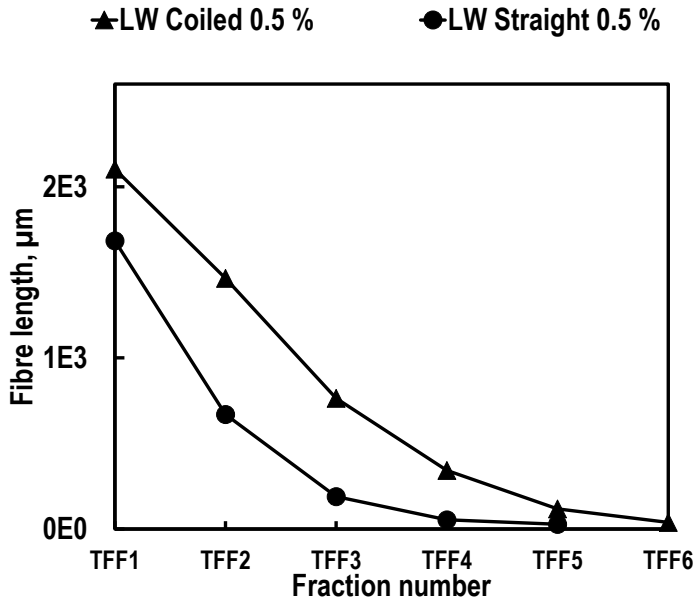

Figure 4-15 *Length weighted tube flow fractions of mechanical pulp (PGW) obtained at a volume flow of 5.2 l/min.*

Mass balances for 2.5 l/min and 5.2 l/min fractions for a coiled setup

To verify the model described above, a separate evaluation of the outer and the inner cross section of the tube was performed. An adapter (Figure 4-16) was designed which divides the flow into an inner (IA) and outer area (OA). This adapter was designed, to investigate the influence of the secondary flow. To do so, fiber mass balances and measurements of the mean fiber length have been performed using samples taken from the inner (IA) and the outer part (OA) of the cross section. Table 4-5 shows the results of the mass balances at 2.5 l/min and 5.2 l/min. To obtain enough material, three fractionation trials for each volume flow were performed. The samples from the inner and outer area of each trial were collect in two bins and used for the determination of the mass balances. Based on the fiber mass ratio between the inner and outer cross section it is apparent that a higher flow velocity and the above proposed concentration of long fibers is present in the outer region.

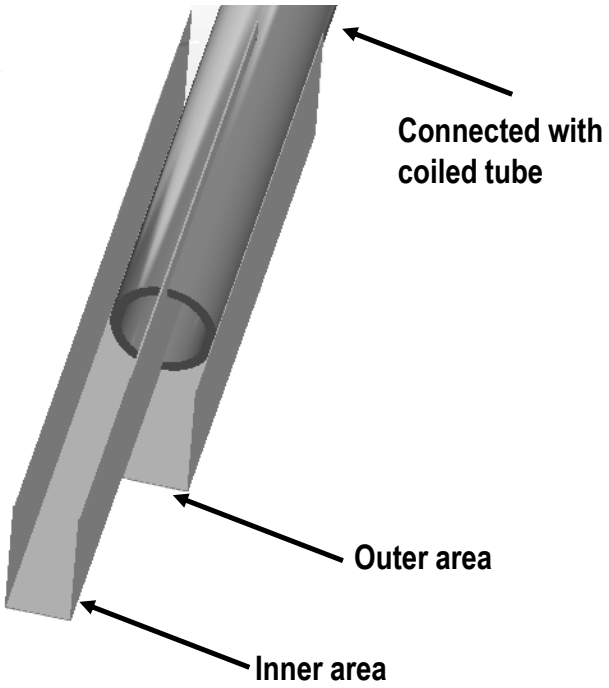

Figure 4-16 *Schematic view of the mass balance adapter.*

Table 4-6 shows a higher average fiber length of the sample taken from the outer region which is also supporting the theory.
At an increased volume flow of 5.2 l/min the fiber mass ratio decreases compared to 2.5 l/min. This effect can be explained by the secondary flow that causes mixing of the fibers over the entire cross section. Compared to 2.5 l/min, there is almost no difference in the mean fiber length at 5.2 l/min between the outer and inner area due to mixing.

Volume flow	2.5 l/min	5.2 l/min
Mean fiber mass inner area (IA), g	0.137	0.1595
Mean fiber mass outer area (OA), g	0.26	0.2325
Total fiber mass, g	0.397	0.391
STD inner area (IA), g	0.003	0.0015
STD outer are (OA), g	0.012	0.0045
Ratio fiber mass OA/IA	**1.8978**	**1.4577**

Table 4-5 *Fiber mass distribution of sulfite pulp in a coiled tube at different volume flow rates.*

	Mean fiber length LW
2.5 l/min IA	1.647
2.5 l/min OA	2.238
5.2 l/min IA	1.892
5.2 l/min OA	2.0275
Difference OA-IA at 2.5 l/min	**0.591**
Difference OA-IA at 5.2 l/min	**0.1355**

Table 4-6 *Mean fiber length values of sulfite pulp samples in a coiled tube at different volume flow rates (AR represents the arithmetic mean fiber length and LW represents the length weighted fiber length.*

Distribution of fines in a tube flow separation process

Fig 4-17 shows the behavior of fibers and fine particles in a suspension fractionated in the straight set up at a volume flow of 2.5 l/min. The x axis presents the timeline and the y axis shows the normalized particle number of fibers and fines as measured with the L&W Fiber Tester Plus. The graph clearly shows that the fibers tend to be captured by the faster flow and exit the tube faster than the fines i.e. longer particles come out first (indicated by the average length weighted fiber length).

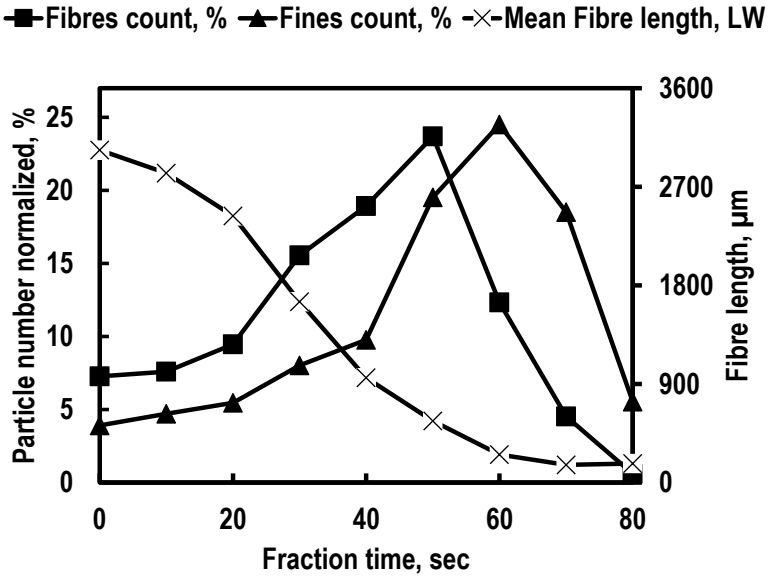

Figure 4-17 *The distribution of fibers and fines in a tube flow fraction of straight setup and the mean fiber length at a certain time interval at 2.5 l/min.*

Fines seem to be more evenly distributed. This can be explained by their smaller size. Due to this, the tendency to reach out to a faster flowing region and to be

dragged along is much lower than for fibrous particles. Still, fine material is to some extent dragged along with the longer fibers. Therefore fines do not show a normal distribution but are as well somewhat shifted to the long fiber fraction.
It should be kept in mind that all effects described above are related to long fibers being dragged along with faster flowing regions. Since the fines fraction is almost evenly distributed over the cross section, these particles may not be affected at all or at least only to a small extent by the secondary flow in the coiled configuration.

Conclusions

An investigation on the influence of secondary flow in a coiled tube set-up of a tube flow fractionation device has been performed by changing parameters such as curvature and flow velocity.
Based on the results obtained from different investigations on the secondary flow in a coiled tube it is evident that different settings strongly affect the fractionation characteristics. If a sharp separation between long fibers and short fibers/fines is required, fractionation in a coiled tube at low flow velocities seems beneficial. If a wider distribution of long fibers, short fibers and fines is required, fractionation with a straight tube at low flow velocities will lead to better results. Furthermore it has been shown that in a coiled tube setup an increased volume flow leads to a decrease in the selectivity between fibers and fines and similar fractions like in the straight set up are obtained. Since a straight setup is not very applicable in the laboratory, knowledge about the effect of secondary flow and the possibility to affect the separation in a coiled setup is of considerable interest.

4.2 Implementation of a laboratory pressure screen for separation of fines

4.2.1 Introduction

The primary application area of screening is to remove contaminants, that deteriorate the appearance and strength properties of paper. Nowadays, pressure screens are increasingly used to fractionate or separate different fiber fractions for targeted processing.
Fiber fractionation is defined by the separation of pulp fibers by quality (fiber length, coarseness, specific area etc.) to improve the final value of a product. It is an efficient method of producing higher quality and a more uniform pulp.
In softwood kraft pulping, pressure screens are used to produce top and base stock

from a single high yield cook to make multiply board. In TMP production, the fractionation with pressure screens of high freeness pulp and subsequent long fiber refining has shown to improve strength. Furthermore, the fractionation of low freeness pulp and long fiber refining has shown to improve sheet structure, optical and printing characteristics (Corson et al. [1996], Corson et al. [1997]). In case of recycled fiber production and subsequent refining of the long fiber fraction, fiber fractionation improves strength, brightness and reduces energy consumption in the papermaking process (Scott and Abubakr [1994], Mayovsky [1998], Lapierre et al. [1998]).
Today, fiber fractionation with pressure screens is also used for several other applications including improving the reinforcement potential of the pulp by increasing the tensile strength and freeness or to separate different fiber and fines fractions for further applications (Björk et al. [2015].

4.2.2 Pressure screening design

In the following chapters, literature review on pressure screen design and mathematical descriptions of separation performance are to a large extent based on the review "A Lecture on Pressure Screening" by Olson [2003].

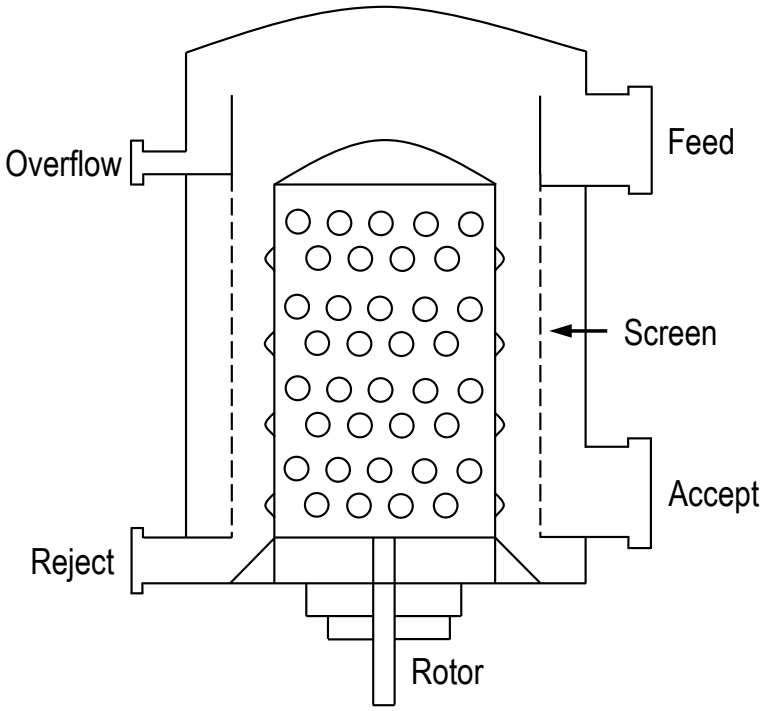

Figure 4-18 *Schematic view of a pressure screen (adapted from Olson [2003]).*

In a pressure screen, pulp and contaminants are transported through the feed port. The pulp fibers flow down between the screen plate and the rotor where pulp fibers preferentially pass through the screen and out through the accept port. The remaining pulp and contaminants pass the reject port.
In case of fiber fractionation, small fibers pass through the screen while the long fiber fraction is retained in the pressure screen. Figure 4-18 shows a schematic view of a pressure screen.

Configurations and rotors

Three different configurations of pressure screens are mainly used (see Figure 4-19). The **outflow** configuration is the most common screen. Pulp is transported from the inside of the screen plate cylinder to the outside. Long fibers and contaminants are retained inside the plate and pass the reject port. The rotor is mounted on the inside of the screen plate. In contrast to the outflow configuration, in the **inflow** pressure screen setup, pulp flows from the outside of the screen cylinder to the inside. Long fibers and contaminants are retained outside the screen plate cylinder. The rotor is mounted at the outside of the screen plate. Due to the outside rotor configuration, centrifugal forces keep heavy contaminants away from the screen.
The **inflow/outflow** configuration provides higher screen plate area for the size of the screen. This setup is typically used for headbox screens.
In pressure screening, **rotors** are used to create negative and positive pressure pulses that prevent pulp accumulations on the screen plate. This can be achieved by having either foil rotors or specialized bumps on a rotor drum moving at a high velocity near the screen plate. The magnitude of the pressure pulses is the main difference between the various types of rotor designs available. The higher the magnitude of pressure pulse of the rotor, the higher the screen capacity is.

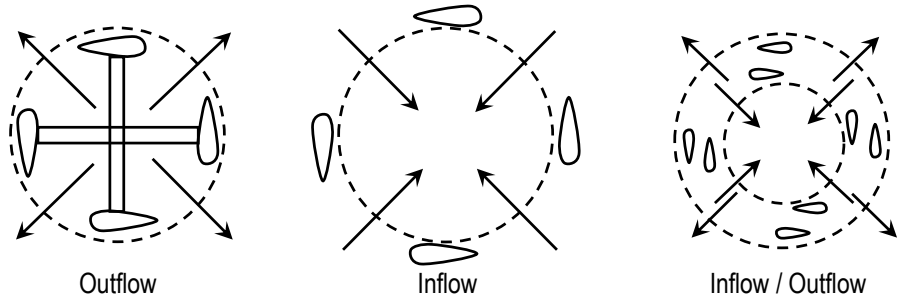

Figure 4-19 *Different types of pressure screens (adapted from Olson [2003]).*

By increasing the rotational velocity the pulse frequency also increases and therefore the capacity increases by clearing the apertures more often.

In case of barrier screening, high pulse rotors are preferred. In barrier screening, oversized particles are removed from the pulp because they are physically larger than the screenplate holes and therefore they do not pass through the apertures. In probability screening (fractionation and small shives) low pulse rotors are used. Here, particles are smaller than the apertures and have therefore some probability to pass through the apertures. Rotors also generate a high tangential fluid velocity at the surface of the screen plate. This effect increases the screening efficiency and hinders contaminants to enter the screen plate. Due to the high rotor velocity, pulp gets fluidized which prevents the area near the screen plate to have a too high pulp consistency.
The most commonly used rotor types are:

- Foiled rotors
  A positive and negative pressure pulse is generated by passing an airfoil shaped blade over a screen basket surface. The amplitude of pressure pulse can be controlled by the distance between the foil and screen basket. Figure 4-20 shows a schematic view of pressure pulses created by a foil rotor.
- Pump rotors
  Bump rotors consists of protruding parts (bumps) which are mounted on a solid core. They create the required pressure pulses.
- Lobe and S-rotors
  They are high amplitude pulse rotors, for medium consistency applications.

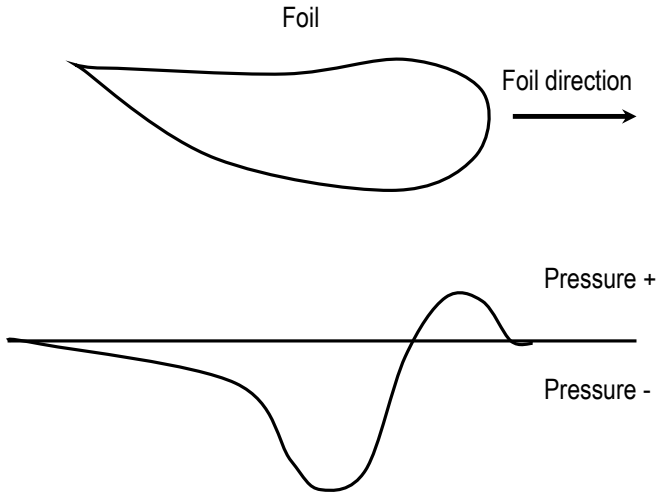

Figure 4-20 *Schematic view of the pressure pulse generated by a foil rotor (adapted from Olson [2003]).*

Screen plates

Screen plates affect the screening performance to the highest extent. The first screen baskets were smooth screens with round holes drilled in them and they are still widely used. They are easy to manufacture and therefore cheaper than slotted screen plates. Holed screen plates are often used as protection or as fractionation screens. Smooth holed screen plates separate fibers by length better than slotted screen plates. The drawback of holed screen plates is, that they have a poor ability of removing contaminants.
Due to the fact that holed screen plates efficiently fractionate long fibers into the reject port, there is a considerable increase of the consistency in the reject port, especially at low volumetric reject ratios. An increased consistency in the reject port can lead to screen failure by plugging of the screen plate or the reject port.
Today, contours are used for holed screen plates to increase the capacity (Olson [2003]).
In the case of contaminants removal, pressure screens are equipped with slotted screen plates. Since the implementation of contours, the capacity of slotted screens has increased to a point where slot widths are small enough to be an effective barrier to remove most of the contaminants. Nowadays, the state-of-the-art pressure screen device which is equipped with a slotted screen plate can have slot widths of 0.2 mm for softwood kraft pulp screening and 0.15 mm for softwood TMP pulps.

4.2.3 Theory of screening

This section describes the fundamental mechanisms of screening and the derivation of performance equations to design and optimize pressure screen devices.

Probability and barrier screening

In pressure screening, the passage of contaminant particles is limited by either barrier screening or probability screening. In barrier screening, oversized particles cannot fit through the apertures under any condition. This type of screening, called "ideal screening" has 100 % efficiency and 0 % loss.
In probability screening, particles can fit through, but they have some probability of passing through the aperture. Therefore, small shives fit through the screen, but still their passage is inhibited by other factors such as particle orientation or interaction with other particles.
In fact, fiber fractionation is always probability screening since every fiber is able to fit through the screen. Therefore, screening is always less than 100 % efficient and

further sensitive to screen design and operation (Olson [2003], Olson [1996]).
The mechanisms of particle passage through a screen plate in probability screening is still largely unconfirmed. However, there are several mechanisms described in literature.
A simple description about the retention of long fibers is given by the fiber mat theory. This theory states that long fibers are blocked to flow through a screen plate because they are blocked by a fiber mat. Studies based on high speed video analysis have shown that a properly operated screen does not show a fiber mat on the screen plate.
The turning and alignment theory both described the inability of long particles (fibers) to turn sufficiently at an aperture opening to pass through the aperture. The alignment theory proposes that particles which are close to the screen plate are forced to follow the tangential flow direction. This effect enhances the turning effect on the screen plate.
The wall effect theory (see Figure 4-21) describes a fiber length dependent concentration gradient at the screen plate surface. This means, that small fibers have a higher probability to pass through the screen because of their closer proximity to the plate. Long fibers tend to be farther away from the screen and therefore do not pass as easy as short fibers (Olson [1996]).
Today, extensive rotor foil and screen basket studies based on CFD flow simulations were carried out to find new ways of controlling pressure screen throughput efficiency, increased capacity and quality of screening as well a reduction in energy consumption (Feng et al. [2005], Lindroos and Puro [2007]).

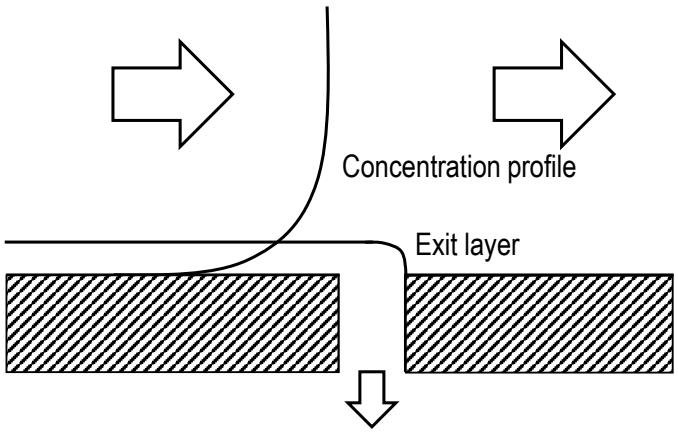

Figure 4-21 *Concentration gradient theory (adapted from Olson [2003]).*

4.2.4 Performance equations

Due to the lack of theoretical understanding of particle passage through a screen, performance equations have been introduced to describe consistency changes and contaminant removal and to design and operate pressure screens.

Consistency changes

During the separation process between the fine and coarse fraction in a pressure screen device, different consistencies of the feed, reject and accept flow occur. The accept flow has a lower consistency than the feed flow and consequently, the reject consistency increases. This effect is known as "reject thickening" which can lead to screen failure. This phenomenon occurs, if the consistency of the reject pulp is too high and therefore blocks the reject pipe. If the pulp consistency of the feed increases, plugging of the screen plate apertures can occur.
The particle passage ratio P can be explained by the particle concentration (contaminants, fibers, pulp) passing through a single aperture divided by the particle concentration of the remaining pulp in the pressure screen.

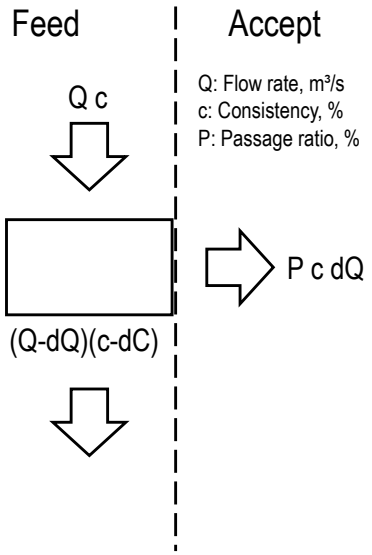

Figure 4-22 *Mass balance through a screen cross sectional element (adapted from Olson [2003]).*

According to Olson [2003], this model can be used, if the control volume, which is an element of cross section (see Figure 4-22), is located in the middle of the pressure screen. Further, it is assumed that on the one hand the flow between the rotor and the screen plate is a plug flow and on the other hand the flow in the tangential

direction is ideal mixed.
Figure 4-22 shows the mass balance through a screen cross sectional element.
The average passage ratio of pulp (P_{pulp}) is defined as:

$$P_{pulp} = \frac{c_{single \cdot pulp}}{c_{total \cdot pulp}} \tag{4.3}$$

$c_{single \cdot pulp}$ is defined as the the consistency of pulp after passing a single screen aperture and $c_{total \cdot pulp}$ is defined as the consistency of the pulp inside the pressure screen. After mathematical simplification to:

$$(P_{pulp} - 1)\frac{dQ}{Q} = \frac{dc}{c} \tag{4.4}$$

And integrating from the feed port to the reject port ($Q = Q_F$ and $C = C_F$, $Q = Q_R$ and $C = C_R$) :

$$\int_{Q_F}^{Q_R} (P_{pulp} - 1)\frac{dQ}{Q} = \int_{c_F}^{c_R} \frac{dc}{c} \tag{4.5}$$

or

$$\frac{c_R}{c_F} = \left(\frac{Q_R}{Q_F}\right)^{P_{pulp}} \tag{4.6}$$

or

$$T = {R_v}^{P_{pulp}-1} \tag{4.7}$$

$R_v = Q_R/Q_F$ is referred to as the volumetric ratio and $T = c_R/c_F$ is known as the reject thickening factor. The consistency drop of the accept stream, defined as $D = c_A/c_F$ can be calculated and is given by

$$D = \frac{c_F - c_A}{c_F} = \frac{{R_v}^{P_{pulp}} - R_v}{1 - R_v} \tag{4.8}$$

Fines screening efficiency

According to Olson [2003], the contaminant removal efficiency, E, or shive removal efficiency is defined as:

$$E = \frac{Debris\ in\ Feed - Debris\ in\ Accept}{Debris\ in\ Feed} \tag{4.9}$$

In case of fines screening, a new parameter is introduced which describes the fines removal efficiency E_{fines} as:

$$E_{fines} = \frac{Mass\ content\ in\ Feed - Mass\ content\ in\ Reject}{Mass\ content\ in\ Feed} \tag{4.10}$$

or

$$E_{fines} = \frac{\dot{m}_{A_{fines}}}{\dot{m}_{F_{fines}}} = \frac{c_{A_{fines}}}{c_{F_{fines}}} \frac{Q_A}{Q_F} \tag{4.11}$$

where $c_{A_{Fines}}$ is the mass concentration of fines in the accept stream and $c_{F_{Fines}}$ is the mass concentration of fines in the feed stream.

4.2.5 Design of a laboratory pressure screen for separation of fines

As mentioned in Chapter 2.8.3, conventional laboratory fractionation devices for fiber-fines fractionation are the Bauer McNett fractionator and the Britt Dynamic Drainage Jar (BDDJ) tester. The main drawback when using these devices is the small amount of pulp that can be treated in a single step (10 g BMcN, 5 g BDDJ) i.e. only small amounts of fines can be produced. To allow further processing, thickening of such a highly diluted suspension is needed.
Recently research does increasingly focus on the fines fraction. Therefore the need for new technologies for fines separation in a laboratory and industrial scale is of utmost importance in this research field to be able to conduct respective trials with reasonable effort.
One aim of this thesis was to provide a new laboratory method of continuous fines separation where quantities of fines fractions of more than 100 g/h of oven dried material can be produced. Therefore, a lab-pressure screen was implemented to carry out this task. The design and implementation of the pressure screen as well detailed results are presented in the following chapters.

Considerations to the design and construction of the pressure screen

Based on the application of the pressure screen, considerations regarding the design and construction are described below:

- Barrels of 60 l maximum capacity are used to collect the accept and reject flow to allow handling of the barrels in the laboratory. In case of the assumption, that the pressure screen can be operated at an volumetric accept/reject ratio of 80/20, a resulting accept flow of 12 l/min allow running the device at least 5 minutes which shows a suitable period of time for changing and preparation

of the 60 l barrels. Therefore a maximum feed flow of 15 l/min can be used for fines separation.

- The height of the corpus is 50 mm flat to avoid thickening along the height of the pulp suspension in the pressure screen.
- The diameter of the foil rotor (230 mm) was chosen in order to achieve a rotor velocity of 17 m/s at 1405 rpm (comparable value to industrial devices)
- All the other dimensions of the pressure screen are the result of the considerations taken above

4.2.6 Overview of the technical data and the design of the pressure screen at the IPZ

The laboratory pressure screen which was implemented at the Institute of Paper, Pulp and Fiber Technology at Graz University of Technology was designed based on a collaboration with the Institute of Paper Technology and Mechanical Process Engineering at the Technical University in Darmstadt. Their lab-pressure screen was designed to simulate the PMV pilot pressure screen (type Voith MS 0) at volumetric flows 20 times lower than those of the pilot screen. To get comparable results to the pilot pressure screen (industrial pressure screen design), screen diameter and rotor setup are the same (Ewald et al. [2014]).
The pressure screen which was implemented at the IPZ is however an evolution from its original design having several detail improvements and new features which are presented in this chapter. Figure 4-23 gives an detailed view of the pressure screen including main dimensions of the device.
The height of the pressure screen is 50 mm in order to avoid thickening of the pulp suspension along the height of the device. The screen area (19.8 cm^2) was relatively small designed in order to be able to change the screen plates easily and to reduce excessive volumetric accept flow (reject thickening). There are several Bauer McNett equivalent screens (30, 50, 100 mesh) available for subfractionation of different pulp suspensions. For separation of fines fractions, a 100 µm (laser perforated spring steel) hole screen was implemented (see Figure 4-24).

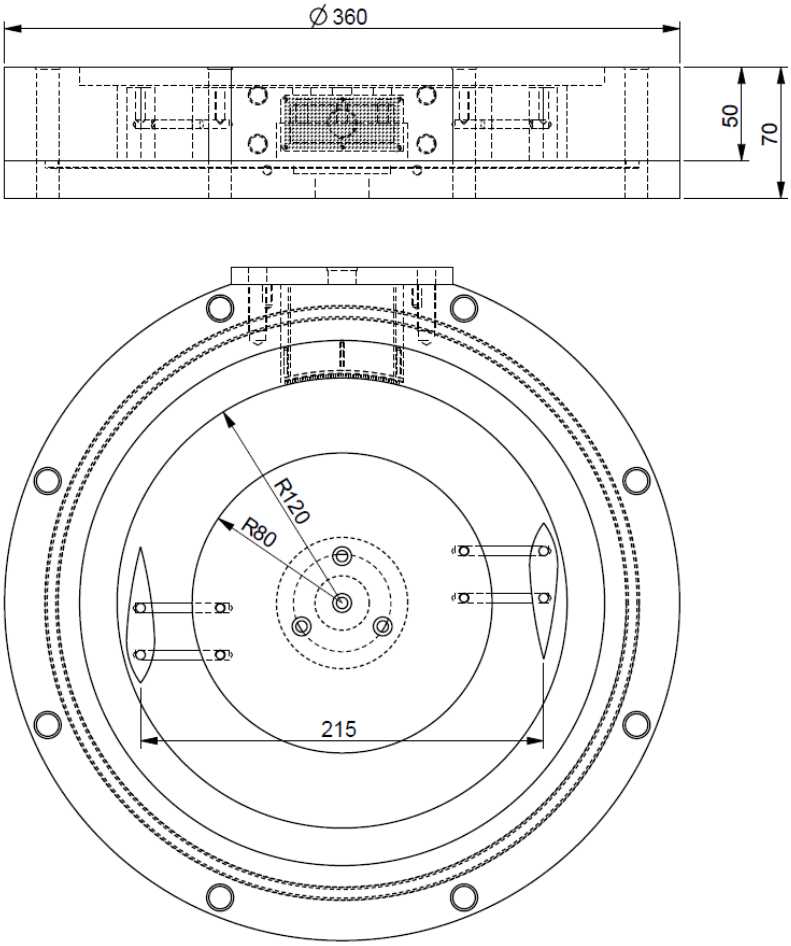

Figure 4-23 *Detail view of the pressure screen device at the IPZ.*

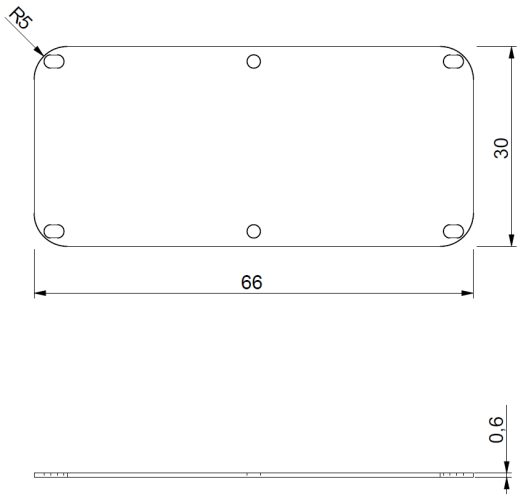

Figure 4-24 *Detail view of the 100* µm *screen plate used for fines separation.*

First evaluation results showed, that the fines fraction obtained from the 100 µm screen can be compared to those from the BDDJ fines fraction (see Chapter 4.2.9).

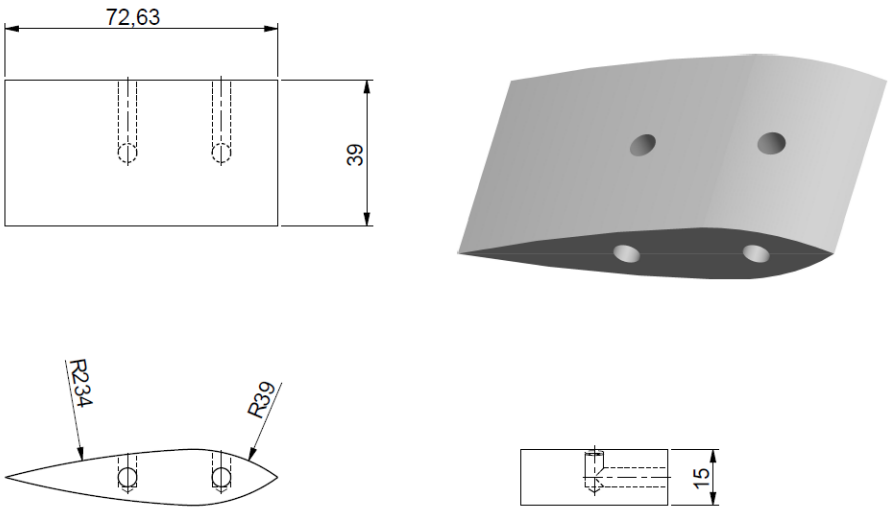

Figure 4-25 *Detail view of the pressure screen foil.*

A pulp suspension enters and leaves the pressure screen tangentially while the accept flow suspension leaves the pressure screen radially. The inlet as well outlet ports are connected with ball valves to control volume flow ratios and the internal pressure of the pressure screen device. A deaeration ball valve is mounted on the transparent top cover of the pressure screen to remove air inside the device during the starting process.
Further, the deaeration ball valve is needed for emptying and cleaning the pressure screen (see Figure 4-30). The cover of the pressure screen consists of a transparent material which allows visualization of the separation process inside the screen. For an easy access for cleaning the device in case of stock changes or plugging of screens, the cover is mounted and fixed by three clips.
The foil rotor is driven by an electric engine and as a results of the outer foil diameter (see Figure 4-23), 17 m/s tangential rotor velocity can be achieved at maximum rotation velocity of the electric engine. This foil rotor accelerates the pulp inside the chamber to a high tangential velocity. To avoid vibrations from the electric motor, the rotor is mounted on a claw coupling. Figure 4-26 gives an overview about the whole laboratory pressure screen unit. The pulp suspension is pumped from a feed tank to the pressure screen through the inlet where the separation process takes place.

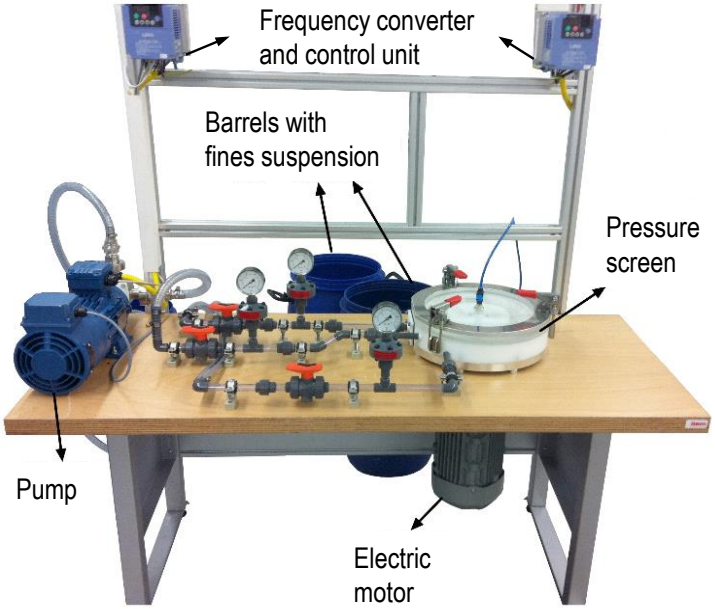

Figure 4-26 *Overview of the pressure screen device at the IPZ.*

The fines suspension (accept flow) is collected in a separate container and the remaining pulp is either transferred back to the feed tank through the outlet port (reject flow) or in a separate container. Several washing cycles are carried out in order to remove the fines from the pulp.

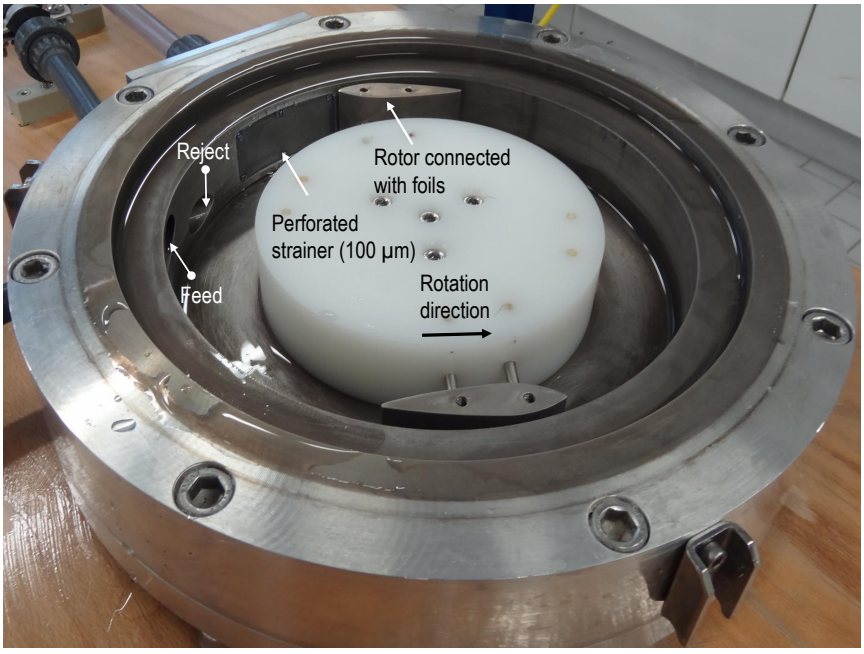

Figure 4-27 *Detailed view of the foil rotor inside the pressure screen.*

Positive pressure pulses are generated at the leading edge of the airfoil shaped rotor blades (see Figure 4-25) which push the fines through a perforated strainer (hole diameter 100 µm). Negative pressure pulses at the rear side of the foils remove fibers from the strainer to prevent plugging (see Figure 4-28 and 4-29). Furthermore, the foil rotor also introduces turbulence, which mixes the suspension and keeps the pulp fluidized (see Figure 4-27).

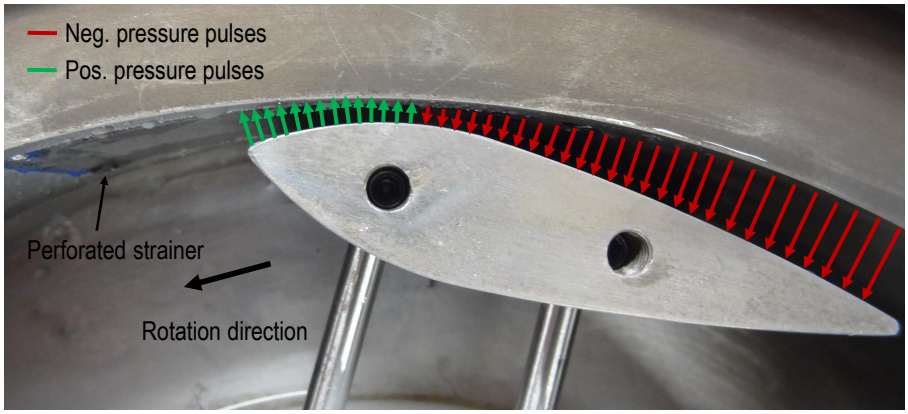

Figure 4-28 *Positive and negative pressure pulses generated by a foil rotor.*

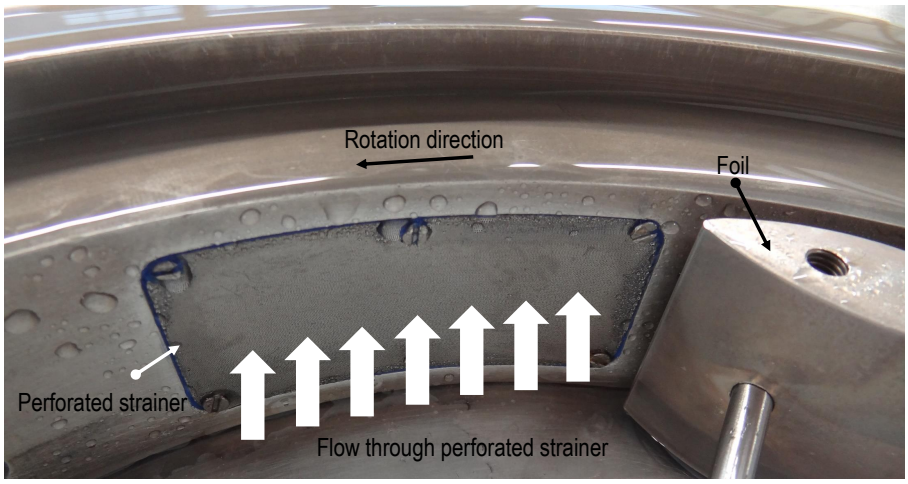

Figure 4-29 *Detailed view of the perforated strainer and the foil rotor.*

Figure 4-28 and Figure 4-29 show the principle of fines separation through a screen including a visualization of negative and positive pressure pulses induced by a rotating foil.

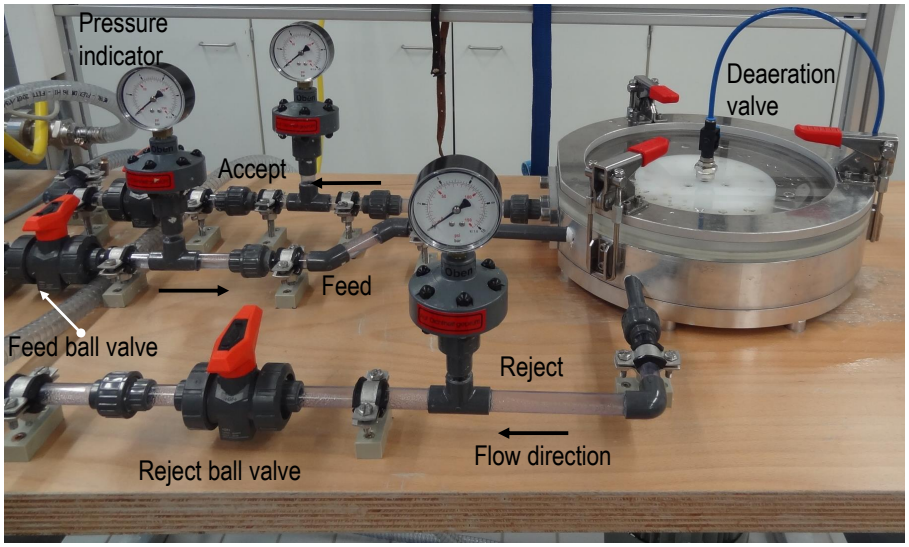

Figure 4-30 *General view of the pressure screen device, including ball valves and flow directions of feed, reject and accept flow.*

4.2.7 Repeatability of pressure screening

Based on three independent separation trials (bleached unrefined kraft pulp), it is evident that the pressure screen has a high repeatability. The three trials were performed using equal parameters such as feed flow, accept-reject ratio and consistency of the pulp (see Figure 4-31).

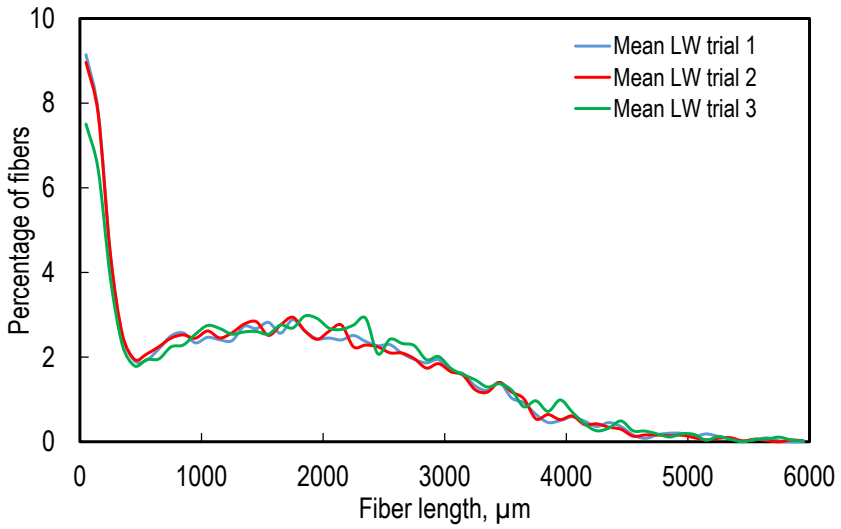

Figure 4-31 *Repeatability length weighted fiber length distribution of the reject flow of three different trials of a bleached unrefined kraft pulp.*

Table 4-7 shows the mean length weighted fibre length including the standard deviation and the 95 % confidence interval of three independent trials.

	Mean fiber length	Stand. Dev.	95% conf.
Reject, arithmetic	0.2385	0.0206	0.0165
Reject, length weighted	1.6633	0.0709	0.0568

Table 4-7 *Mean fiber length, standard deviation and 95 % confidence interval of the reject flow of three independent trials.*

4.2.8 Evaluation results of process parameters

In order to determine the relevant process parameter on separation performance of the pressure screen device, evaluation trials have been performed. In these experiments, the process parameters volumetric accept-reject ratio (**A**), volumetric feed flow (**B**) and feed consistency (**C**) were changed.
This investigation was based on a statistical experimental design of third order including the mean fiber length results of each trial and is illustrated in Table 4-8. The volumetric accept-reject ratio, volumetric feed flow and the feed consistency, (see Table 4-8) were varied to determine the most relevant parameter (A, B, C) for separation performance.
A bleached unrefined sulfite pulp was used (50l total volume in barrel) where the reject pulp was transferred back into feed tank. For each trial, separation with the pressure screen was performed for 15 minutes. The reject fractions obtained from evaluation experiments were then collected in separate barrels. To ensure a constant feed pulp consistency during separation, additional water was pumped into the feed tank to balance the loss of water caused by the removal of fines (accept flow out of the pressure screen). Afterwards the fiber morphology - the arithmetic mean fiber length - of each fraction was determined using a L&W Fiber Tester Plus.
Table 4-8 shows the influence of parameter A, B and C on separation performance based on arithmetic mean fiber lengths obtained from the reject pulp. This means, that if a higher amount of fines is removed from the pulp, the arithmetic mean fiber length increases in the reject pulp flow.

Trial number	A	B	C	Arithmetic mean fiber length, mm
0	50	12	0.35	0.569
1	30	8	0.1	0.336
2	70	8	0.1	0.789
3	30	14	0.1	0.452
4	70	14	0.1	1.144
5	30	8	0.6	0.307
6	70	8	0.6	0.657
7	30	14	0.6	0.365
8	70	14	0.6	0.914

Table 4-8 *Statistical experimental design of third order and arithmetic mean fiber length results obtained from each fraction.*

A statistical analysis based on the statistical plan was performed using Minitab. Figure 4-32 shows the Pareto diagramm of standardized effects (95 % confidence level). Based on this diagram it is evident that only parameter A and parameter B have a significant influence on fractionation results obtained from fiber length measurements. The combination of the main parameters (A, B, C) also does not show a statistical significance. Therefore, only the main parameters A, B and C were used in the current linear statistical model (see Equation 4.12).

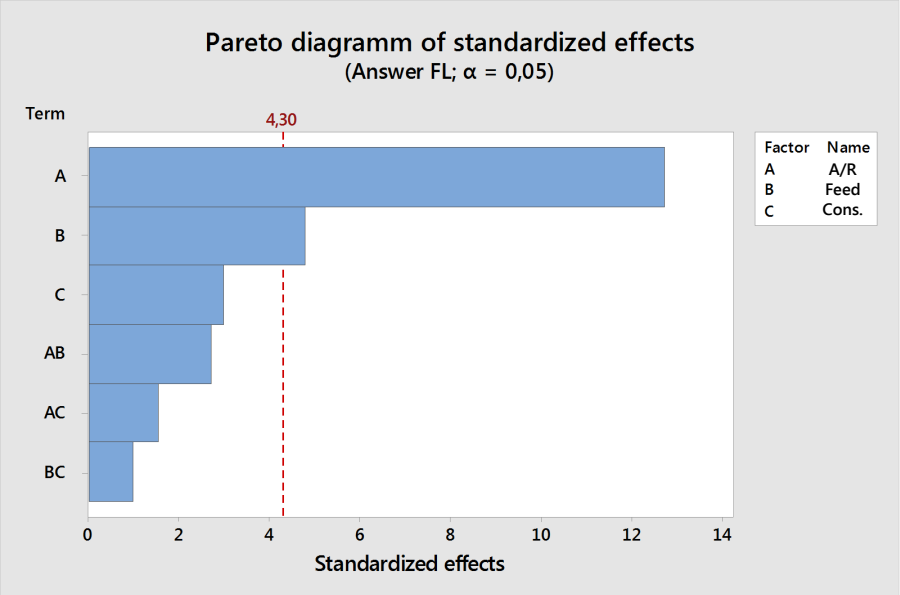

Figure 4-32 *Pareto diagram of standardized effects (95 % confidence level).*

$$FL = -0.293 + 0.01278 \cdot A + 0.0317 \cdot B - 0.239 \cdot C \tag{4.12}$$

Table 4-9 gives an overview about the main statistical parameters obtained for this model:

D	R^2	R^2 corr.
0.0905753	93.83	90.13

Table 4-9 *Main statistical parameters obtained for the current statistical model. D is defined to be the standard distance between the data points and regression line.*

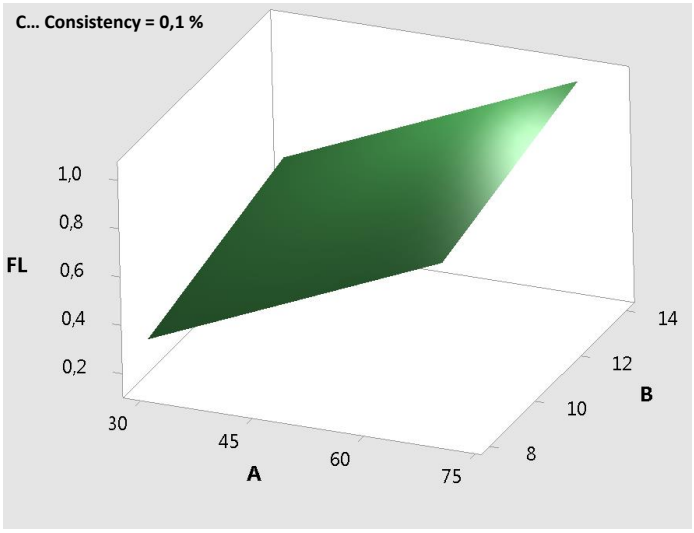

Figure 4-33 *Evaluation results of parameter A and parameter B based on fiber length at 0.1 % consistency.*

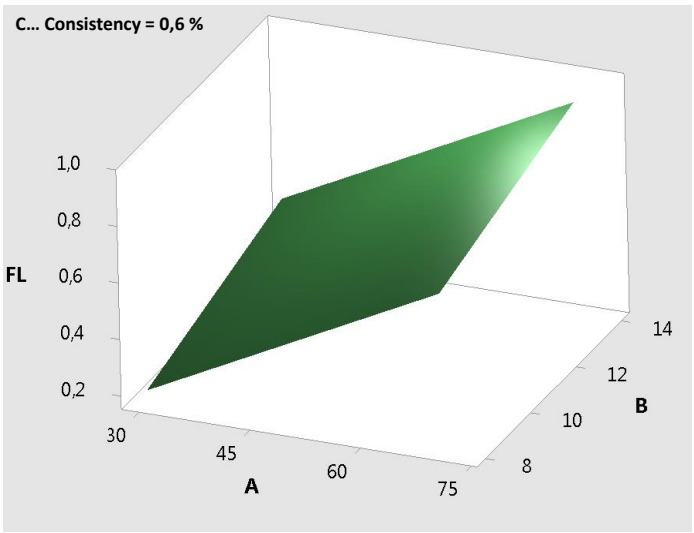

Figure 4-34 *Evaluation results of parameter A and parameter B based on fiber length at 0.6 % consistency.*

Figure 4-33 and Figure 4-34 both illustrate the influence of parameter A and parameter B on the fiber length of the reject flow at 0.1 % consistency and 0.6 % consistency. It has to be pointed out here, that an increase in fiber length refers to a high separation efficiency of the pressure screen and a low fiber length refers to a bad separation efficiency, respectively.
Based on these figures, it is evident that a high separation efficiency of fines can be obtained at high accept-reject ratios (70/30) and increased feed flow (14 l/min).

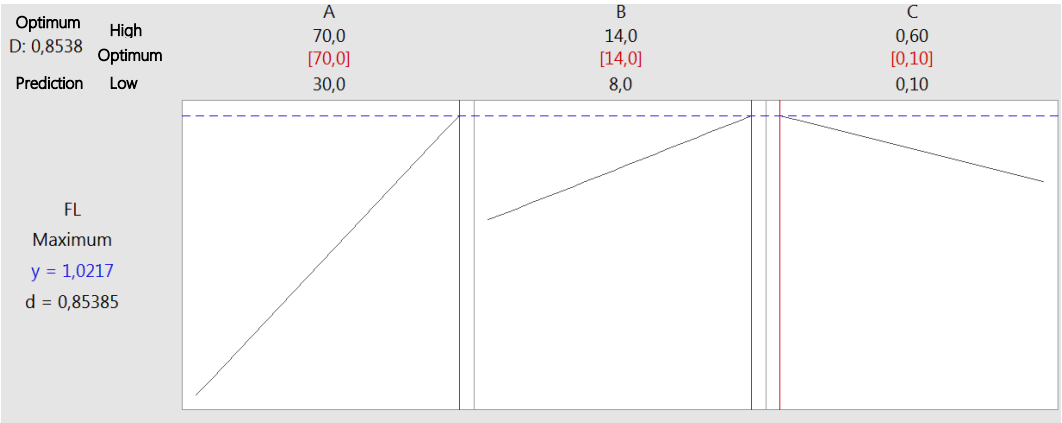

Figure 4-35 *Optimization results of process parameters A, B and C.*

Figure 4-35 shows a statistical optimization for the process parameters (A, B, C) of the pressure screen. Again, it is evident that high accept-reject ratios and high feed flows show the highest separation efficiency of fines.

4.2.9 Results of fines screening

The pressure screen can be operated either in a cyclic procedure, where the reject is transported back into the feed tank or in one pass where reject and accept are collected separately in different barrels. In case of the cyclic procedure, additional water has to be given to the feed tank to balance the feed flow consistency of the pressure screen. The reason for this is the reject thickening effect, where the major part of the water is transported away with the accept flow, which is then collected separately. The thickened reject flow is transported back to the feed tank where the pulp consistency would increase constantly.
In case of cyclic operation, the amount of fines separated from the pulp depends on several parameters, such as the total pulp amount in the feed tank, pulp consistency, feed volume flow, volumetric accept-reject ratio and operating time.
In the following chapter, performance equations and evaluation results are based on the one pass operation method. Several parameters influence the separation behav-

ior of the device. The main parameters which can be controlled are feed consistency, feed volume flow, reject thickening factor and the total pulp amount in the feed tank as well the operating time.

Reject thickening factor

The thickening effect of the reject flow, called "reject thickening" occurs because the accept flow has a lower consistency than the reject flow due to the fact that more water flows through the accept port than through the reject port (volume separation due to the volumetric accept-reject ratio). If the reject flow is too thick, failure in screening can occur or it blocks the screen or the reject pipe.
In these experiments, the pressure screen was operated based on the one pass method and a volumetric feed flow of 12 l/min was chosen for the testing procedure.
Figure 4-36 shows the reject thickening factor (T) of two different pulp types and pulp consistencies as a function of the volumetric reject ratio (R_v). It demonstrates too, how the volumetric reject ratio affects the consistency of the reject pulp, as predicted in Equation 4.7.

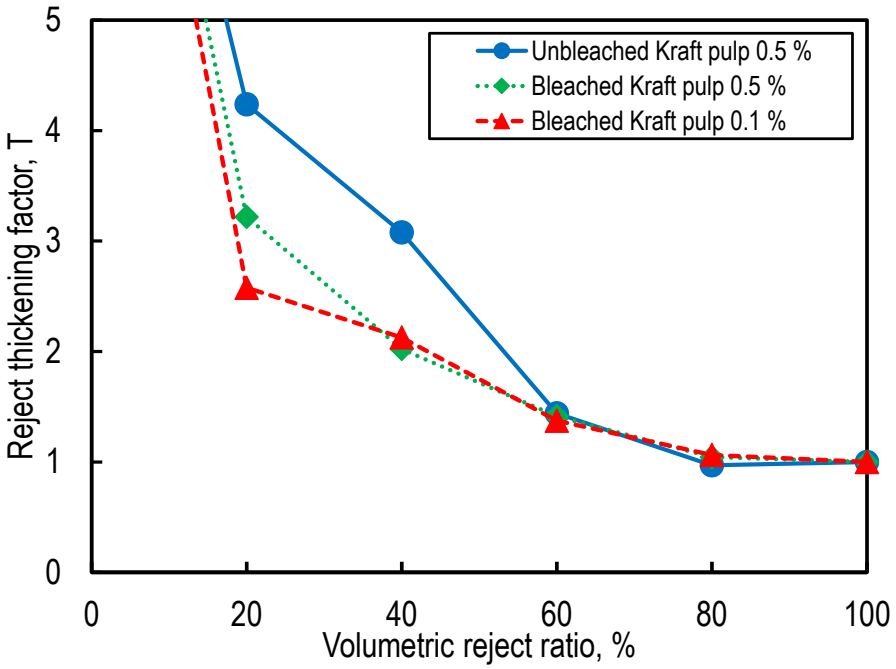

Figure 4-36 *Reject thickening factor, T, as a function of volumetric reject ratio, R_v at one pass operation of the pressure screen.*

Based on Figure 4-36 it is evident that at low volumetric reject flows, thickening of the pulp in the reject flow can be up to more than four times the feed flow. It has

to be point out here that due to this thickening effect, a higher feed consistency can lead to plugging of the reject port. Based on the investigations of reject thickening, it was possible to define the operating window for the feed consistency. It turned out that the maximum suitable feed consistency for efficient fines separation ranges between 0.1 % and 1 %.

Probability screening efficiency

The contaminant removal efficiency, or in our case the fines removal efficiency is defined in Equation 4.10 and demonstrates the ratio of the mass concentration of fines in the accept stream to the mass concentration of fines in the feed pulp stream. The fines removal efficiency on a probability basis is theoretically related to the accept-reject ratio, following the same analysis than for reject thickening (R_v).
Based on these investigations, it was shown that more than 60 % of fines can be removed in case of one pass operation of the pressure screen. This can be achieved by a volumetric accept reject ratio of 80/20 where large quantities of water are forced to flow through the screen and therefore dilution of the fines suspension occurs. This effect indicates the need of further processing steps in order to thicken the highly diluted fines suspension produced with the pressure screen.
Figure 4-37 demonstrates how efficiency differs with reject ratio, which is predicted by equation 4.10.

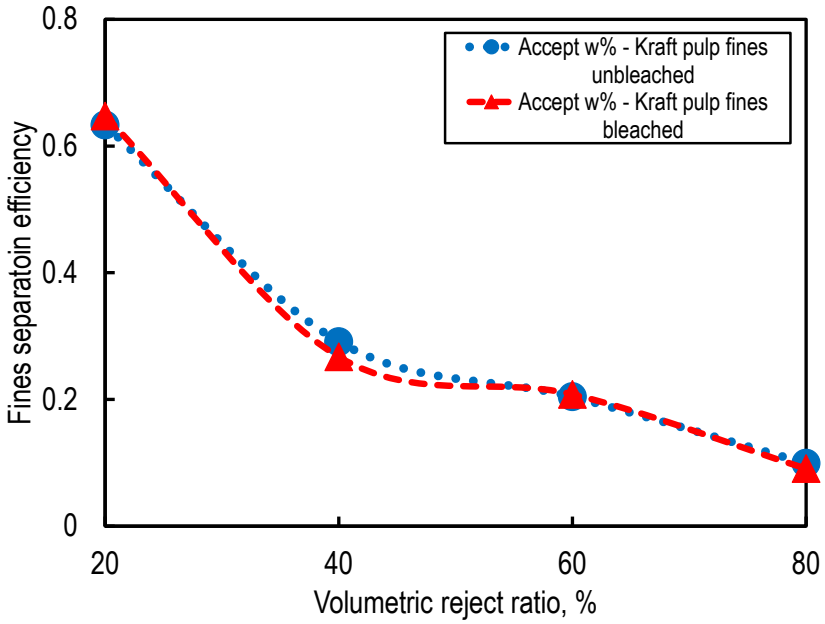

Figure 4-37 *Fines removal efficiency, E, of two different pulp types at a given feed consistency, as a function of the volumetric reject ratio R_v at one pass operation of the pressure screen.*

In Figure 4-38, a comparison between an original unbleached kraft pulp sample and the corresponding fines fraction is shown. From this figure and from figure 4-37 it is evident that the laboratory pressure screen has a high separation efficiency (**65% fines removal**). The majority of the produced fines fraction (> 80%) consists of particles which are smaller than 100 µm (see Figure 4-38).

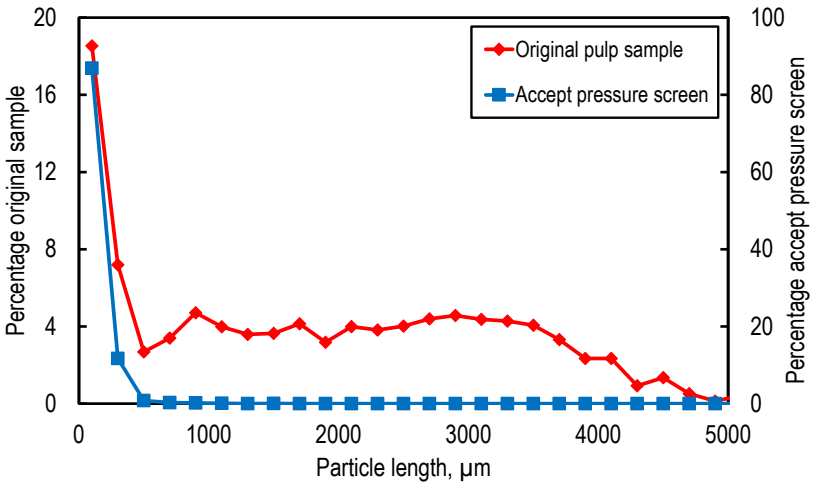

Figure 4-38 *Fines screening system example at one pass operation of the pressure screen.*

Comparison to conventional laboratory fines separation

The most common technical solution for isolating the fines fraction in the lab is the Britt Dynamic Drainage Jar (BDDJ) tester. In order to produce suitable fines fractions with the pressure screen for further laboratory investigations and applications, the obtained fines fractions has to be similar to those obtained with the BDDJ tester. Figure 4-39 shows a comparison based on length weighted fiber length distribution of fines fractions obtained from the BDDJ tester and from the pressure screen of a bleached unrefined kraft pulp.
Based on Figure 4-39 and Table 4-10 it is obvious that the pressure screen produces fines fractions with an equal length distribution than those produced with the BDDJ tester. Additionally, the mean length values of fines fractions of both devices show similar results.

	Pressure screen	BDDJ
Mean arithmetic particle length, mm	0.058	0.059
Mean length weighted particle length, mm	0.0945	0.094

Table 4-10 *Mean values of comparison measurements between the pressure screen and the BDDJ tester.*

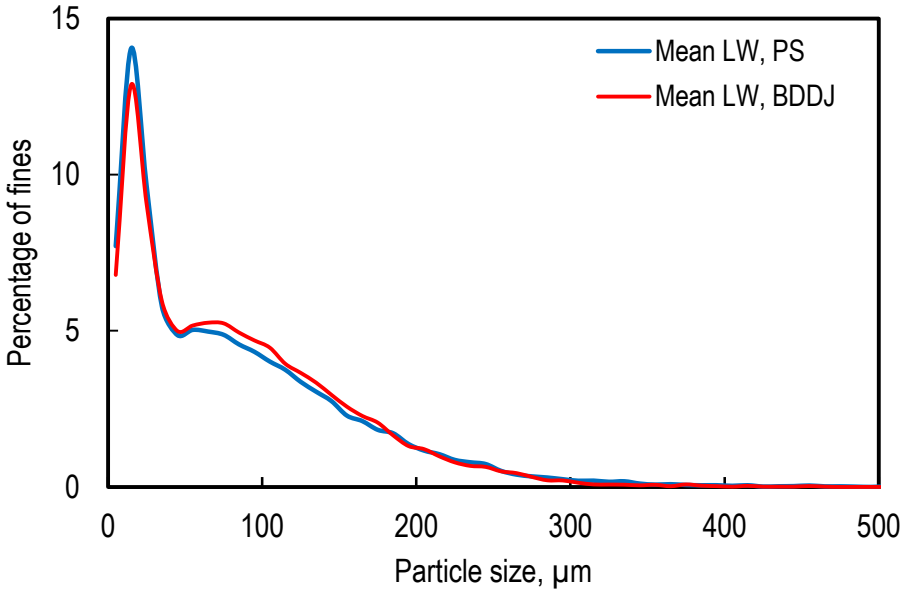

Figure 4-39 *Comparison measurements based on length weighted particle length distribution between the pressure screen (PS) and the Britt Dynamic Drainage Jar (BDDJ) tester.*

Example of a fines removal mass balance calculation

The example below illustrates a calculation based on one pass operation of the pressure screen representing the hourly screening capacity, global efficiency and the reject ratio of the system at the optimum operating point. The produced fines fraction has a low consistency (0.0145%). The diluting of the fines fraction is generated due to the volumetric accept/reject ratio (80/20) where large quantities of water are forced to exit through the screen (accept port).
In case of 15 l/min feed flow (0.5 % consistency) and a volumetric accept-reject ratio of 80/20:

Starting conditions:

$$\dot{m}_{F_{pulp}} = 4500\ g/h\ oven\ dried\ pulp\ or$$
$$F_{pulp} = 900\ l/h\ pulp\ suspension$$
$$\frac{R_{pulp}}{F_{pulp}} = 0.2$$
$$c_{\mathrm{fines_A}} = \mathbf{0.017\%}$$

Fines Material Balance:

$$E_{fines} = \frac{\dot{m}_{\mathrm{A}_{fines}}}{\dot{m}_{\mathrm{F}_{fines}}} = \frac{\dot{m}_{\mathrm{F}_{fines}} - \dot{m}_{\mathrm{R}_{fines}}}{\dot{m}_{\mathrm{F}_{fines}}} = \mathbf{0.65}$$

$$\dot{m}_{\mathrm{F}_{fines}} = \dot{m}_{\mathrm{A}_{fines}} + \dot{m}_{\mathrm{R}_{fines}}$$

$$\dot{m}_{\mathrm{F}_{fines}} = F_{\mathrm{pulp}} \cdot c_{\mathrm{fines_F}} = \mathbf{189.9\ g/h}\ \textit{oven dried fines}$$

$$\dot{m}_{\mathrm{A}_{fines}} = E_{fines} \cdot \dot{m}_{\mathrm{F}_{fines}} = \mathbf{123.4\ g/h}\ \textit{oven dried fines}$$

$$\dot{m}_{\mathrm{R}_{fines}} = \dot{m}_{\mathrm{F}_{fines}} - \dot{m}_{\mathrm{A}_{fines}} = \mathbf{66.5\ g/h}\ \textit{oven dried fines}$$

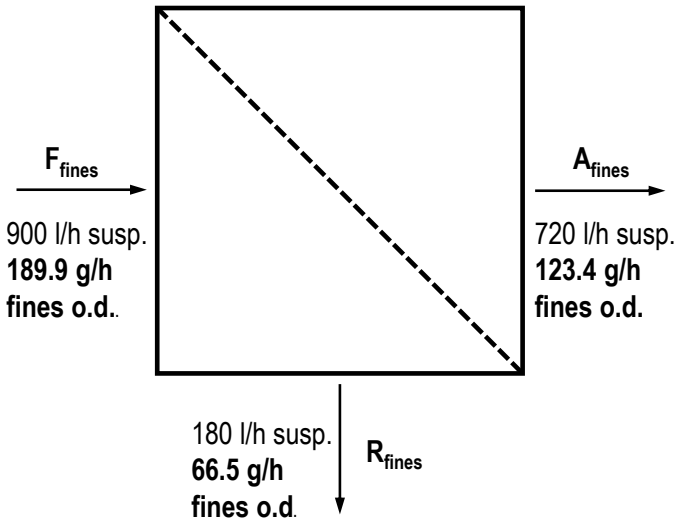

Figure 4-40 *Example of fines screening.*

Trials using different amounts of pulp showed that depending on the original fines content of a pulp, (5 - 40 % mass content Krogerus et al. [2002]) quantities up to 100 g of fines (oven dry mass) can be produced within one hour on the laboratory pressure screen. The solids content of the produced fines suspensions range from 0.01

to 0.1 %. In figure 4-40 the volume flow balance of the pressure screen shows that several hundred liters of suspension are produced within one hour. This indicates that for further processing an additional thickening step is needed.

4.2.10 Conclusions

Results from pressure screening show a high separation efficiency of more than 60 % for unbleached and bleached kraft pulps. The majority of the produced fines fraction (> 80 %) consists of particles which are smaller than 100 µm (see Figure 4-38).
Based on evaluation results, it was shown that the optimum working point for fines removal can be achieved with a high reject thickening factor, a high volumetric feed flow and a low pulp feed consistency.
Trials using different amounts of pulp showed that depending on the original fines content of a pulp (5 - 40 % mass content Krogerus et al. [2002]) quantities of more than 100 g of fines (oven dry mass) can be produced within one hour. Due to the low solids content of the fines fraction (accept flow) further treatments such as chemical modification or formation of handsheets are more difficult to perform. This indicates that for further processing an additional thickening step is needed to generate suitable fines suspensions.

4.3 Design and development of a dissolved air flotation cell for thickening of fines suspensions

The current chapter is divided into two different parts. The first section describes the general principles of dissolved air flotation (DAF). The most important principles of DAF such as bubble formation and size, particle-interactions and a bubble size distribution measurement method are described in this section. The second section deals with the design and construction of a lab-scale DAF device for thickening of fines as well with performance and evaluation results.

4.3.1 Introduction

The current literature review on DAF is partly based on the review paper of J.K. Edzwald "Dissolved air flotation and me" (Edzwald [2010]).
Dissolved air flotation technique was used as a method to separate particles, especially mineral ores in the early 1900's. In 1905, a US patent was issued for a technique using pressurized aeration followed by a pressure release to generate small air bubbles.
From these early beginnings, DAF has been used for several applications including: mineral separation, clarification of paper mill waste water or municipal and industrials waste sludge thickening.
Today, DAF is mainly used for drinking water clarification and will emerge as a new and important technology in western countries because of stricter regulations of filtration of surface waters.

4.3.2 Theoretical basics of DAF

General description of a DAF plant

Figure 4-41 illustrates a DAF plant for clarification of water. In general, DAF is a separation process where air bubbles are used to remove particles from its suspension.
The DAF tank can be divided into two zones where the front end is defined as the contact zone and the rear end as the separation zone. A baffle divides the contact zone from the separation zone.
Air bubbles are transported into the DAF cell. First, the air is dissolved under pressure in a vessel called saturator. The total amount of dissolved air depends on the saturator pressure. A typical overpressure value for saturator units is 500 kPa. Small

air bubbles are generated by an eventual pressure drop which have sizes between 10 - 100 µm. These small air bubbles generate a milky water-air bubble suspension in the DAF tank.
In the contact zone, collisions and attachment of particles or flocs with air bubbles takes place. Air bubbles which are attached to flocs are called floc bubble-aggregates. The suspension which is composed of floc-aggregates, free air bubbles and particles is transported to the separation zone. In the separation zone, bubble aggregates and single particles attached to air bubbles rise to the surface of the tank. The float layer at the surface of the tank consists of a mixture of air bubbles and particles attached to air bubbles. This layer is called float.
Over the time the float is concentrated producing a sludge that is removed from the tank by a scrapper.
The clarified water is removed from the bottom of the tank.

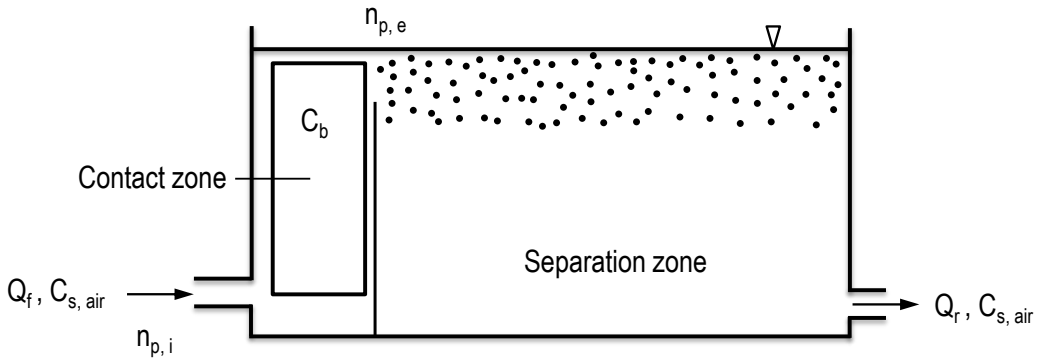

Figure 4-41 *Schematic view of the DAF tank used in the current work showing the contact zone and separation zone (partly adapted from Haarhoff and Edzwald [2004]).*

Bubble formation

In a DAF plant, bubbles are generated by the injection of pressurized water into a flotation tank and a subsequent pressure release. The process of bubble growth follows two steps: nucleation and subsequent bubble growth.
Due to the pressure difference, small nuclei are formed spontaneously according to the thermodynamic principle of minimizing the free energy. If air is assumed as an ideal gas, the critical diameter for homogenous nucleation is defined as:

$$d_{\mathrm{cb}} = 4\,\sigma\,/\Delta P \tag{4.13}$$

d_{cb} = critical bubble diameter, mm
σ = surface tension of water, N/m

ΔP = pressure difference across the nozzle, kPa

Different publications of bubble size measurements show, that DAF systems use bubble sizes in a range of 10 to 100 µm (Takahashi et al. [1979]). To achieve suitable bubble sizes, a rapid pressure drop has to be generated. Higher pressures produce smaller bubbles, but there is a limiting point in reducing the bubble size. Increasing the pressure more than 500 kPa has a small effect on bubble size (Heinanen et al. [1992]).
Figure 4-43 illustrates the critical bubble size diameter of the bubble nucleus as a function of the pressure change. It is evident that smaller bubbles are formed at higher pressure differences. The minimization of the free energy change is easier in a contaminated system or other surface containing scratches or crevices. After the nuclei growth, bubbles are formed in a second step.

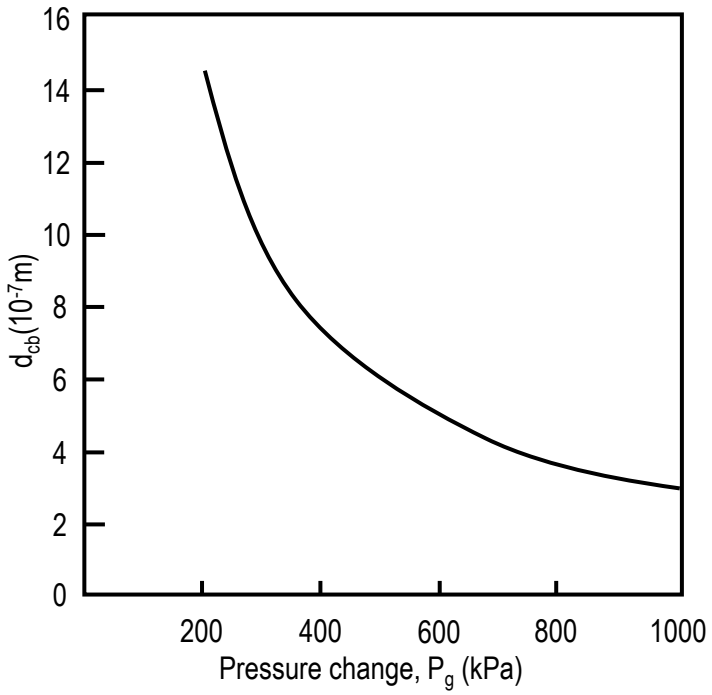

Figure 4-42 *Critical bubble diameter (d_{cb}) of bubble nucleus of air in water at 20°C as a function of the pressure change (adapted from Edzwald [1995]).*

The bubble rise velocity can be described with the Stokes law under laminar conditions. It is obvious that larger bubbles have higher rise velocities than smaller ones (see Figure 4-43). They exist either as ellipsoids (1 to 10 mm) or as spherical bubbles (<10 mm). For Stokes laminar flow conditions (for bubbles < 100 µm) the

bubble rise velocity can be calculated from:

$$u_b = g\, {d_b}^2 (\rho_w - \rho_b) / 18\, \mu \tag{4.14}$$

d_b = bubble diameter, mm
g = gravitational constant, m/s^2
μ is the dynamic viscosity of water, Pa s
ρ_w, ρ_b = density of water and air, kg/m^3
u_b = bubble rise velocity (fluid motion around the bubble relative to the bubble), m/s

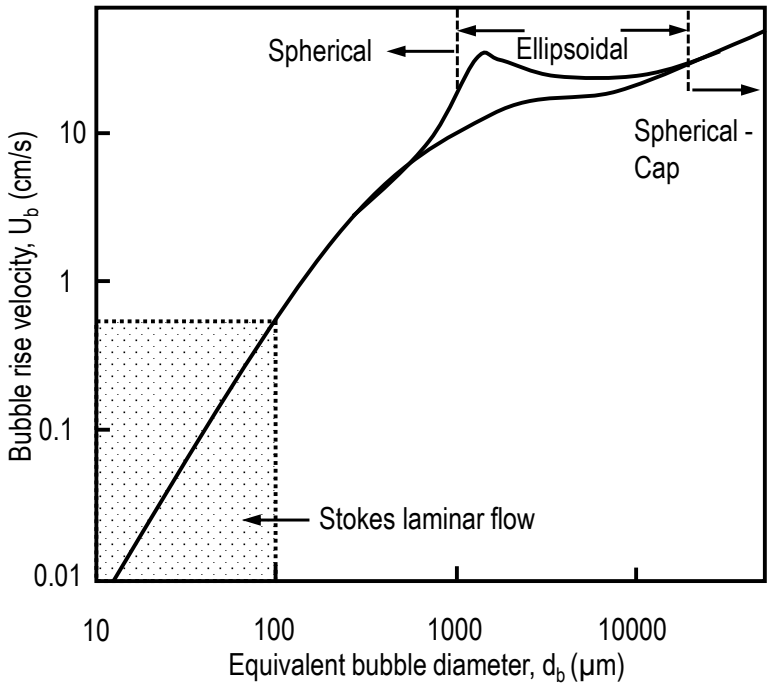

Figure 4-43 *Bubble rise velocity of air in water at 20°C. Bubbles <100 µm follow Stokes law (adapted from Edzwald [1995]).*

Bubble particle interactions

According to literature, there are three possible mechanisms for formation of aggregates consisting of bubbles and particles:
The first mechanism describes the entrapment of bubbles into flocs, where flocs are much larger than bubbles. The second mechanism describes the growth of a bubble on particles and the third mechanism deals with particle collisions and adhesion with bubbles. It has to be pointed out here, that mechanism three is the most important

mechanism in DAF systems (Kitchener and Gochin [1981]).
The main parameter to measure the floatation of particles by bubbles is the contact angle. The contact angle must be finite and large enough that the work of energy of adhesion for the water phase to the solid particle is less than the energy of cohesion of water. A larger contact angle shows hydrophobicity and good adhesion. The magnitude of the contact angle depends however on the size scale of bubbles and particles.
According to literature (Edzwald [1995]), there is an universal agreement and experimental evidence that two conditions are necessary for flotation: charge neutralization and production of hydrophobic particles.
Figure 4-45 gives an overview about the scale of bubbles and particles used for DAF and the contact angle between the absorbed bubble and particle.

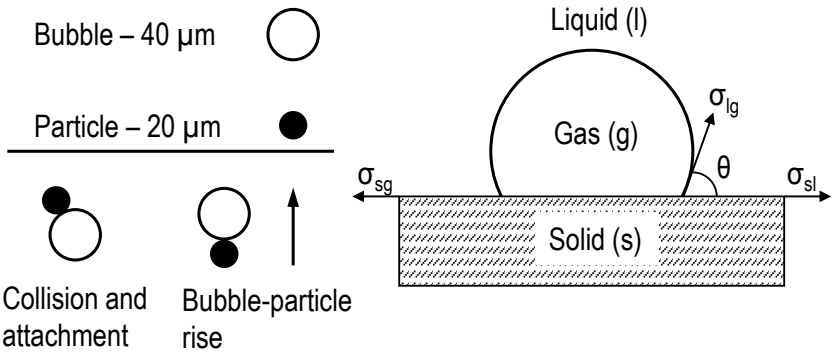

Figure 4-44 *Contact angle for bubble attachment to solid surfaces and scale of bubbles and particles in DAF systems (partly adapted from Edzwald [1995]).*

Charge neutralization

In general, flotation is not successful without the addition of a coagulant. For instance, polyaluminium chloride (PACl) is a positive charged polymeric aluminum species that affect particle destabilization via charge neutralization. Due to the addition of coagulant, the negative charge on the particle surface is reduced and flotation performance is enhanced. Overdosing of PACl or other coagulants lead to charge restabilization of the particles.

Hydrophobic particles

The adhesion or attachment of particles requires hydrophobic particles surfaces or at least hydrophobic spots on particles (e.g. hydrophobic parts of fines). The hy-

drophobicity of particles is increased by reducing the negative charge (Gochin and Solari [1983]).

Bubble generation and calculation of bubble supply

The injection and the subsequent pressure release causes saturated air to be released into the flotation tank. The concentration of air bubbles in the flotation system affects the bubble-particle collisions and is therefore an important parameter for the design and operation of a DAF plant. Based on the Henry's Law, the equilibrium mass concentration of dissolved air, after the pressure release, can be calculated. In case of the assumption that air is an ideal gas,

$$C_{\mathrm{sat}} = f\, P_{\mathrm{t}} / H_{\mathrm{air}} \tag{4.15}$$

$C_{\mathrm{sat}} =$ saturated mass concentration of air, mg/L
$f =$ saturator efficiency,
$P_{\mathrm{t}} =$ total air pressure of the saturator (plus one atmosphere), kPa
$H_{\mathrm{air}} =$ Henry's Law constant (4.18 kPa/mg/L at 20°C)

It has to be mentioned here, that air is an mixture of several gases consisting primarily of nitrogen and oxygen. Due to its nature, oxygen has a higher solubility than nitrogen under overpressure. The saturator efficiency can be expected between 60-70 % for unpacked saturators and 90 % for packed saturators (Edzwald et al. [1999]). The saturator efficiency is defined as the ratio of the air feed from the device to the amount of dissolved air in water.

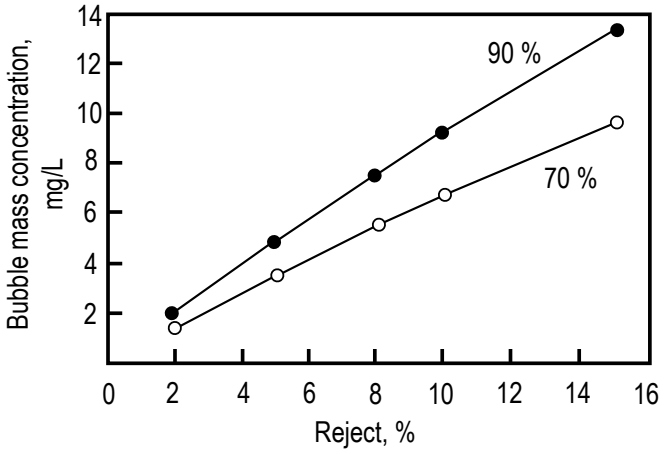

Figure 4-45 *Bubble mass concentration as a function of reject stream for two different saturator efficiencies (partly adapted from Edzwald [1995]).*

The mass concentration of the pressure release valve are calculated from Equation 4.15. The mass concentration describes the mass of air per unit volume of water in the reaction zone of the flotation tank. Figure 4-45 illustrates the bubble mass concentrations as a function of feed volume flow of saturated air of a conventional DAF plant (mass concentration data adopted from Edzwald [1995]).

Flocculation of fines suspensions

In flotation, the main approach to increase the separation efficiency is to increase the size of particles (d_p). Figure 4-46 shows a schematic example of separation efficiency as a function of particle size. It also shows an increase of separation efficiency with increasing particle diameter.

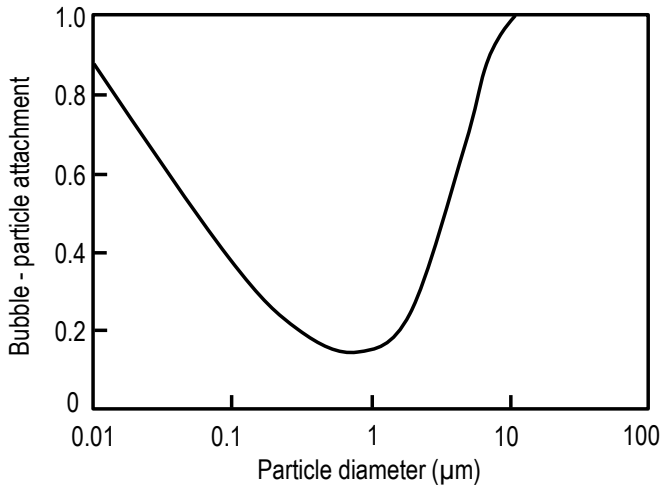

Figure 4-46 *Effect of particle-bubble attachment as a function of particle or floc size (model data adapted from Haarhoff and Edzwald [2004]).*

According to Edzwald [2010], the flotation tank can be divided into two different zones (Figure 4-41). In the contact zone, bubbles and particles should get in contact and the separation zone should provide smooth conditions for particle-bubble agglomerates to rise to the surface. In the paper "Principles and applications of dissolved air flotation" by Edzwald [1995], he described a model for particle collection by bubbles in the reaction zone.

4.3.3 Performance equations

Separation zone performance - The ideal case

The separation design and performance model according to Edzwald [2010] of particle-floc and free bubbles removal and an idealized DAF tank with a vertical plug flow in the separation zone is both illustrated in Figure 4-47.
Particle - bubble agglomerates (flocs) and free bubbles are removed if their rise velocity (u_b, u_{fb}) is higher than the separation zone hydraulic loading ($v_{sz\text{-}hl}$). The separation zone hydraulic loading is the downward water velocity in the separation zone (see Figure 4-47).

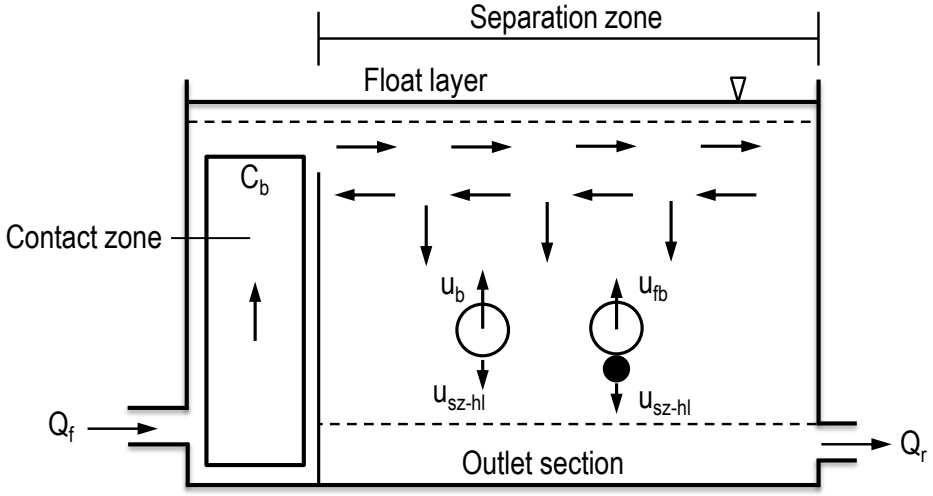

Figure 4-47 *Schematic view of an idealized DAF tank showing the float layer, vertical flow section for clarification, horizontal flow section and the outlet (partly adapted from Edzwald [2010]).*

According to Edzwald [2010], conventional DAF systems have hydraulic loadings between 5-15 m/h.
Figure 4-47 also shows a stratified flow in a DAF system. Due to density differences between the top of the tank where the air concentration of the bubbles is the highest and the bottom of the tank where the concentration is the lowest, different flow pattern arise. The bubble blanket (layer with high concentration of bubbles) can penetrate deeper in the DAF tank at higher reject flow or lower water temperature (Edzwald et al. [1999]).

Performance equations

The overall separation efficiency is defined as the ratio between the fines mass concentration in the reject flow to the fines mass concentration in the feed flow of the DAF system (see Equation 4.16).

$$E_{\text{fines}} = \frac{\dot{m}_{\text{F, fines}} - \dot{m}_{\text{R, fines}}}{\dot{m}_{\text{F, fines}}} \tag{4.16}$$

The hourly productivity of fines removed from the feed flow is illustrated in Equation 4.17 and the flow balance of the DAF system is illustrated in Figure 4-48.

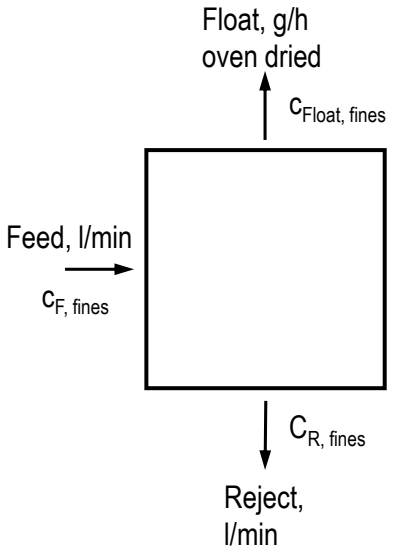

Figure 4-48 *Process flow diagram of the DAF device.*

$$Float = \dot{m}_{\text{F}}\, c_{\text{F}} - \dot{m}_{\text{R}}\, c_{\text{R}} \tag{4.17}$$

Here, it is assumed that the volume flow of the feed port is equal to the volume flow of the reject port due to the thickening effect of the float and the fact, that more than 99 % of water is removed from the float layer.

4.3.4 Design of a DAF system for continuous separation of fines suspensions

The current work is based on DAF separation technique, but it differs from the main application, where in general water clarification is the main application field. In this work, a laboratory DAF cell was developed with a clear focus on thickening of the

fines float layer and the following specifications:

- Operating the DAF cell without the use of coagulants or any other chemical additives
- The DAF should be operating in-line with the pressure screen
- The DAF device should be mobile in order to perform industrial trials at different locations

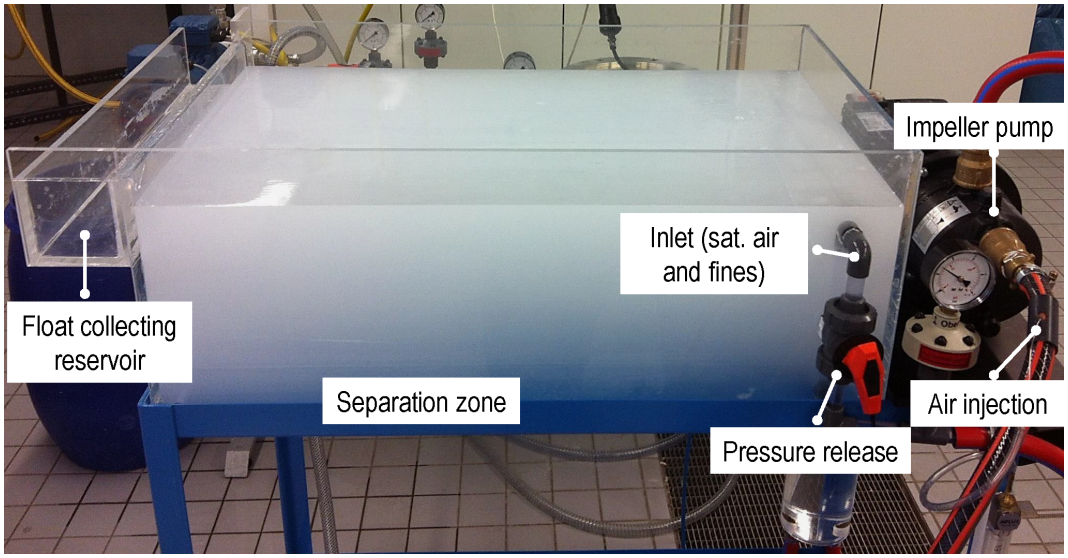

Figure 4-49 *Laboratory DAF cell at the IPZ.*

Figure 4-49 shows an image of the dissolved air flotation cell. The DAF cell consists of three main components: A jet pump for saturating the suspension and subsequent transportation into the DAF tank, an air cushion for deaeration of excess air and the DAF tank for separation and thickening of fines.
The fines suspension is transported from a feed container through the jet pump to the flotation cell. A needle in the suction tube of the jet pump injects a defined amount of air. The air gets sucked into the tube due to a low pressure inside the tube. High shear forces and an overpressure introduced by the impeller of the jet pump lead to collapse of the air bubbles and finally to dissolution. The amount of air can be adjusted by a control valve. Due to a pressure drop controlled by a valve, the dissolved air is released in the form of fine bubbles. The volume flow into the DAF cell can be adjusted by a control valve. It should be noted here that the

suspension flow control valve has an indirect proportional behavior between volume flow and the pressure increase. This means that if there is an decrease in volume flow the pressure increases.
The bubbles and the fines flow into the flotation tank. Different flow zones are defined inside the flotation cell to achieve good separation efficiency. A stable froth layer (float) is formed on the surface which contains the fines particles (thickened fines flocs). This froth is removed by a hand-operated scraper.
Pre-trials showed, that the DAF cell can be operated in a range of feed flow between 2.5 l/min and 7 l/min.

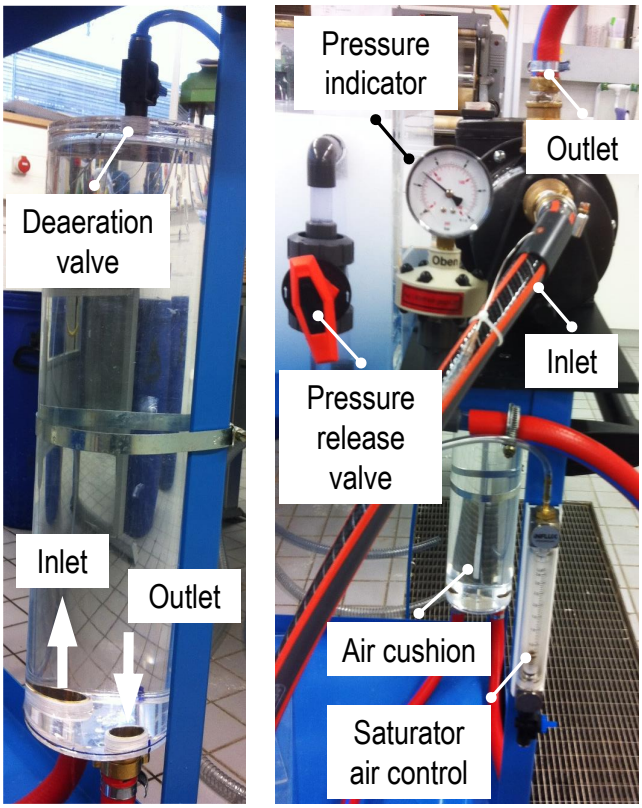

Figure 4-50 *Air cushion for deaeration (left side); pressure control and indication unit (right side).*

Figure 4-50 is divided into two parts. The left side illustrates the air cushion which is used for deaeration of excess air. After the deaeration step the suspension consists only of water, saturated air and fines. The removal of non-dissolved air bubbles before the pressure release is of utmost importance. The transportation of air bubbles through the pressure release leads to an aggressive expansion of the bubbles. This expansion and subsequent growing effect of the air bubbles generates disturbances and turbulence in the DAF tank which cause poor formation of the float layer on

the surface.
The right side of Figure 4-50 illustrates the air saturation unit including a needle for air injection, a jet pump and a pressure release valve.

Saturator unit

The current method of air saturation differs from the industrial method. Here, a simple method using a jet pump (turbo mixing device) was developed to dissolve a certain amount of air in water and to transport a suspension into the flotation tank. In general, the jet pump generates an overpressure and merges a gas and liquid that is not readily soluble, mixes them, dissolve them and force-feed them. In contrast, a conventional DAF system is equipped with a chemical charging pump, compressor, large size dissolving tank, pressurization tank, agitator, static mixer and other attachment parts.

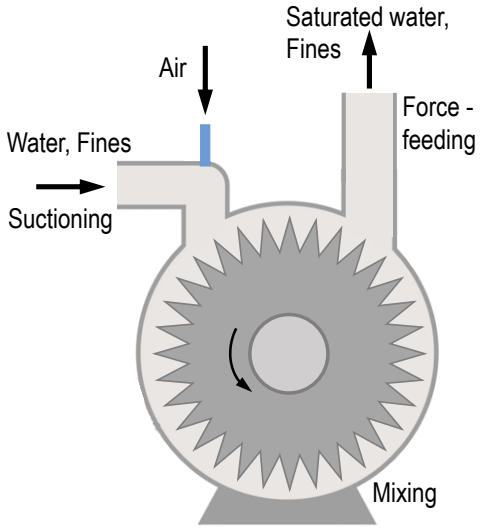

Figure 4-51 *Saturator unit (impeller jet pump) for micro bubble production.*

The jet pump sucks in air, water and the fines suspension. After transportation into the pump, mixing and dissolving takes places due to high shear forces and an overpressure up to 4.5 bar. After the mixing procedure, the jet pump provides high-pressure feeding of the dissolved liquid mixture. Figure 4-51 gives a schematic overview about the design of the saturator unit used for dissolved air flotation.

Calculation of saturator efficiency

In order to determine the saturator efficiency, a calculation based on the ideal gas law was done. It is not possible to dissolve 100 % of the injected air with the jet pump and therefore, an air cushion was installed to collect the non dissolved air bubbles. The collected air in the air cushion lowers the level of water at increasing time. At a certain time period, a certain water level occurs and therefore a certain amount of pressurized air is collected in the air cushion.
It is possible to measure the height of the air column in the air cushion (see Figure 4-52) and to calculate the volume of air. Subsequent it is possible to calculate the total volume of air at 1 atmosphere pressure based on the ideal gas law (see equation 4.19).

$$p_1 V_1 = R T_1 \tag{4.18}$$

$$p_2 V_2 = R T_2 \tag{4.19}$$

After simplification of equation 4.18 and 4.19 (inserting 6.4 cm air column height) and assuming that T_1=T_2, the total air volume of non dissolved air at 1 atmosphere pressure can be calculated according:

$$V_2 = \frac{p_1 V_1}{p_2} \tag{4.20}$$

After 10 minutes running the DAF device the hight of the air column was measured. In addition, the total amount of air was measured by an air flow meter. Table 4-11 illustrates the specific air quantities from the suction side of the saturator and the air cushion.

Cumulative air flow (10 min)	Value
Suction side	30 l
Non dissolved	2.58 l

Table 4-11 *Specific air quantities from the suction side of the saturator and the air cushion.*

The saturator efficiency f is defined as the ratio between the actual saturated air and the injected air into the jet pump (Equation 4.21).

$$f = \frac{Cumulative\ air - Non\ dissolved\ air}{Cumulative\ air} = \frac{30 - 2.58}{30} = \mathbf{91.4\,\%} \tag{4.21}$$

After substitution of the known values into equation 4.21 a saturator efficiency of 91.4 % can be achieved with this device. To simplify the subsequent evaluations, an overall saturator efficiency of 90 % was assumed for all further calculations.

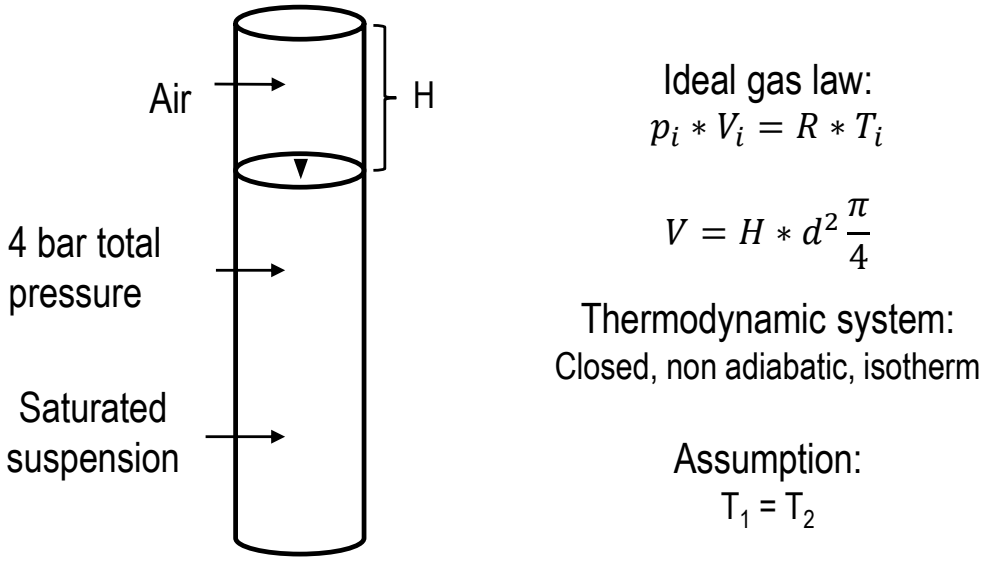

Figure 4-52 *Schematic view of the determination method of saturator efficiency calculation.*

Calculation of the air to solid ratio in the current DAF

In order to compare the current DAF device with industrial DAF plants, the air to solid ratio was determined. The air to solids ratio is a calculation of how much air is being applied to a given amount of suspended solids within the DAF process. This value is defined as g of air to g of solids. According to Table 4-12, the current DAF generates 86.41 mg/l saturated air (401.33 kPa) with a feed consistency of 0.02% (produced with pressure screen, 60 l total volume). Further, based on 60 l total volume of the DAF tank, 12 g of oven dried fines are collected in the tank.

$$\frac{AR}{SO} = \frac{sat.air\ at\ 401.33\ kPa}{0.02\%\ solids\ content} = \frac{5.16\ g\ air}{12\ g\ fines} = \mathbf{0.43} \tag{4.22}$$

According to Equation 4.22, the current DAF device shows an air to solids ratio of **0.43** which is significantly higher than the air to solids ratio of industrial devices (0.0023 to 0.091 g air/g solids (Ross et al. [2000])).

4.3.5 Results of fines thickening

Figure 4-53 illustrates the influence of different saturated air quantities on fines separation performance based on the concentration of fines in the recycle flow. The x-axis is defined as the amount of saturated air per volume unit and the y-axis is defined as the mass concentration of fines in the recycle stream.
Based on figure 4-53, it is evident that an increased amount of saturated air leads to

a better separation of fines from the liquid phase, as the consistency in the recycle stream becomes lower. Additionally it can be seen that fines from two different pulp types were used in this experiments. The first pulp was an unbleached kraft pulp (100 % spruce) and the second pulp was a bleached kraft pulp (100 % spruce). Figure 4-53 thus also illustrates the influence on separation performance based on different pulp fines. It is evident, that for both data points, unbleached fines are easier to separated from the liquid phase than bleached pulp fines. Due to their higher amount of lignin and extractives on the surface, they have more hydrophobic areas which lead to better flotation.
It has to be mentioned here, that only primary fines were used for thickening trials. Preliminary tests showed, that there is no significant difference in thickening of secondary fines.

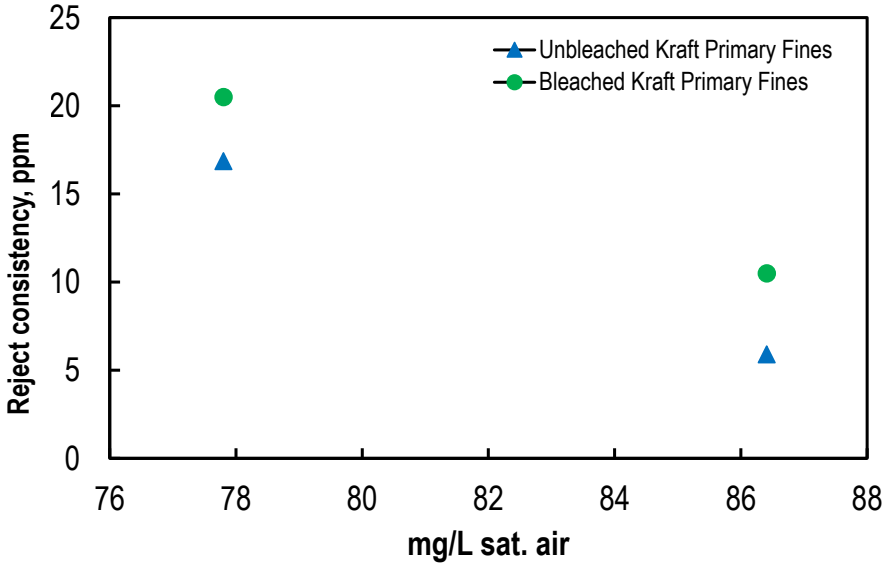

Figure 4-53 *Influence of saturated air quantities on fines separation performance expressed as the concentration of fines in the reject flow.*

Table 4-12 shows the consistency in the recycle stream, the overpressure and the saturated air amount at different volumetric feed flows.

Feed 2.5 l/min	Reject cons. ppm	Pressure + 1 atm kPa	Sat. air amount mg/l
Unbleached kraft	16.87	361.33	77.8
Bleached kraft	20.5	361.33	77.8
Feed 5 l/min	Reject cons. ppm	Pressure + 1 atm kPa	Sat. air amount mg/l
Unbleached kraft	5.90	401.33	86.41
Bleached kraft	10.5	401.33	86.41

Table 4-12 *Overview about consistencies in the recycle stream, overpressure and the saturated air amount at different volumetric feed flows.*

In addition to experiments on the influence of saturated air quantities on flotation performance, investigations about the selective separation behavior in the DAF tank have been performed. Table 4-13 shows the mean particle diameter of the flotation sludge layer and the mean particle diameter of the recycle stream. Based on Table 4-13, it is evident that there is no significant difference of mean particle diameter between the float layer and the recycle stream. Therefore, selective separation (fractionation) can be neglected for the used DAF device.

	Mean particle size - arithmetic, mm	Mean particle size - length weighted, mm
Flotation sludge	0.052	0.0705
Recycle stream	0.051	0.067

Table 4-13 *Mean particle length values of kraft pulp fines of the float layer and of the recycle stream at 5.0 l/min feed flow (arithmetic mean fiber length and length weighted fiber length included).*

Evaluation results based on kraft pulp fines

In order to determine the fines thickening performance of the DAF device, trials using unbleached kraft pulp fines have been performed. Pre trials at different volumetric reject flows were carried out to determine the "operating window" of the DAF device. There is just a small region of volumetric feed flow where flotation can be performed. At low volumetric feed flow, low quantities of air are transported into the DAF cell. In this case, air bubbles are not distributed randomly in the DAF tank. This leads to bubble rising in the front end of the tank. Therefore, flotation of fines is limited. If the volumetric feed flow increases, turbulence in the DAF tank occur, which leads to a dissolution of fines-flocs. As a result of strong turbulence, separation performance of the DAF device decreases.

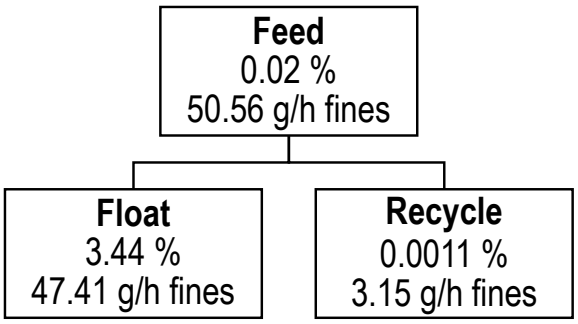

Figure 4-54 *Schematic overview about the flotation process and the mass balance including consistencies at each port for unbleached kraft pulp fines.*

Figure 4-54 and Table 4-14 show the mass balance including consistencies at each port. The results are based on a volumetric feed flow of 5 l/min. It is evident that this process has a high separation efficiency where fines are thickened from 0.02 % to 3.44 % mass concentration (consistency). The hourly amount of oven dried fines is illustrated in Figure 4-54 and in Table 4-14.
One important aspect of this method is that it is operated without the use of any chemicals (e.g. flocculation agents, oils etc.) to avoid contamination of the material. Only water and small air bubbles are used for thickening of fines.

	Fines oven dried g/h	Consistency %
Feed	50.56	0.02
Float	47.41	3.44
Recycle	3.15	0.0011

Table 4-14 *Hourly amount of oven dried fines (unbleached kraft) produced with the DAF and consistencies at each port.*

Results from these investigations of the DAF unit show a high separation efficiency of 93.8%.

$$E_{\text{fines}} = \frac{\dot{m}_{\text{fines,F}} - \dot{m}_{\text{fines,R}}}{\dot{m}_{\text{fines,F}}} = \frac{50.56 - 3.15}{50.56} = \mathbf{93.8\,\%} \tag{4.23}$$

Figure 4-55 and Table 4-15 show the mass balance including consistencies of the flotation process for bleached kraft pulp fines. The trials were performed at 5 l/min volumetric feed flow. Again, it is evident that this process has a high separation efficiency (81 %), but less than for unbleached kraft pulp fines. Fines from bleached kraft pulp have a smaller amount of lignin and extractives on their surface which leads to a smaller hydrophobicity and therefore weaker separation performance. In these experiments, fines are thickened from 0.01 % to 1.49 % mass concentration.

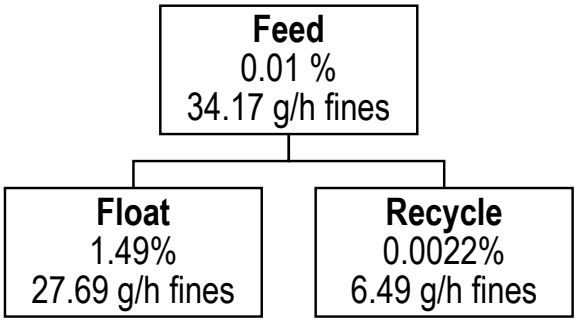

Figure 4-55 *Schematic overview about the flotation process and the mass balance including consistencies at each port for bleached kraft pulp fines.*

	Fines oven dried g/h	Consistency %
Feed	34.17	0.01
Flotation sludge	27.69 g/h	1.49
Recycle	6.49	0.0022

Table 4-15 *Hourly amount of oven dried fines (bleached kraft) produced with the DAF and consistencies at each port.*

Results from these investigations with the DAF device show a high separation efficiency of 81 %.

$$E_{\text{fines}} = \frac{\dot{m}_{\text{fines,F}} - \dot{m}_{\text{fines,R}}}{\dot{m}_{\text{fines,F}}} = \frac{34.17 - 6.49}{34.17} = \mathbf{81\,\%} \tag{4.24}$$

4.3.6 Closed circuit production

As already described in chapter 4.2.9, the pressure screen can be operated either in a cyclic procedure or in a one pass procedure. In case of the cyclic procedure, additional water has to be pumped into the feed tank to balance the feed flow consistency.
However, it is now possible to combine both aggregates where the recycle flow of the DAF cell can be used as dilution water for the feed tank balance. This procedure is called "closed circuit production" where no additional external water is needed for separation of fines from pulp and subsequent fines thickening.

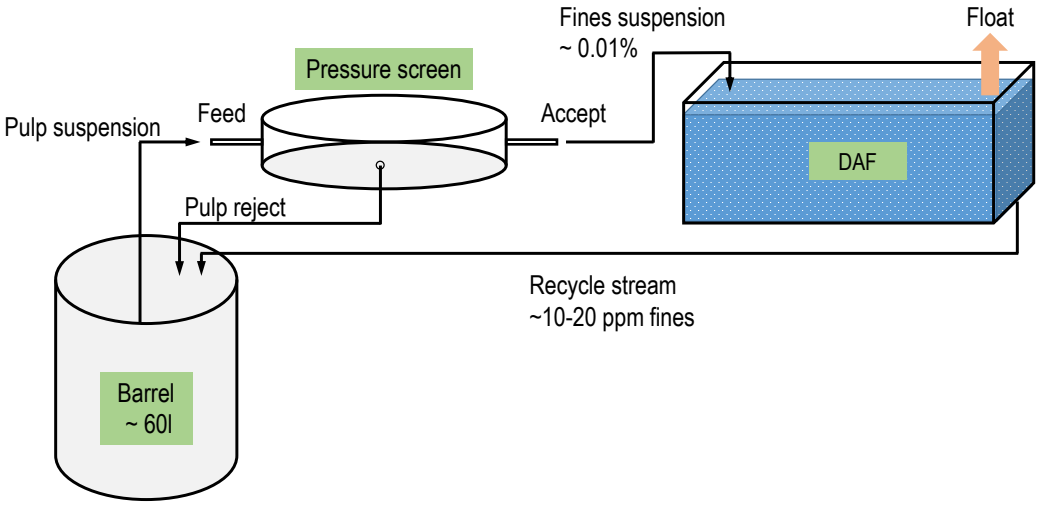

Figure 4-56 *Schematic overview of the "closed circuit" production procedure.*

Figure 4-56 illustrates the "closed circuit" procedure, where the pressure screen is connected with the DAF device. From this figure it is evident that the recycle stream (fines mass concentration 10-20 ppm) is transported back into the feed tank barrel. This procedure is aborted, if most of the fines (>90 %) are removed from the pulp suspension.

As an example of this method, both the pressure screen and the DAF unit can be used to separate and thicken fines from industrial streams. In this case, the pressure screen can be operated in the one pass operation method to maximize the separation of fines and further to maximize the float consistency from fines thickening. It is evident, that based on this method quantities of up 1000 g of oven dried fines can be produced within one day.

4.4 Bubble size distribution measurement via image analysis

In order to evaluate the current DAF method and to compare it to literature data, the bubble size distribution (BSD) was measured. Table 4-16 gives an overview on the bubble sizes reported for the DAF method in literature.

Bubble sizes µm	Conditions	Reference
10-120	Needle valve: bubbles 40-90 µm	Zabel (1984)
33-75 (median sizes)	Hague nozzle; larger bubbles at a pressure of 350 kPa compared to 500 and 620 kPa	De Rijk et al. (1994)
15-85	Mean sizes of 30 µm for pressures of 350-608 kPa	Han et al. (2002)
Albert plant	Full-scale plants	Leppinen and Dalziel (2004)
70-84 (median: contact zone)	Observed bubble clusters	
72-145 (median: separation zone)		
Graincliffe plant		
40-60 (contact zone)		
50-150 (separation zone)		

Table 4-16 *Bubble sizes in DAF systems (adapted from Edzwald [2010]).*

In order to compare the current DAF with results from literature, a transparent viewing chamber was installed for measuring the bubble size distribution (BSD). The apparatus consists of a tube attached to a sealed viewing chamber with rear illumination (Figure 4-57). The tube is connected to a bypass which allows control of the volume flow of saturated water. The viewing chamber is connected to a jet pump from the DAF unit and is filled with water where images are captured (see Table 4-17. Images are captured and processed off-line to yield BSD data.
According to literature (Kracht et al. [2013]), the accuracy of this method is hard to establish (there is no "gold standard" against which to compare), but the approach is now widely used. Although this technique is being widely used, there are still some issues that may affect its accuracy such as bubble evolution or limitations to the image analysis process.

Equipment	Detailed description
Nikon D5100	16 megapixel
Lens Nikon ED	200 mm 1:4 D

Table 4-17 *Equipment used for BSD determination.*

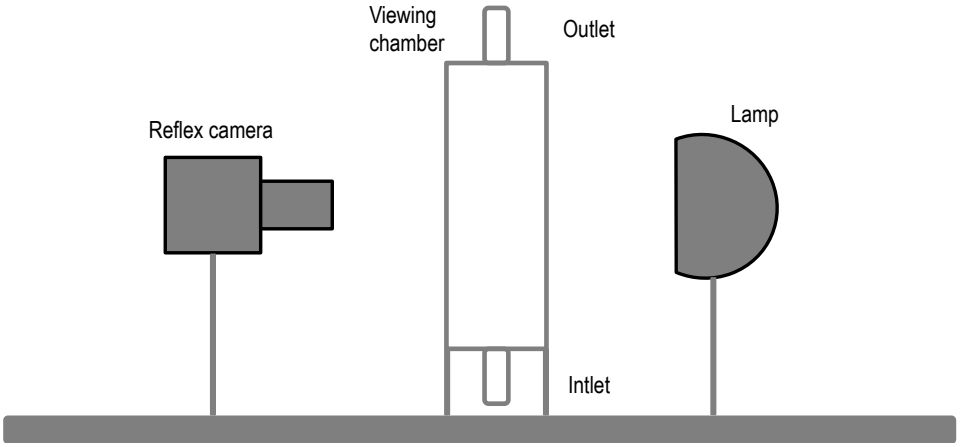

Figure 4-57 *Schematic image of the sampling device for measuring the BSD.*

Image analysis

Once the images are generated, they are first modified using wavelet filter transformation to treat the out of focus area. Subsequently, they are converted into binary images using MATLAB and processed in order to identify different objects. Those objects are later characterized according to a series of metrics such as maximum and minimum diameter, mean diameter and area. Figure 4-58 shows the original picture of bubbles and the binary version.
Figure 4-58 also shows, that bubbles appear either as single bubbles or as several bubbles touching each other (bubble clusters). After the segmentation step, the objects are classified into categories by their position and metrics.
Bubble clusters are difficult to handle and therefore would require specific analysis procedures. In the setup used for this procedure, bubble clusters occur and are included into the calculation of the bubble size distribution. Nevertheless, these clusters are quite rare compared to single bubbles and therefore they have a minor influence on the bubble size distribution results. The results obtained from this method are described in the following chapter.

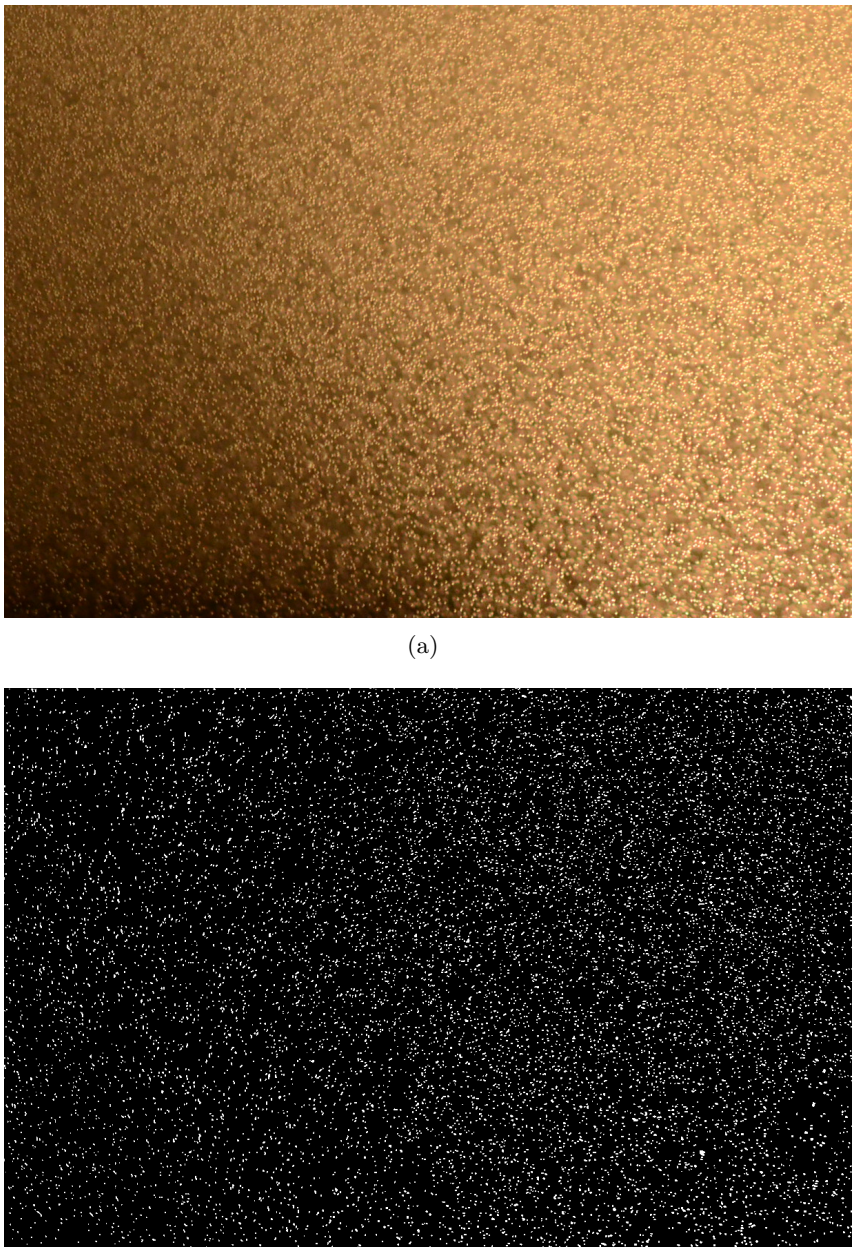

(a)

(b)

Figure 4-58 *Example image of bubbles generated in the DAF device. Original image (a) and binary image (b).*

4.4.1 Results of bubble size distribution evaluation

Figure 4-59 shows an exemplary result of a bubble size distribution of a single sample. In this figure, the x-axis is defined as the pixel size and the y-axis is defined as the frequency of bubbles detected. In order to convert the pixel to µm, a ruler was installed into the measuring cell. With this method, it is possible to include a scale

in every picture and therefore convert it from pixel to µm.
Based on Figure 4-59, it is evident that the DAF device produces a small and sharp bubble size distribution.
Table 4-18 shows results of the bubble size measurements at different pressure levels and comparative measurements using 50 µm polyamide particles. It is evident that there is no significant difference in bubble mean size between the two pressure levels. Measurements based on 50 µm polyamide calibration particles show that there is only a minor deviation of the results from the given diameter of these particles.

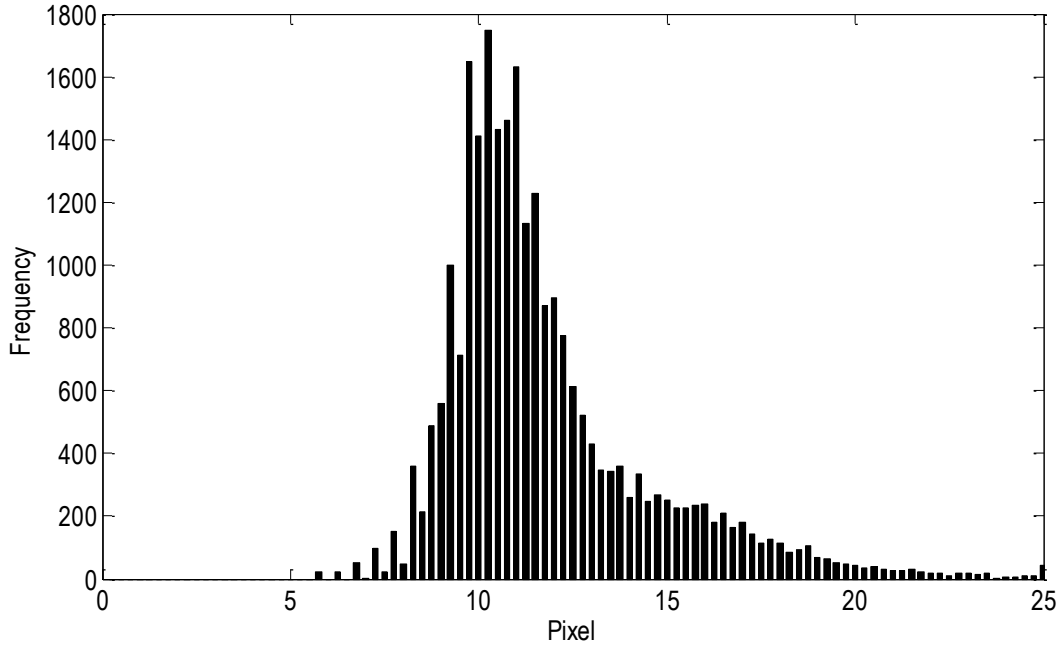

Figure 4-59 *Exemplary result of a bubble size distribution of a single sample.*

Based on these results a comparison to literature (see Table 4-16) shows that the current DAF cell produces bubbles within the range of a conventional DAF plant.

Sample ID	Mean diameter, µm
Bubbles 3.5 bar	63.952 ± 2.288
Bubbles 2.2 bar	62.321 ± 0.795
Polyamide 50 µm	44.988 ± 2.267

Table 4-18 *Mean bubble/particle diameter of each pressure level including the standard deviation.*

Bubble rise velocity

The bubble rise velocity can be calculated according the the Stoke's law for particles <100 µm.

Parameter	Value
d_b	63.95 µm
g	9.81 m/s^2
ρ_w	998.21 kg/m^3
ρ_b	1.188 kg/m^3
μ_w	1002.7 $\mu Pa\,s$

Table 4-19 *Mean bubble diameter at 3.5 bar and physical properties of water at 20°C (Kurzweil et al. [2008]).*

Substituting these values (Table 4-19) into Equation 4.25, yields a bubble rise velocity of **0.266 cm/s** (see also Figure 4-43).

$$U_b = g\,{d_b}^2(\rho_w - \rho_b)/18\,\mu = \mathbf{0.266\ cm/s} \tag{4.25}$$

4.4.2 Conclusions

Experiments with different pulp fines show that the dissolved air flotation process has a high separation efficiency (93.8 % max.) where fines are thickened from 0.01 % up to more than 3 % mass concentration (consistency). One important aspect of this method is that it is operated without the use of any chemicals (e.g. flocculation agents, oils etc.) to avoid contamination of the material. Only water and small air bubbles are used for thickening of fines.
The device can be used in-line with the pressure screen to yield large quantities (up to 80 g/h oven dried fines at 7 l/min feed flow DAF unit) for further experiments.
It has been demonstrated that different pressure levels have no influence on bubble growth and size distribution.
It was also demonstrated that different pulp types (unbleached - bleached) show a different separation behavior due to their hydrophobicity. In some cases the use of coagulant should be taken into account to achieve higher separation efficiency. In particular, if the fines consistency is lower than 0.01 %.

5 General conclusions and outlook

This thesis investigated both analytical fractionation and fines separation and thickening in the lab-scale. In case of the analytical fractionation part, the focus was set on the investigation of the influence of secondary flow in a coiled tube set-up of a tube flow fractionation device by changing parameters such as curvature and flow velocity.

It has been proven that in a coiled set-up, different settings strongly affect the fractionation characteristics due to the secondary flow (Dean flow).

The main drawback when using the tube flow fractionation device is the small amount of pulp used and therefore the even smaller fractions which can be produced for subsequent analysis or application.

Another aim of the thesis was to provide larger quantities of fines (> 100 g oven dried material) from different pulp sources for further investigation and applications. A pressure screen was implemented to separate the fines fraction from the fiber fraction.

Results from pressure screening show a high separation efficiency of more than 60 % for unbleached and bleached kraft pulps. Trials using different amounts of pulp show that depending on the original fines content of a pulp more than 100 g of fines (oven dry mass) can be produced within one hour.

Arising from the screening process the task was to find a new technology to increase the consistency of the fines suspension produced. Therefore, a laboratory dissolved air flotation cell (DAF) was developed with a clear focus on thickening of the fines in the float layer. Experiments with different pulp fines showed that the dissolved air flotation process has a high separation efficiency (93.8 % max.) where fines are thickened from 0.01 % up to more than 3 % mass concentration. Furthermore, the device can be used in-line with the pressure screen to yield large quantities (up to 50 g/h oven dried) of fines for further experiments.

Although, the technologies mentioned above provide suitable amounts of fines in the

lab-scale, there is still a lack of knowledge on industrial application of fines thickening. In the current work, trials using industrial devices from industry partners within the Flippr° project as well as from external partners were performed to investigate different fines thickening technologies. Three different industrial devices including a chamber filter press, disc separator and a decanter centrifuge were used to thicken different fines suspensions. Results from the chamber filter press show a high thickening ability where a suspensions was thickened from 0.1 % mass concentration up to 12 %.

Trials using a disc separator and decanter centrifuge showed that both devices can provide large quantities of fines and excellent thickening abilities (11 % for disc separator and 32 % for decanter centrifuge).

However, these industrials devices show high energy consumption and therefore there is still a need for pre-thickening of fines suspensions. The dissolved air flotation seems to be the key technology as a first thickening step where more than 99 % of water can be removed combined with low energy costs.

Bibliography

Asikainen, S. (2013). Reinforcing ability of fractionated softwood kraft pulp fibres. *Nordic Pulp and Paper Research Journal*, 28(2):290–296.

Asikainen, S., Fuhrmann, A., Ranua, M., and Robertsén, L. (2010a). Effect of birch kraft pulp primary fines on bleaching and sheet properties. *BioResources*, 5(4):2173–2183.

Asikainen, S., Fuhrmann, A., and Robertsén, L. (2010b). Birch pulp fractions for fine paper and board. *Nordic Pulp and Paper Research Journal*, 25(3):269–276.

Bäckström, M., Kolar, M., and Htun, M. (2008). Characterisation of fines from unbleached kraft pulps and their impact on sheet properties. *Holzforschung*, 62(5):546–552.

Bergelin, E. and Holmbom, B. (2008). Reactions and distribution of birch extractives in kraft pulp oxygen delignification. *Journal of Wood Chemistry and Technology*, 28(4):261–269.

Berger, S., Talbot, L., and Yao, L. (1983). Flow in curved pipes. *Annu. Rev. Fluid Mech*, 15:461–512.

Björk, E., Vomhoff, H., and Bouveng, M. (2015). Production of a fine fraction using micro-perforated screens. In *PaperCon2015, April 19-22, Georgia World Congress Center, Atlanta, GA*.

Björklund, J. and Nilvebrant, N.-O. (2009). *Wood chemistry and wood biotechnology*, chapter 7. Wood extractives, pages 147–172. De Gruyter: Berlin, Germany.

Blom, U., Nevalainen, P., and Arhippainen, B. (1981). Development of the alva prehydrolysis process ii. mill scale application. *Tappi Proc. Pulp. Conf., Denver*, pages 401–416.

Brecht, W. and Holl, M. (1939). Schaffung eines normalverfahrens zur gutebewertung von holzschliffen. *Der Papier-fabrikant*, 10(24):74–86.

Brecht, W. and Klemm, K. H. (1952). Das strukturgemisch eines holzschliffes als schlüssel für die kenntnis seiner technologischen eigenschaften. *Wochenblatt für Papierfabrikation*, 80(11):364–370.

Brännvall, E. and Lindström, M. E. (2006). A study on the difference in tensile strength between industrially and laboratory-cooked pulp. *Nordic Pulp and Paper Research Journal*, 21(2):222–226.

Chen, H., Park, A., Heitmann, J., and Hubbe, M. (2009). Importance of cellulosic fines relative to the dewatering rates of fiber suspensions. *Industrial & Engineering Chemistry Research*, 48(20):9106–9112.

Cole, C., Hubbe, M. A., and Heitmann, J. A. (2008). Water release from fractionated stock suspensions. part 1 - effects of the amounts and types of fiber fines. *Tappi Journal*, 7(7):28–32.

Corson, S., Wakelin, R., and Loyd, M. (1996). Tmp furnish development strategies, part 1: fractionation and long fibre removal. *Pulp and Paper Canada*, 97(12):446–449.

Corson, S., Wakelin, R., and Loyd, M. (1997). Tmp furnish development strategies, part 2: Sheet properties. *Pulp and Paper Canada*, 98(1):41–44.

Cuming, H. (1952). The secondary flow in curved pipes. *Rep. Mem. 2880, Aeronaut. Res. Counc.*

De Silveira, G., Zhang, X., Berry, R., and Wood, J. R. (1996). Location of fines in mechanical pulp handsheets using scanning electron microscopy. *Journal of Pulp and Paper Science*, 22(9):J315–J320.

Dean, W. (1928). The stream-line motion of fluid in a curved pipe. *The London, Edinburgh, and Dublin Philosophical Magazine and Journal of Science Series 7*, 5(30):673–695.

Edzwald, J., Tobiason, J., Amato, T., and Maggi, L. (1999). Integrating high-rate daf technology into plant design. *Journal / American Water Works Association*, 91(12):41–53. cited By 24.

Edzwald, J. K. (1995). Principles and applications of dissolved air flotation. *Wat. Sci. Tech*, 31(3-4):1–23.

Edzwald, J. K. (2010). Dissolved air flotation and me. *Water Research*, 44(7):2077 – 2106.

Ek, M., Gellerstedt, G., and Henriksson, G., editors (2009). *Pulping Chemistry and Technology*, volume 2. Berlin, Boston: De Gruyter.

Eustice, J. (1910). Flow of water in curved pipes. *Proc. R. soc. London Ser. A*, 84(568):107–118.

Eustice, J. (1911). Experiments of streamline motion in curved pipes. *Proc. R. soc. London Ser. A*, 85(576):119–131.

Ewald, C., Kröling, H., and Schabel, S. (2014). New laboratory screen for simulation and optimization of fractionation processes in industrial pressure screens. In *18th International Papermaking Conference*, pages 1–17. SPP.

Fardim, P., editor (2011). *Chemical Pulping Part 1, Fibre Chemistry and Technology, Book 6 (Part 1), Second Edition, Totally updated version.* Paper Engineers' Association/ Paperi ja Puu Oy.

Feng, M., Gonzalez, J., and Olson, J. A. (2005). Numerical simulation and experimental measurement of pressure pulses produced by a pulp screen foil rotor. *Journal of Fluids Engineering*.

Fengel, D. (1969). The ultrastructure of cellulose from wood. *Wood Science and Technology*, 3(3):203–217.

Fengel, D. (1970). The ultrastructure of cellulose from wood. *Wood Science and Technology*, 4(1):15–35.

Fengel, D. and Wegener, G. (1984). *Wood: chemistry, ultrastructure, reactions*. de Gruyter, Berlin and New York.

Fengel, D. and Wegener, G. (2003). *Wood - Chemistry, Ultrastructure, Reactions*. Verlag Kessel.

Flippr° (2013). http://www.flippr.at/, 21.02.2017, 11:48.

Forgacs, O. (1963). The characterization of mechanical pulps. *Pulp Pap Mag Can*, 64:T–89–T–118.

Gavelin, G., Kolmodin, H., and Treiber, E. (1975). Critical point drying of fines from mechanical pulps. *Sven Papperstidn*, 78:603–608.

Gochin, R. and Solari, J. (1983). The role of hydrophobicity in dissolved air flotation. *Water Research*, 17(6):651 – 657.

Haarhoff, J. and Edzwald, K. (2004). Dissolved air flotation modelling: insights and shortcomings. *Journal of Water Supply: Research and Technology - AQUA*, 53(3):127–150.

Hafrén, J., Fernando, D., Gorski, D., Daniel, G., and Salomons, F. A. (2014). Fiber- and fine fractions-derived effects on pulp quality as a result of mechanical pulp refining consistency. *Wood Science and Technology*, 48(4):737–753.

Halonen, L. and Ljokkoi, R. (1989). Improved screening concepts. In *Proceedings of Tappi Pulping Conference, Atlanta, GA*, pages 61–66.

Hawes, J. and Doshi, M. (1986). The contribution of different types of fines to the properties of handsheets made from recycles paper. Technical report, Appleton, USA: The Institute of Paper Chemistry.

Hawthorne, W. (1951). Secsecond circulation in fluid flow. *Proc. R. Soc. London Ser.*, A 206(1086):374–387.

Heijnesson, A., Simonson, R., and Westermark, U. (1995a). Metal ion content of material removed from the surface of unbleached kraft fibres. *Holzforschung*, 49:75–80.

Heijnesson, A., Simonson, R., and Westermark, U. (1995b). Removal of lignin-rich surface material from unbleached kraft fibers. *Holzforschung*, 49:313–318.

Heinanen, J., Jokela, P., and Peltokangas, J. (1992). Experimental studies on the kinetics of flotation. In Klute, R. and Hahn, H., editors, *Chemical Water and Wastewater Treatment 2*, pages 247–262. Springer-Verlag, New York, USA.

Holik, H., Gamsjäger, N., Westerkamp, A., Schmitt, M., Morton, A., Stetter, A., Tietz, M., Feldmann, R., Wohlfahrt, M., and Mirsberger, P. (2006). *Paper and Board Manufacturing*, chapter 6, pages 219–331. Wiley-VCH Verlag GmbH & Co. KGaA.

Hubbe, M. (2002). Fines management for increased paper machine productivity. In *Proc. Sci. Tech. Advan. Wet End Chemistry, Pira, Barcelona.*

Hyll, K., Farahani, F., and Mattsson, L. (2016). Optical methods for fines and filler size characterization. Technical report, KTH Royal Institute of Technology and Innventia AB.

Ilvessalo-Pfäffli, M.-S. (1995). *Fiber atlas: identification of papermaking fibers.* Springer, Berlin [u.a.].

Jagiello, L. (2013). Implementation of a tube flow fractionator. y, Graz University of Technology, Austria.

Johansson, B. and Kubát, J. (1956). An axial separation effect in fflowi pulp suspensions. *Svensk Papperstidn.*, 59(23):845–846.

Johansson, H., Olgård, G., and Jernqvist, . (1970). Radial particle migration in plug flow - a method for solid-liquid separation and fractionation. *Chem. Eng. Sci.*, 25(3):365–372.

Kangas, H. and Kleen, M. (2004). Surface chemical and morphological properties of mechanical pulp fines. *Nordic Pulp and Paper Research Journal*, 19(2):191–199.

Karjalainen, M., Ämmälä, A., Rousu, P., and Niinimäki, J. (2013). Fractionation of wheat straw pulp cells in a hydrocyclone. *Nordic Pulp and Paper Research Journal*, 28(2):282–289.

Karlsson, A. and Agnemo, R. (2010). High consistency hydrogen peroxide bleaching of mechanical pulps with varying amounts of fines. *Nordic Pulp and Paper Research Journal*, 25(3):256–268.

Kellomäki, S., editor (2009). *Forest Resources and Sustainable Management, Totally updated version.* Paper Engineers' Association/Paperi ja Puu Oy.

Kibblewhite, R. (1975). Interrelations between pulp refining treatments, fiber and fines quality and pulp freeness. *Pap Puu*, 57:519–526.

Kitchener, J. and Gochin, R. (1981). The mechanism of dissolved air flotation for potable water: basic analysis and a proposal. *Wat. Res.*, 15:585–590.

Kleen, M., Kangas, H., and Laine, C. (2003). Chemical characterization of mechanical pulp fines and fiber surface layers. *Nordic Pulp and Paper Research Journal*, 18(4):361–368.

Kracht, W., Emery, X., and Paredes, C. (2013). A stochastic approach for measuring bubble size distribution via image analysis. *International Journal of Mineral Processing*, 121:6 – 11.

Krogerus, B., Eriksson, L., Sundberg, A., Mosbye, J., Ahlroth, A., Östlund, I., and Sjöström, L. (2002). Fines in closed circuits - final report. *SCAN Forsk report: 740.*

Krogerus, B. and Fagerholm, K. (2003). Analytical fractionation of pulps by tube flow. *Paperi ja Puu - Paper and Timber*, 85:209–213.

Krogerus, B., Fagerholm, K., and Löytynoja, L. (2003). Analytical fractionation of pulps by tube flow. *Paperi ja Puu/Paper and Timber*, 85(4):209–213.

Kurzweil, P., Frenzel, B., Eichler, J., and Schiewe, B. (2008). *Physik Aufgabensammlung.* Vieweg+Teubner.

Laitinen, O. (2011). *Utilisation of tube flow fractionation in fibre and particle analysis.* PhD thesis, Department of Process and Environmental Engineering, Acta Univ Oul C382. 62 p.

Laitinen, O., Kemppainen, K., Stoor, T., and Niinimaki, J. (2011). Fractionation of pulp and paper particles selectively by size. *Bioresources*, 6(1):672–685.

Lapierre, L., Pitre, D., and Bouchard, J. (1998). Bleaching of deinked recycled pulp: benefits of fibre fractionation. *Pulp and Paper Report*, 1357.

Lübbe, E. (2013). *Farbbeschreibung und Farbmessung.* Springer Vieweg.

Li, H., Ni, Y., and Sain, M. (2002). Characterization of bctmp fines and their effect on sizing. *Tappi Journal*, 1(9):3–7.

Liimatainen, H., Taipale, T., Haapala, A., and Niinimäki, J. (2008). Influence of mechanical pulp fines on clay retention. *Tappi Journal*, 7(12):10–16.

Liitiä, T., Maunu, S., and Horting, B. (2001). Solid state nmr studies on inhomogeneous structure of fibre wall in kraft pulp. *Holzfoschung*, 55:503–510.

Lindholm, C. A. (1980). Comparison of some papermaking properties of groundwood, pressure groundwood, and thermomechanical pulp by means of artificial blends of pulp fractions. part 1. primary results. *Pap Puu*, 62:593–606.

Lindqvist, H., Salminen, K., Kataja-aho, J., Retulainen, E., Fardim, P., and Sundberg, A. (2011). The effect of fines on dewatering, wet and dry web properties, pages 887-894. *PaperCon Conference.*

Lindqvist, H., Salminen, K., Kataja-aho, J., Retulainen, E., Fardim, P., and Sundberg, A. (2012). The effect of fibre properties, fines content and surfactant addition on dewatering, wet and dry web properties. *Nordic Pulp and Paper Research Journal*, 27(1):104–111.

Lindroos, K. and Puro, M. (2007). Superior tools for adjustable screening process. In *8th Research Forum in Recycling, Progress in Paper Recycling.*

Lindström, T. and Glad-Nordmark, G. (1978). Chemical characterization of the fines fraction from unbleached kraft pulps. *Svensk Papperstidn.*, 81(15):489–492.

Lindström, T. and Söremark, C. (1977). The influence on paper strength of dissolved and colloidal substances in the white water. *Svensk Papperstidning*, 80(11):341–345.

Lönnberg, B., editor (2009). *Mechanical Pulping - Book 5.* Paper Engineers' Association/ Paperi ja Puu Oy.

Lorentzen&Wettre (2016). Fiber tester+ data sheet, http://new.abb.com/pulp-paper/abb-in-pulp-and-paper/products/lorentzen-wettre-products, 22.02.2017 10:45.

Luukko, K. (1998). On the characterization of mechanical pulp fines: A review. *Paperi ja Puu/Paper and Timber*, 80(6):441–448.

Luukko, K. and Paulapuro, H. (1999). Mechanical pulp fines: Effect of particle size and shape. *Tappi Journal*, 82(2):95–101.

Mayovsky, J. (1998). Fractionation of occ. how can it help you? In *Recycling Symposium*, pages 407–416.

Miles, K. and Karnis, A. (1991). The response of mechanical and chemical pulps to refining. *Tappi J.*, 74(1):157–164.

Ämmälä, A. (2001). *Fractionation of thermomechanical pulp in pressure screening*. PhD thesis, University of Oulu.

Mohlin, U.-B. (1977). Distinguishing character of tmp. *Pulp Pap Can*, 78:83–88.

Mosbye, J. (2003). *Colloidal wood resin: analyses and interactions*. PhD thesis, Norwegian University of Science and Technology.

Mosbye, J., Laine, U., and Moe, S. (2003). The effect of dissolved substances on the adsorption of colloidal extractives to fines in mechanical pulp. *Nordic Pulp and Paper Research Journal*, 18(1):63–68.

Niinimäki, J. (1998). *On the Fundamentals of Pressure Screening - An experimental study of conditions and phenomena in the screen basket*. PhD thesis, University of Oulu.

Niinimäki, J., Ämmälä, A., and Jokinen, H. (2007). Fractionation of fibres - possibilities and limits. In *PulPaper 2007 Conference*.

Niskanen, K., editor (2008). *Paper Physics - Book 16*. Paper.

Nylund, J., Byman-Fagerholm, H., and Rosenholm, J. B. (1993). Physico-chemical characterization of colloidal material in mechanical pulp. *Nord.Pulp Pap.Res.J.*, 8(2):280–283.

Obadas, N., Henniges, U., Potthast, A., and Rosenau, T. (2016). Cellulosic fines: Properties and effects. *Progress in Materials Science*, 83:574–594.

Olgård, G. (1970). Fractionation of fiber suspensions by liquid column flow. *Tappi J.*, 53(7):1240–1246.

Olson, J. (1996). *The effect of fibre length on passage through narrow apertures*. PhD thesis, Dept. of Chemical Engineering, The University of British Columbia.

Olson, J. A. (2003). A lecture on pressure screeninng. Technical report, Mechanical Engineering Department: University of Columbia.

Osong, S. H., Norgren, S., and Engstrand, P. (2013). An approach to produce nano-lignocellulose from mechanical pulp fine materials. *Nordic Pulp and Paper Research Journal*, 28(4):472–479.

Paavilainen, L. (1990). Importance of particle size - fibre length and fines - for the characterization of softwood kraft pulp. *Paperi Ja Puu*, 72(5):516–526.

Panula-Ontto, S., Fuhrmann, A., and Robertsén, L. (2002). Effect of cell-wall thickness and fines on bleaching. In *Tappi International Pulp Bleaching Conference*, pages 161–169.

Parham, R. A. and Gray, R. L. (1984). *Formation and Structure of Wood*, chapter 2, pages 3–56.

Pascal, R. and Silvy, J. (1993). 1993. *Conduite et commande des proceeds/ coord: C. Jallut*, 7(29):233–238.

Piazza, I. D. and Ciofalo, M. (2011). Transition to turbulence in toroidal pipes. *Journal of Fluid Mechanics*, 687:72–117.

Redlinger-Pohn, J., Jagiello, L., Bauer, W., and Radl, S. (2016). Mechanistic understanding of size-based fibre separation in coiled tubes. *International Journal of Multiphase Flow*, 83:239–253.

Retulainen, E., Luukko, K., Fagerholm, K., Pere, J., Laine, J., and Paulapuro, H. (2002). Papermaking quality of fines from different pulps - the effect of size, shape and chemical composition. *Appita J 55(6)*, 467:457–460.

Retulainen, E., Moss, P., and Nieminen, K. (1993). Effect of fines on the properties of fibre networks. *Products of papermaking*, pages 727–770.

Richter, G. A. (1941). Cellulose from hardwoods. wood pulp purification. *Industrial & Engineering Chemistry*, 33(12):1518–1528.

Ross, C., Smith, B., and Valentine, G. (2000). Rethinking dissolved air flotation design for industrial pretreatment. In *2000 WEF and Purdue University Industrial Wastes Technical Conference*.

Ruck-Florjancic, M. and Ruck, H. (1961). Elektronenoptische untersuchungen an holzschliff-feinstoffen. 2. teil. *Das Papier*, 15:715–725.

Rundlöf, M. (2002). *Interaction of dissolved and colloidal substances with fines of mechanical pulp: influence on sheet properties and basic aspects of adhesion*. PhD thesis, Sweden: Royal Institute of Technology.

Rundlof, M., Htun, M., Hoglund, H., and Wagberg, L. (2000). Importance of the experimental method when evaluating the quality of fines of mechanical pulps. *Journal of Pulp and Paper Science*, 26(9):301–307.

SCAN (2000). Chemical pulp - water retention value. standard c 62:002000.

SCAN (2005). Mechanical and chemical pulps - fines content. standard cm 66:052005.

Scott, G. and Abubakr, S. (1994). Fractionation of secondary fibre - a review. *Progress in Paper Recycling*, 3(3):50–59.

Sirvio, J. and Nurminen, I. (2003). Systematic changes in paper properties caused by fines. pages 205 – 208, Quebec City, Que., Canada. Dynamic drainage jar;Fiber processing;Fibrillar mechanical pulp fines;.

Sjöström, E. (1993). *Wood Chemistry: Fundamentals and Applications*. Academic Press, New York, 2. Edition.

Stark, H. and Eichinger, R. (1979). Magnefite-zellstoff in der papiererzeugung. *Wochenblatt für Papierfabrikation 2*.

Sundberg, A. and Holmbom, B. (2004). Fines in spruce tmp, btmp and ctmp - chemical composition and sorption of mannans. *Nordic Pulp and Paper Research Journal*, 19(2):176–182.

Sundberg, A., Pranovich, A., and Holmbom, B. (2000). Distribution of anionic groups in tmp suspensions. *Journal of Wood Chemistry and Technology*, 20(1):71–92.

Sundberg, A., Pranovich, A. V., and Holmbom, B. (2003). Chemical characterization of various types of mechanical pulp fines. *Journal of Pulp and Paper Science*, 29(5):173–180.

Sundholm, J. (1999). *What is mechanical pulping? - Mechanical Pulping, Book 5 of the Series Pappermaking Science and Technology*. Fapet Oy, 1st edition, 427p.

Swerin, A., Ödberg, L., and Wågberg, L. (1993). Preparation and some properties of the colloidal pitch fraction from a thermomechanical pulp. *Nordic Pulp Paper Res.J.*, 8(3).

Taipale, T., Holappa, S., and Laine, J. (2011). Isolation and characterization of cellulosic pulp fines and their interactions with cationic polyacrylamides. *Journal of Dispersion Science and Technology*, 32(6):863–873.

Taipale, T., Österberg, M., Nykänen, A., Ruokolainen, J., and Laine, J. (2010). Effect of microfibrillated cellulose and fines on the drainage of kraft pulp suspension and paper strength. *Cellulose*, 17(5):1005–1020.

Takahashi, T., Miyahara, T., and Mochizuki, H. (1979). Fundemental study of bubble formation in dissolved air pressure flotation. *Jour. Chem. Engr. Japan*, 12:275–280.

Thalib, T. and Hultén, A. H. (2006). Xps in combination with mercurization - incorporation of mercury into different morphological parts of an unbleached softwood kraft pulp. *Holzforschung*, 60(1):9–13.

Timmel, T. (2014). Flippr° - future lignin pulp proprocess research. http://flippr.at/jart/prj3/flippr/main.jart.

Vogel, H. (1974). *Chemiker-Kalender*. SpringeSpringer, Berlin Heidelberg New York.

Wagner, W. and Kruse, A. (1998). *Properties of Water and Steam*. Spinger-Verlag, Berlin Heidelberg New York.

Webster, D. and Humphrey, J. (1997). Traveling wave instability in helical coil flow. *Phys. Fluids*, 9(2):407–418.

Westermark, U. and Capretti, G. (1988). Influence of ray cells on the bleachability and properties of ctmp and kraft pulps. *Nord.Pulp Pap.Res.J.*, 3(2):95–99.

Westermark, U., Hardell, H.-L., and Iversen, T. (1986). The content of protein and pectin in the lignified midle lamella/primary wall from spruce fibers. *Holzforschung*, 40:65–68.

Wågberg, L. and Björklund, M. (1993). Adsorption of cationic potato starch on cellulosic fibres. *Nord Pulp Pap Res J*, 8(2):399–404.

Willför, S., Sundberg, A., Hemming, J., and Holmbom, B. (2005a). Polysaccharides in some industrially important hardwood species. *Wood Sci Technol*, 39:601–617.

Willför, S., Sundberg, A., Hemming, J., and Holmbom, B. (2005b). Polysaccharides in some industrially important softwood species. *Wood Sci Technol*, 39:245–257.

Wood, J. R. and Karnis, A. (1996). Determination of specific surface area of mechanical pulp fines from turbidity measurements. *Paperi ja Puu/Paper and Timber*, 78(4):181–186.

Yin, X., Lin, T., and Nazhad, M. (2013). Influence of chemical pulp fines´ origin on fines quality. *IPPTA: Quarterly Journal of Indian Pulp and Paper Technical Association*, 25(2):83–87.

List of Figures

List of Tables